



KADIR HAS UNIVERSITY
SCHOOL OF GRADUATE STUDIES
DEPARTMENT OF ENGINEERING AND NATURAL SCIENCE

**HIGH-PASS AND LOW-PASS MIXED ELEMENT
LOSSLESS TWO-PORT NETWORKS AS PHASE
SHIFTERS**

GÖKHAN ÇAKMAK

DOCTOR OF PHILOSOPHY THESIS

ISTANBUL, JULY, 2022

GÖKHAN ÇAKMAK

Ph.D Thesis

2022

**HIGH-PASS AND LOW-PASS MIXED ELEMENT
LOSSLESS TWO-PORT NETWORKS AS PHASE
SHIFTERS**

GÖKHAN ÇAKMAK

DOCTOR OF PHILOSOPHY THESIS

A thesis submitted to
the School of Graduate Studies of Kadir Has University
in partial fulfillment of requirements for the degree of
Doctor of Philosophy in Electronics Engineering

Istanbul, JULY, 2022

APPROVAL

This thesis titled **HIGH-PASS AND LOW-PASS MIXED ELEMENT LOSSLESS TWO-PORT NETWORKS AS PHASE SHIFTERS** submitted by **GÖKHAN ÇAKMAK**, in partial fulfillment of the requirements for the degree of Doctor of Philosophy in Electronics Engineering, is approved by

Prof. Metin Şengül (Advisor)
Kadir Has University

.....

Assoc. Prof Atilla Özmen
Kadir Has University

.....

Asst. Prof. Yalçın Şadi
Kadir Has University

.....

Prof. Ahmet Sertbaş
Istanbul University - Cerrahpaşa

.....

Asst. Prof. Ertuğrul Saatçı
Istanbul Kültür University

.....

I confirm that the signatures above belong to the aforementioned faculty members.

Prof. Mehmet Timur Aydemir

Director of the School of Graduate Studies

Date of Approval: 22.07.2022

DECLARATION ON RESEARCH ETHICS AND PUBLISHING METHODS

I, GÖKHAN ÇAKMAK, here by declare

- that this Ph.D. of Science Thesis that I have submitted is entirely my own work, and I have cited and referenced all material and results that are not my own in accordance with the rules;
- that this Ph.D. of Science Thesis does not contain any material from any research submitted or accepted to obtain a degree or diploma at another educational institution;
- and that I commit and undertake to follow the “ Kadir Has University Academic Codes of Conduct “ prepared in accordance with the “ Higher Education Council Codes of Conduct”.

In addition, I acknowledge that any claim of irregularity that may arise in relation to this work will result in disciplinary action in accordance with the university legislation.

Gökhan Çakmak

Date (22.07.2022)



To my Dearest Family...

ACKNOWLEDGEMENTS

People in their life may have some difficulties to reach their targets. These difficulties are sometimes so formidable without someone's advice and guidance. Only the lucky ones have a patient and determined counselor around them. I think I am one of the lucky ones to have a supervisor Prof. Metin Şengül. With your help, I can have the power and determination to finish the Ph.D. thesis and continue my academic career.



Thanks, Professor

HIGH-PASS AND LOW-PASS MIXED ELEMENT LOSSLESS TWO-PORT NETWORKS AS PHASE SHIFTERS

ABSTRACT

Phase shifters are one of the sub-units in many systems. In active-phased array radar (APAR) systems, digital phase shifters (switched line, reflection, loaded-line, and high-pass/low-pass which is the smallest in volume [17]) are used. High-pass/low-pass phase shifters was introduced over 50 years ago [28,40,44]. Besides the size advantage, if their power and phase-bandwidth capabilities are compared with other type phase shifters [7,23,39], high-pass/low-pass phase shifters are the best choice [28]. From the more complicated versions [46] to simple versions [43], the usage of the high-pass/low-pass shifters has increased in the last 20 years. For a system designed to be small in size, all the sub-units must be as small as possible. Therefore, in practice, high-pass/low-pass phase shifters are implemented using lumped elements. However, the connection points will deteriorate the frequency response of the phase shifter at microwave frequencies. Therefore, these points must be considered as distributed elements, circuits must be designed to contain mixed lumped and distributed elements. In this thesis, phase shifting properties of four different mixed element lossless two-port networks have been studied: Two high-pass networks (with inductors and capacitors separated by distributed elements and with capacitors separated by distributed elements), two low-pass networks (with inductors and capacitors separated by distributed elements and with capacitors separated by distributed elements). In the design of these networks, a real frequency-based approach is utilized. Namely, free parameters are initialized, and then optimized to get the desired response. Obtained circuit functions are used to calculate the normalized component values. In the thesis, a new component value calculation process is defined. Calculated normalized values are denormalized to get real component values. In the last section of the thesis, high-pass and low-pass sections are designed. Then real component values are calculated for different frequency values, and performances of the phase shifters are obtained and compared.

Key Words: Phase Shifters, Lumped Elements, Distributed Elements

FAZ KAYDIRICI OLARAK YÜKSEK GEÇİREN VE ALÇAK GEÇİREN KARMA ELEMANLI KAYIPSIZ İKİ KAPILI DEVRELER

ÖZET

Faz kaydırıcılar birçok sistemin alt sistemlerinden biridir. Aktif Faz Dizinli Radar sistemlerinde (hat anahtarlama, yansıma, yüklü hat ve yüksek geçiren / alçak geçiren, ki en az yer kaplayan [17]) dijital faz kaydırıcılar kullanılmaktadır. Yüksek geçiren / alçak geçiren faz kaydırıcılar 40 yılı aşkın bir süre önce ortaya çıkmıştır [28,40,44]. Boyut avantajının yanı sıra, güç ve faz- bant kabiliyetleri, diğer tip faz kaydırıcıları [7,23,39] ile kıyaslandığında yüksek geçiren / alçak geçiren faz kaydırıcılar en iyi seçenektir [28]. Daha karışık versiyonlardan [46] basit versiyonlara [43], yüksek geçiren / alçak geçiren kaydırıcıların kullanılması son 15 yılda artış göstermiştir. Tasarlanan bir sistemin küçük boyutlarda olması için, bütün alt sistemlerin de olabildiğince küçük olması gerekir. Bu yüzden, pratikte yüksek geçiren / alçak geçiren faz kaydırıcılarda toplu elemanlar kullanılır. Şu var ki, bağlantı noktaları mikrodalga frekanslarda faz kaydırıcıların performansını kötüleştirir. Bu yüzden, bağlantı noktalarının dağınık eleman olduğu farz edilmeli, toplu ve dağınık elemanları içeren karma elemanlı devreler tasarlanmalıdır. Bu tezde, dört farklı iki-kapılı kayıpsız karma elemanlı faz kaydırıcı devrenin faz kaydırma özellikleri incelenmiştir: Bobin ve kondansatörlerin dağınık elemanlarla ayrıldığı yüksek geçiren devre, kondansatörlerin dağınık elemanlarla ayrıldığı yüksek geçiren devre, bobin ve kondansatörlerin dağınık elemanlarla ayrıldığı alçak geçiren devre, kondansatörlerin dağınık elemanlarla ayrıldığı alçak geçiren devre. Bu devrelerin tasarımlarında, gerçek frekans tabanlı bir yaklaşım kullanılmaktadır. Yani, serbest parametrelere başlangıç değerleri atanır ve sonra istenilen cevap elde edebilmesi için optimal hale getirilir. Elde edilen devre fonksiyonları normalize edilmiş devre elemanlarının değerlerini hesaplamakta kullanılır. Bu tezde, eleman değerlerinin hesaplanmasında yeni bir yaklaşım tanımlanmıştır. Hesaplanan normalize edilmiş elemanları değerleri, gerçek eleman değerlerinin bulunması için denormalize edilir. Tezin son kısmında, yüksek geçiren ve alçak geçiren bölümler tasarlandı. Sonra gerçek eleman değerleri farklı frekans değerleri için hesaplandı ve faz kaydırıcıların performansları elde edildi ve karşılaştırıldı.

Anahtar Sözcükler: Faz kaydırıcılar, Toplu elemanlar, Dağınık elemanlar

TABLE OF CONTENTS

ACKNOWLEDGEMENT	v
ABSTRACT	vi
ÖZET	vii
LIST OF FIGURES	x
LIST OF SYMBOLS	xiii
LIST OF ACRONYMS AND ABBREVIATIONS	xiv
1. INTRODUCTION	1
2. LITERATURE	3
3. SCATTERING PARAMETERS	5
3.1 Scattering Parameters via Incident and Reflected Waves	5
3.2 Scattering Parameters Defined via Polynomials	10
4. HIGH-PASS AND LOW-PASS MIXED ELEMENT NETWORK	14
4.1 LPPSN via Series Inductors and Shunt Capacitors Separated by UE	14
4.1.1 One unit element and one lumped element	16
4.1.2 One unit element and two lumped elements	16
4.1.3 Two unit elements and one lumped element	17
4.1.4 Two unit elements and two lumped elements	18
4.1.5 Two unit elements and three lumped elements	19
4.2 HPPSN via Series Capacitors and Shunt Inductors Separated by UE	20
4.2.1 One unit element and one lumped element	21
4.2.2 One unit element and two lumped elements	22
4.2.3 Two unit elements and one lumped element	23
4.2.4 Two unit elements and two lumped elements	24
4.2.5 Two unit elements and three lumped elements	25
4.3 LPPSN via Shunt Capacitors Separated by UE	25
4.3.1 One unit element and one shunt capacitor	27
4.3.2 One unit element and two shunt capacitors	27
4.3.3 Two unit elements and one shunt capacitor	28
4.3.4 Two unit elements and two shunt capacitors	29
4.3.5 Two unit elements and three shunt capacitors	30

4.4	HPPSN via Series Capacitors Separated by UE.....	31
4.4.1	One series capacitor and one unit element.....	31
4.4.2	Two series capacitors and one unit element.....	32
4.4.3	One series capacitor and two unit elements.....	33
4.4.4	Two series capacitors and two unit elements.....	34
4.4.5	Three series capacitors and two unit elements.....	35
5.	COMPONENT VALUE CALCULATIONS	37
5.1	HPN via Series Capacitor Separated by UE.....	39
5.2	LPN via Shunt Capacitor Separated by UE.....	41
5.3	HPN via Series Capacitors and Shunt Inductors Separated by UE.....	43
5.4	LPN via Shunt Capacitors and Series Inductors Separated by UE.....	45
6.	OPTIMIZATION PROCESS.....	48
7.	HIGH-PASS AND LOW-PASS NETWORKS.....	55
7.1	HPN via Series Capacitor Separated by UE	56
7.2	LPN via Shunt Capacitors Separated by UE.....	65
7.3	LPN via Series Inductors and Shunt Capacitors Separated by UE.....	68
7.4	HPN via Shunt Inductors and Series Capacitors Separated by UE.....	71
8.	PHASE SHIFTER NETWORKS.....	74
8.1	PSN via Series or Shunt Capacitors Separated by UE.....	74
8.2	PSN via Capacitors and Inductors Separated by UE.....	100
9.	CONCLUSION.....	125
	REFERENCES.....	128

LIST OF FIGURES

Figure 3.1 A two-port network with waves.....	06
Figure 5.1 HPN via series capacitors separated by UE.....	39
Figure 5.2 LPN via shunt capacitors separated by UE.....	41
Figure 5.3 HPN via series capacitors and shunt inductors separated by UE.....	43
Figure 5.4 LPN via shunt capacitors and series inductors separated by UE.....	44
Figure 6.1 Calculation Process of circuit component values.....	54
Figure 7.1 Synthesis of HPN via series capacitors separated by UE.....	56
Figure 7.2 TPG response of HPN via series capacitors separated by UE.....	64
Figure 7.3 Synthesis of LPN via shunt capacitors separated by UE.....	65
Figure 7.4 TPG response of LPN via shunt capacitors separated by UE.....	67
Figure 7.5 Synthesis of LPN via shunt capacitors and series inductors separated by UE.....	68
Figure 7.6 TPG of LPN via shunt capacitors and series inductors separated by UE.....	70
Figure 7.7 Synthesis of HPN via SC and SHI separated by UE.....	71
Figure 7.8 TPG of HPN via series capacitors and shunt inductors separated by UE.....	73
Figure 8.1 LPPSN via shunt capacitors separated by UE	74
Figure 8.2 HPPSN via series capacitors separated by UE	78
Figure 8.3 PRN via series capacitors or shunt capacitors separated by UE at 1 GHz....	80
Figure 8.4 TPG of network via SC or SHC separated by UE at 1 GHz.....	81
Figure 8.5 PRN via series capacitors or shunt capacitors separated by UE at 5 GHz....	82
Figure 8.6 TPG of network via SC or SHC separated by UE at 5 GHz.....	82
Figure 8.7 PRN via series capacitors or shunt capacitors separated by UE at 10 GHz....	83
Figure 8.8 TPG of network via SC or SHC separated by UE at 10 GHz.....	84
Figure 8.9 PRN via series capacitors or shunt capacitors separated by UE at 20 GHz....	85
Figure 8.10 TPG of network via SC or SHC separated by UE at 20 GHz.....	86
Figure 8.11 PRN via series capacitors or shunt capacitors separated by UE at 25 GHz....	87
Figure 8.12 TPG of network via SC or SHC separated by UE at 25 GHz.....	88
Figure 8.13 PRN via series capacitors or shunt capacitors separated by UE at 30 GHz....	89
Figure 8.14 TPG of network via SC or SHC separated by UE at 30 GHz.....	90
Figure 8.15 PRN via SC or SHC separated by UE at 100 GHz.....	91

Figure 8.16 TPG of network via SC or SHC separated by UE at 100GHz.....	92
Figure 8.17 Insertion loss of network via SC or SCH separated by UE at 1 GHZ.....	93
Figure 8.18 PRN via SC or SCH separated by UE over octave bandwidth at 1 GHZ...	93
Figure 8.19 High/low pass via lumped elements as 90^0 phase shifter at 1 GHZ.....	94
Figure 8.20 PRN via lumped elements over octave bandwidth at 1 GHZ.....	95
Figure 8.21 ILN via lumped elements over octave bandwidth at 1 GHZ.....	95
Figure 8.22 A broadband 90^0 phase shifter via series resonator and transmission line...	96
Figure 8.23 PRN via SC or SHC separated by UE over 129% bandwidth at 5 GHz.....	96
Figure 8.24 ILN via SC or SHC separated by UE over 129% bandwidth at 5 GHz	97
Figure 8.25 PRN via SC or SHC separated by UE over Ku-band at 15 GHz.....	98
Figure 8.26 ILN via SC or SHC separated by UE over Ku-band at 15 GHz	99
Figure 8.27 LPPSN via mixed lumped elements separated by UE at 1 Ghz.....	100
Figure 8.28 HPPSN via mixed lumped elements separated by UE at 1 Ghz.....	104
Figure 8.29 TPG of network via mixed lumped elements separated by UE at 1 GHZ...	106
Figure 8.30 PRN via mixed lumped elements separated by UE at 1 GHZ.....	107
Figure 8.31 TPG of network via mixed lumped elements separated by UE at 5 GHz...	108
Figure 8.32 PRN via mixed lumped elements separated by UE at 5 GHz.....	108
Figure 8.33 TPG of network via mixed lumped elements separated by UE at 10 GHz .	109
Figure 8.34 PRN via mixed lumped elements separated by UE at 10 GHz.....	110
Figure 8.35 TPG of network via mixed lumped elements separated by UE at 20 GHz .	111
Figure 8.36 PRN via mixed lumped elements separated by UE at 20 GHz.....	112
Figure 8.37 TPG of network via mixed lumped elements separated by UE at 25 GHz ..	113
Figure 8.38 PRN via mixed lumped elements separated by UE at 25 GHz.....	114
Figure 8.39 TPG of network via mixed lumped elements separated by UE at 30 GHz ..	115
Figure 8.40 PRN via mixed lumped elements separated by UE at 30 GHz.....	116
Figure 8.41 TPG of network via mixed lumped elements separated by UE at 100 GHz.	117
Figure 8.42 PRN via mixed lumped elements separated by UE at 100 GHz.....	118
Figure 8.43 PRN via mixed lumped elements separated by UE over octave bandwidth.	120
Figure 8.44 ILN via mixed lumped elements separated by UE over octave bandwidth..	120
Figure 8.45 PRN via mixed lumped elements separated by UE for % 129 bandwidth...	121
Figure 8.46 ILN via mixed lumped elements separated by UE for % 129 bandwidth...	122
Figure 8.47 PRN via mixed lumped elements separated by UE for Ku-band.....	123

Figure 8.48 ILN via mixed lumped elements separated by UE for Ku-band.....123



LIST OF SYMBOLS

Δ - Desired Phase Angle



LIST OF ACRONYMS AND ABBREVIATIONS

HPN	HIGH PASS NETWORK
HPPSN	HIGH PASS PHASE SHIFTER NETWORK
ILN	INSERTION LOSS OF NETWORK
LPN	LOW PASS NETWORK
LPPSN	LOW PASS PHASE SHIFTER NETWORK
MMIC	MONOLITHIC MICROWAVE INTEGRATED CIRCUIT
PRN	PHASE RESPONSE OF NETWORK
PSN	PHASE SHIFTER NETWORK
SC	SERIES CAPACITOR
SHC	SHUNT CAPACITOR
SHI	SHUNT INDUCTOR
TPG	TRANSDUCER POWER GAIN
UE	UNIT ELEMENT

1. INTRODUCTION

Phase shifters are one of phased array system elements used to control electronic beam direction and fast beam scanning in communication and radar systems, like flight control, collision avoidance, missile prevention, and global positioning systems [10,18,20,24,41,42]. The phased array antenna uses the phase shifter to change the phase of the generated radiation main beam so that the system can scan over the specific area without mechanical movement of the antenna [21,27]. Different phase shifters are generated according to bandwidth needs, insertion loss, circuit size, and power consumption. The phase shifters, in literature, are switched phase shifters, loaded phase shifters, and reflection-type phase shifters [7,22,44,49]. Compared with these phase shifters, high/low pass phase shifters possess advantages such as small circuit size, low power consumption, and phase-to-bandwidth capabilities [17]. The distributed elements are insufficient due to sizes in low frequencies as lumped elements. The lumped elements are beneficial in low frequencies, but inductors are bulky and produce magnetic fields caused parasitic in the LC ladder network at high frequencies. These circumstances negatively affect the civilian and military applications' phase response [26]. With these conditions, utilizing the lumped and distributed elements together becomes inevitable. The proximity of inductors with capacitors can be resolved by placing the transmission line between the lumped elements or replacing the transmission lines with inductors in LC ladder networks. This thesis uses the transmission line with characteristic impedance and commensurate delay as a circuit component, like lumped elements. This thesis has two configurations for phase shifters with mixed elements in high-pass and low-pass ladder networks. One type of ladder network as phase shifters consists of two different lumped elements separated by transmission lines. The other type has only series and shunt capacitors separated by transmission lines individually. Two independent variable scattering parameters can verify the system functions. Complex frequency p defines the lumped elements. Richards' variable λ defines the distributed components. The two variable scattering parameters can define reflections, phase, and transducer power gain responses in both directions at two port networks [1-3]. The restrictions will be

determined according to the scattering parameters for optimization methods to get the desired amplitude and phase responses. The calculation of component value is at the end of the design process.



2. LITERATURE

The high-pass and low-pass phase shifters consist of lumped and distributed elements, individually or together. The performance of a phase shifter is based on the number of components in the design process at high-pass and low-pass networks [6]. The performance of phase shifters with lumped elements in high-pass and low-pass π /T topologies is analyzed in [14]. The design for π and T type circuits, consisting of inductors and pin diodes, acts as a capacitor in reverse conditions to get 0° to 180° phase response for high-pass and low-pass phase shifters at extra high frequencies [11]. The study for π and T type circuits possessed capacitors, inductors, and pin diodes (in reverse biased act like a capacitor and in forward biased as a short circuit) according to design 0° - 360° high-pass and low-pass phase shifters for each four different generated LC circuits [12]. The study for the execution of a numerical method is about the minimization of insertion loss and increase in bandwidth against the parasitic effects and performance loss of three lumped elements in high-pass and low-pass symmetrical ladder networks [13]. The design of two types of symmetrical LC lattice networks contains capacitors, inductors, and pin diodes used to generate efficient high-pass and low-pass phase shifters due to wide bandwidth and 0° - 360° wide phase shifters [15]. In all these studies, the phase response and amplitude responses are calculated according to admittance, impedance methods, or the ABCD matrix used to define the scattering matrix.

The study of high-pass and low-pass 0° - 360° phase shifters via lumped elements uses three canonic polynomials to represent scattering parameters to designate conditions and restrictions for the definition of the algorithm. Moreover, this design does not execute the switching process [29]. There are restricted studies about the high-pass and low-pass two-port lossless ladder networks via lumped elements separated by distributed components. These studies are based on scattering parameters defined by three canonic two different variables polynomials to determine mathematical analysis for matching or filter design for good transducer power gain results. The lumped elements are represented with p

(complex frequency), and the unit element (distributed component) is represented with (Richards' variable) λ . The design concerns low-pass ladder networks with two types of lumped elements (inductor and capacitor) separated by transmission lines [17]. The analysis of high-pass, band-pass, and stop-band networks with inductors and capacitors separated by unit elements is defined in [8]. A broadband matching network design with mixed elements is described in [30]. The study about structures of ladder networks with shunt capacitors separated by transmission lines is defined in [32]. There are two different topologies for high-pass and low-pass via mixed element two-port networks as phase shifters. One is a high-pass and low-pass phase shifter with capacitors and inductors separated by transmission lines. The other one has only series capacitors or shunt capacitors separated by transmission lines. The mathematical analysis of the ladder network with series capacitors separated by transmission lines is the subject of this thesis [34]. The analysis of these networks as phase shifters is about the defining restrictions to receive the desired amplitude, phase responses and observation of these results [36]. The circuit component value calculation for each topology is executed at the end of the design process. The synthesis of three configurations is existed in literature and has been tested with mathematical analysis except for the network with series capacitors separated by transmission lines. The synthesis of the network with series capacitors separated by transmission is also the subject of this thesis [33].

3. SCATTERING PARAMETERS

A scattering method with two different types of description will be introduced. The first type is the voltage and current waves used to describe the scattering parameters. In the second type, the three canonic polynomials (g, h, f) are used to define the scattering parameters.

The high-pass and low-pass lossless ladder networks with two different and one type of lumped elements separated with distributed components are described via scattering parameters.

3.1 Scattering Parameters via Incident and Reflected Waves

In literature, many methods like impedance, admittance, and scattering matrices are used to analyze two-port networks at low frequencies. The scattering parameters with admittance and impedance methods are used in microwave and RF frequencies. The loadings are defined as zero or infinity (like Thevenin or Norton) at the ports that scattering parameter becomes an insufficient method at high frequencies. These scattering parameters are defined by using the waves in the forward direction from the source to the network and the backward direction from the network to the source in the first port. In the second port, the wave in the forward direction is from the network to the load resistance. The backward direction is from the load resistance to the network [25].

In Figure 3.1, Z_{int} is the input impedance. a_1 is the incident wave from source to port one of the networks (forward direction). b_1 is the reflected wave from the first port of the network to the source (backward direction). l represents the length of the network. V_1 is the voltage at the first port of the network. V_2 is the voltage at the second port of the network. b_2 is the incident wave from the network to the load impedance. a_2 is the reflected wave from the load (R_L) to the network.

According to Figure 3.1, if the output impedance (Z_{out}) is equal to R_L , the reflection will not occur at the load resistance. The reflection in port one will not occur if the input impedance is equal to the generator impedance (R_{in}).

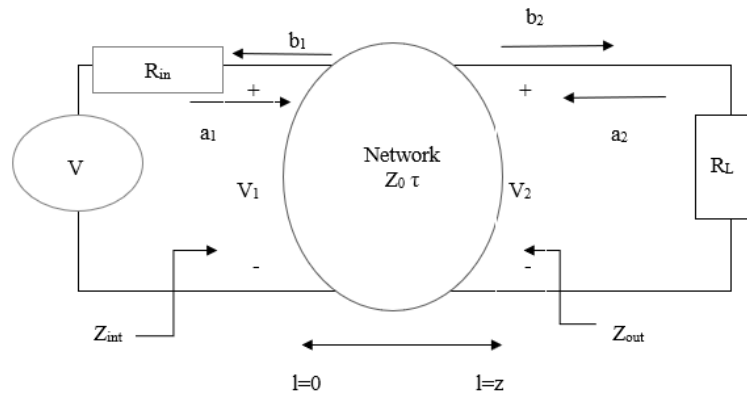


Figure 3.1 A two-port network with waves

The incident and reflected waves at both ports are defined as

$$a_1 = \frac{(V_1 + R_{in} I_{int})}{2\sqrt{R_{in}}}, \quad (3.1)$$

$$b_1 = \frac{(V_1 - R_{in} I_{int})}{2\sqrt{R_{in}}}, \quad (3.2)$$

$$a_2 = \frac{(V_2 + R_L I_0)}{2\sqrt{R_L}}, \quad (3.3)$$

$$b_2 = \frac{(V_2 - R_L I_0)}{2\sqrt{R_L}}. \quad (3.4)$$

The definition of the voltage at port one with the incident waves and reflected waves is shown as

$$V_1 = (a_1 + b_1) / \sqrt{R_{in}}. \quad (3.5)$$

The definition of the current in port one with the incident waves and reflected waves is shown as

$$I_1 = \frac{a_1 - b_1}{\sqrt{R_{in}}}. \quad (3.6)$$

The definition of the voltage at port two with the incident and reflected waves is shown as

$$V_2 = (a_2 + b_2) / \sqrt{R_L} \quad (3.7)$$

The definition of the current at port two with the incident and reflected waves is shown as

$$I_2 = \frac{a_2 - b_2}{\sqrt{R_L}}. \quad (3.8)$$

S_{int} represents the input reflection coefficient.

$$S_{int} = \frac{b_1}{a_1} = \frac{Z_{int} - R_{in}}{Z_{int} + R_{in}}. \quad (3.9)$$

S_{out} represents the output reflection coefficient.

$$S_{out} = \frac{b_2}{a_2} = \frac{Z_{out} - Z_L}{Z_{out} + Z_L}. \quad (3.10)$$

S_{in} represents the reflection coefficient from the generator.

$$S_{in} = \frac{Z_{in} - 1}{Z_{in} + 1} \quad (3.11)$$

S_L represents the load reflection coefficient.

$$S_L = \frac{Z_L - Z_{out}}{Z_L + Z_{out}} \quad (3.12)$$

There are four different scattering parameters for two-port networks. The scattering matrix is defined as

$$b = \begin{bmatrix} b_1 \\ b_2 \end{bmatrix}, a = \begin{bmatrix} a_1 \\ a_2 \end{bmatrix}, S = \begin{bmatrix} S_{11} & S_{12} \\ S_{21} & S_{22} \end{bmatrix} \quad (3.13)$$

The input reflection is defined by

$$S_{11} = \frac{b_1}{a_1} \quad a_2 = 0 \quad (3.14)$$

The parameter of the conductivity from source to terminated load resistance is shown as

$$S_{21} = \frac{b_2}{a_1} \quad a_2 = 0 \quad (3.15)$$

The output reflection at the second port is defined as

$$S_{22} = \frac{b_2}{a_2} \quad a_1 = 0 \quad (3.16)$$

The conductivity from terminated load resistance to source in the reverse direction is defined as

$$S_{12} = \frac{b_1}{a_2} \quad a_1=0 \quad . \quad (3.17)$$

S_{21} is equal to S_{12} if the network is reciprocal in a lossless two-port network. That means the power, amplitude, and phase response will be the same at both ports.

Transpose of S parameter is defined as S^T , and conjugate of S parameter is defined as S^* . The multiplication of the scattering matrix with conjugate and transposing the same scattering matrix is equal to the identity matrix and is defined as

$$S^{*T}S = I \text{ for all } p \quad . \quad (3.18)$$

The relations of the scattering matrix parameters with each other are defined as

$$S_{11}^*S_{11} + S_{21}^*S_{21} = 1, \quad (3.19)$$

$$S_{22}^*S_{22} + S_{12}^*S_{12} = 1, \quad (3.20)$$

$$S_{12}^*S_{11} + S_{21}S_{22}^* = 0, \quad (3.21)$$

$$S_{21}^*S_{22} + S_{12}S_{11} = 0. \quad (3.22)$$

The absolute value of all scattering parameters is equal to or smaller than one for a lossless network. The maximum value of the circuit's amplitude response will equal one.

Transducer power gain defines the performance of power transformation from source to the terminated load resistance. The total power is calculated with the incident and reflected waves in two ports and defined as

$$P_T = a_1 a_1^* - b_1 b_1^* + a_2 a_2^* - b_2 b_2^* \quad . \quad (3.23)$$

In literature, scattering parameters are also defined via ABCD parameters and written as

$$S_{21} = \frac{2}{A + B + C + D} \quad . \quad (3.24)$$

3.2 Scattering Parameters Defined via Polynomials

The admittance and impedance methods are insufficient at high frequencies, with zero and infinite loads. Circuit functions can be defined with the scattering parameters. The three polynomials (g, h, f) have single or two independent variables depending on the type of components. The lumped and distributed components can be used in these networks individually or together. The lumped elements are defined via the frequency variable p. The distributed elements can be represented with Richards' variable λ , and τ is the transmission delay of the unit element.

If lumped and distributed elements are used together, two variable polynomials should be used to define the scattering parameters. High-pass and low-pass ladder networks possess only series and shunt capacitors separated by distributed elements. The unit elements (distributed components) with characteristic impedance and equal length are used to separate lumped elements.

The other two high-pass and low-pass ladder networks contain inductors and capacitors for lumped and unit elements as distributed elements. Unit element has the characteristic impedance and same transmission delay that unit elements are used to separate lumped elements.

The scattering matrix via polynomials is expressed as

$$S = \begin{bmatrix} \frac{h}{g} & \frac{\sigma f^*}{g} \\ \frac{f}{g} & \frac{-\sigma h^*}{g} \end{bmatrix}, \quad (3.25)$$

σ is a constant (+1 or -1), and f^* is the conjugate of f polynomial in equation (3.25)

The representation of the scattering matrix via polynomials is defined as

$$S(p, \lambda) = \frac{1}{g(p, \lambda)} \begin{bmatrix} h(p, \lambda) & \sigma f(-p, -\lambda) \\ f(p, \lambda) & -\sigma h(-p, -\lambda) \end{bmatrix}, \quad (3.26)$$

$$S_{11} = \frac{h(p, \lambda)}{g(p, \lambda)}, S_{12} = \frac{\sigma f(-p, -\lambda)}{g(p, \lambda)}, S_{21} = \frac{f(p, \lambda)}{g(p, \lambda)}, S_{22} = \frac{-\sigma h(-p, -\lambda)}{g(p, \lambda)}. \quad (3.27)$$

If only lumped elements are used, scattering matrix via polynomials is defined as

$$S(p) = \frac{1}{g(p)} \begin{bmatrix} h(p) & \sigma f(-p) \\ f(p) & -\sigma h(-p) \end{bmatrix}, \quad (3.28)$$

$$S_{11} = \frac{h(p)}{g(p)}, S_{12} = \frac{\sigma f(-p)}{g(p)}, S_{21} = \frac{f(p)}{g(p)}, S_{22} = \frac{-\sigma h(-p)}{g(p)}. \quad (3.29)$$

If only distributed elements are used, scattering matrix via polynomials is defined as

$$S(\lambda) = \frac{1}{g(\lambda)} \begin{bmatrix} h(\lambda) & \sigma f(-\lambda) \\ f(\lambda) & -\sigma h(-\lambda) \end{bmatrix}, \quad (3.30)$$

$$S_{11} = \frac{h(\lambda)}{g(\lambda)}, S_{12} = \frac{\sigma f(-\lambda)}{g(\lambda)}, S_{21} = \frac{f(\lambda)}{g(\lambda)}, S_{22} = \frac{-\sigma h(-\lambda)}{g(\lambda)}. \quad (3.31)$$

g polynomial is a strictly Hurwitz polynomial that real parts of all roots of g polynomial are smaller than zero [2]. The roots are in left half plane. f polynomial is an even or odd monic polynomial.

The relations between these polynomials via single and two variables according to lossless two port network are defined as

$$g(p,\lambda)g(-p,-\lambda) = h(p,\lambda)h(-p,-\lambda) - f(p,\lambda)f(-p,-\lambda), \quad (3.32)$$

$$g(p)g(-p) = h(p)h(-p) - f(p)f(-p) \quad \lambda=0, \quad (3.33)$$

$$g(\lambda)g(-\lambda) = h(\lambda)h(-\lambda) - f(\lambda)f(-\lambda) \quad p=0. \quad (3.34)$$

$g(p,\lambda)$, $h(p,\lambda)$, $f(p,\lambda)$ are canonic polynomials [40]. The coefficients of g polynomial are nonzero and positive.

For two-port networks, f can be defined for low-pass and high-pass networks as

$$f(p,\lambda) = p^k \lambda^c (1 - \lambda^2)^{n/2} \quad (3.35)$$

In equation (3.35), k represents the number of capacitors and inductors in the ladder network, c represents the number of open and short transmission lines in a network. n is the number of transmission lines in the network.

M_g is the coefficient matrix of $g(p,\lambda)$ polynomial and defined as

$$M_g = \begin{bmatrix} g_{00} & \cdots & g_{0n} \\ \vdots & \ddots & \vdots \\ g_{kn} & \cdots & g_{kn} \end{bmatrix}. \quad (3.36)$$

M_h is the coefficient matrix of $h(p,\lambda)$ polynomial and defined as

$$M_h = \begin{bmatrix} h_{00} & \cdots & h_{0n} \\ \vdots & \ddots & \vdots \\ h_{k0} & \cdots & h_{kn} \end{bmatrix} . \quad (3.37)$$

Transfer scattering parameters are used in the calculations of circuit components [4-5].

The transfer scattering matrix is written as

$$T(p,\lambda) = \frac{1}{f(p,\lambda)} \begin{bmatrix} \sigma g(-p,-\lambda) & h(p,\lambda) \\ \sigma h(-p,-\lambda) & g(p,\lambda) \end{bmatrix}, \quad (3.38)$$

$$T_{12} = \frac{h(p,\lambda)}{f(p,\lambda)}, T_{11} = \frac{\sigma g(-p,-\lambda)}{f(p,\lambda)}, T_{22} = \frac{g(p,\lambda)}{f(p,\lambda)}, T_{21} = \frac{\sigma h(-p,-\lambda)}{f(p,\lambda)}. \quad (3.39)$$

4. HIGH-PASS AND LOW-PASS MIXED ELEMENT NETWORK

There are four different lossless two-port high pass and low pass networks via lumped elements separated by unit elements.

4.1 LPPSN via Series Inductors and Shunt Capacitors Separated by UE

In literature, a low-pass lossless ladder network with two kinds of lumped elements separated via unit elements was studied in [1]. There are networks from two to five degrees for all configurations. Mathematical analysis is examined to identify the structures of these networks. The equations are derived for one lumped element and one unit element, two lumped elements and one unit element, one lumped element and two unit elements, two lumped elements and two unit elements, three lumped elements and two unit elements. These equations are used to calculate the unknown coefficients of $g(p,\lambda)$ and $h(p,\lambda)$.

The representation of $g(p,\lambda)$ is

$$g(p,\lambda)=p^T M_g \lambda . \quad (4.1)$$

For three capacitors and two distributed elements, the coefficient matrix of g polynomial (M_g) is defined as

$$M_g = \begin{bmatrix} 1 & g_{01} & g_{02} \\ g_{10} & g_{11} & g_{12} \\ g_{20} & g_{21} & 0 \\ g_{30} & 0 & 0 \end{bmatrix} . \quad (4.2)$$

The representation of $h(p,\lambda)$ is defined as

$$h(p,\lambda)=p^T M_h \lambda . \quad (4.3)$$

The coefficient matrix of h polynomial (M_h) is defined as

$$M_h = \begin{bmatrix} 0 & h_{01} & h_{02} \\ h_{10} & h_{11} & h_{12} \\ h_{20} & h_{21} & 0 \\ h_{30} & 0 & 0 \end{bmatrix} . \quad (4.4)$$

In M_g and M_h coefficient matrices, lumped elements are represented via the first column of the matrix ($m=3$). The unit elements ($n=2$) are defined via the first row.

In this study, capacitors and inductors are used as lumped elements, and transmission lines are used as distributed elements to separate the lumped elements of the low-pass ladder network.

The unknown parameters in g and h are g_{11} , g_{21} , g_{12} , and h_{11} , h_{21} , h_{12} . The constant parameters are $g_{00}=1$ and $h_{00}=0$.

The unknown parameters are calculated by using the equations given in [22].

$f(p,\lambda)$ polynomial is defined in equation (3.35)

For $n=1$, $m=1,2$

$$f(p,\lambda)=f(p)f(\lambda)=(1-\lambda^2)^{n/2}=(1-\lambda^2)^{1/2} . \quad (4.5)$$

For $n=2$, $m=1,2,3$

$$f(p,\lambda)=f(p)f(\lambda)=(1-\lambda^2)^{2/2}=(1-\lambda^2) . \quad (4.6)$$

This thesis aims to find conditions and restrictions on S_{21} parameter to achieve sufficient amplitude and desired phase response. S_{21} is defined as

$$S_{21} = \frac{f(p,\lambda)}{g(p,\lambda)} . \quad (4.7)$$

4.1.1 One unit element and one lumped element

Constant coefficients values are $g_{00}=1$ and $h_{00}=0$. Coefficient matrices and equations are defined as

$$M_g = \begin{bmatrix} 1 & g_{01} \\ g_{10} & g_{11} \end{bmatrix} , \quad (4.8)$$

$$M_h = \begin{bmatrix} 0 & h_{01} \\ h_{10} & h_{11} \end{bmatrix} , \quad (4.9)$$

$$g_{11} = g_{01} * g_{10} - h_{01} * h_{10} , \quad (4.10)$$

$$g_{11} = h_{11} * m2 , \quad (4.11)$$

$$g_{10} = h_{10} * m1 . \quad (4.12)$$

For shunt capacitor and unit element, $m1$ is equal to -1, and $m2$ is equal to -1.

For unit element and series inductor, $m1$ is equal to 1, and $m2$ is equal to -1.

For series inductor and unit element, $m1$ and $m2$ are equal to 1.

For unit element and shunt capacitor, $m1$ is equal to -1, and $m2$ is equal to 1.

4.1.2 One unit element and two lumped elements

Constant coefficients values are $g_{00}=1$, $h_{00}=0$, $g_{21}=0$ and $h_{21}=0$. Coefficient matrices and equations are defined as

$$M_g = \begin{bmatrix} 1 & g_{01} \\ g_{10} & g_{11} \\ g_{20} & 0 \end{bmatrix} , \quad (4.13)$$

$$M_h = \begin{bmatrix} 0 & h_{01} \\ h_{10} & h_{11} \\ h_{20} & 0 \end{bmatrix} , \quad (4.14)$$

$$g_{11} = g_{01} * g_{10} - h_{01} * h_{10} \quad , \quad (4.15)$$

$$g_{20} = (1 + h_{20}^2)^{1/2} \quad , \quad (4.16)$$

$$g_{10} = (2 * g_{20} + h_{10}^2)^{1/2} \quad , \quad (4.17)$$

$$h_{11} = g_{11} * m1 \quad . \quad (4.18)$$

For $m1=1$, the order of the circuit components is a series inductor, unit element, and shunt capacitor.

For $m1=-1$, the order of the circuit components is a shunt capacitor, unit element, and series inductor.

4.1.3 Two unit elements and one lumped element

Constant coefficients values are $g_{00}=1$ and $h_{00}=0$. Coefficient matrices and equations are defined as

$$M_g = \begin{bmatrix} 1 & g_{01} & g_{02} \\ g_{10} & g_{11} & g_{12} \end{bmatrix} \quad , \quad (4.19)$$

$$M_h = \begin{bmatrix} 0 & h_{01} & h_{02} \\ h_{10} & h_{11} & h_{12} \end{bmatrix} \quad , \quad (4.20)$$

$$g_{11} = g_{01} * g_{10} - h_{01} * h_{10} \quad , \quad (4.21)$$

$$g_{12} = \frac{g_{11} * g_{02} - h_{11} * h_{02}}{g_{01} - m2 * h_{01}} \quad , \quad (4.22)$$

$$h_{11} = h_{02} \frac{g_{10} - m2 * h_{10}}{g_{01} - m2 * h_{01}} \quad , \quad (4.23)$$

$$h_{12} = g_{12} * m2 \quad , \quad (4.24)$$

$$h_{10} = g_{10} * m1 \quad , \quad (4.25)$$

For $m_1=1$ and $m_2=-1$, the order of the components in the network is a unit element, series inductor, and unit element.

For $m_1=-1$ and $m_2=1$, the order of the components in the network is a unit element, shunt capacitor, and unit element.

4.1.4 Two unit elements and two lumped elements

Constant coefficients values are $g_{00}=1$, $h_{00}=0$, $g_{22} = 0$ and $h_{22} = 0$. Coefficient matrices and equations are defined as

$$M_g = \begin{bmatrix} 1 & g_{01} & g_{02} \\ g_{10} & g_{11} & g_{12} \\ g_{20} & g_{21} & 0 \end{bmatrix}, \quad (4.26)$$

$$M_h = \begin{bmatrix} 0 & h_{01} & h_{02} \\ h_{10} & h_{11} & h_{12} \\ h_{20} & h_{21} & 0 \end{bmatrix}, \quad (4.27)$$

$$g_{11} = g_{01} * g_{10} - h_{01} * h_{10}, \quad (4.28)$$

$$g_{12} = \frac{g_{11} * g_{02} - h_{11} * h_{02}}{g_{01} - m_2 * h_{01}}, \quad (4.29)$$

$$g_{21} = \frac{g_{11} * g_{20} - h_{11} * h_{20}}{g_{10} - m_2 * h_{10}}, \quad (4.30)$$

$$h_{11} = h_{02} \frac{g_{10} - m_2 * h_{10}}{g_{01} - m_2 * h_{01}} + h_{20} \frac{g_{01} - m_2 * h_{01}}{g_{10} - m_2 * h_{10}}, \quad (4.31)$$

$$h_{21} = g_{21} * m_2, \quad (4.32)$$

$$h_{20} = g_{20} * m_1, \quad (4.33)$$

$$h_{12} = g_{12} * m_2. \quad (4.34)$$

For $m_1=1$ and $m_2=1$, the order of the components in the network is a series inductor, unit element, shunt capacitor, and unit element.

For $m_1=-1$ and $m_2=-1$, the order of the components in the network is shunt capacitor unit element, series inductor, and unit element.

For $m_1=1$ and $m_2=-1$, the order of the components in the network is a unit element, series inductor unit element, and shunt capacitor.

For $m_1=-1$ and $m_2=1$, the order of the components in the network is a unit element, shunt capacitor unit element, and series inductor.

4.1.5 Two unit elements and three lumped elements

Constant coefficients values are $g_{00}=1$, $h_{00}=0$, $g_{22} = 0$, $h_{22} = 0$, $g_{31} = 0$, $g_{32} = 0$, $h_{31} = 0$, $h_{32} = 0$. Coefficient matrices are defined in equations (4.2) and (4.4).

The equations are defined as

$$g_{11} = g_{01} * g_{10} - h_{01} * h_{10} \quad , \quad (4.35)$$

$$g_{12} = \frac{g_{11} * g_{02} - h_{11} * h_{02}}{g_{01} - m_2 * h_{01}} \quad , \quad (4.36)$$

$$g_{21} = \frac{g_{11} * g_{20} - h_{11} * h_{20} - g_{01} * g_{30} + h_{01} * h_{30}}{g_{10} - m_2 * h_{10}} \quad , \quad (4.37)$$

$$h_{11} = h_{02} \frac{g_{10} - m_2 * h_{10}}{g_{01} - m_2 * h_{01}} + h_{20} \frac{g_{01} - m_2 * h_{01}}{g_{10} - m_2 * h_{10}} \quad , \quad (4.38)$$

$$h_{21} = g_{21} * m_1 \quad , \quad (4.39)$$

$$h_{30} = g_{30} * m_1 \quad , \quad (4.40)$$

$$h_{12} = g_{12} * m_1 \quad . \quad (4.41)$$

For $m_1=1$, the order of the components in the network is a series inductor, unit element, shunt capacitor, unit element, and series inductor.

For $m_1=-1$, the order of the components in the network is a shunt capacitor, unit element, series inductor, unit element, and shunt capacitor.

4.2 HPPSN via Series Capacitors and Shunt Inductors Separated by UE

In literature, the high-pass lossless ladder networks with two kinds of lumped elements separated by unit elements were studied in [8]. There are networks from two-to-five-degree for all configurations. This thesis consists of five different high-pass mixed-element network configurations as phase shifters. Some equations are derived for one lumped element and one unit element, two lumped elements and one unit element, one lumped element and two unit elements, two lumped elements and two unit elements, three lumped elements, and two unit elements. These equations are used to calculate the unknown coefficients of $g(p,\lambda)$ and $h(p,\lambda)$.

For three capacitors and two unit elements, the coefficient matrix of g polynomial (M_g) is defined as

$$M_g = \begin{bmatrix} g_{00} & 0 & 0 \\ g_{10} & g_{11} & 0 \\ g_{20} & g_{21} & g_{22} \\ 1 & g_{31} & g_{32} \end{bmatrix}. \quad (4.42)$$

The coefficient matrix of h polynomial (M_h) is defined as

$$M_h = \begin{bmatrix} h_{00} & 0 & 0 \\ h_{10} & h_{11} & 0 \\ h_{20} & h_{21} & h_{22} \\ 0 & h_{31} & h_{32} \end{bmatrix}. \quad (4.43)$$

The first column represents the lumped elements ($\lambda=0$), and the last row represents the distributed elements ($p=0$). The unknown parameters are g_{11} , g_{21} , g_{22} , and h_{11} , h_{21} , h_{22} .

$f(p,\lambda)$ polynomial for lossless reciprocal high/low pass network from equation (3.35) are written as

For $k=1$ and $n=1$

$$f(p,\lambda)=f(p)f(\lambda)=p^1(1-\lambda^2)^{1/2} . \quad (4.44)$$

For $k=1$ and $n=2$

$$f(p,\lambda)=f(p)f(\lambda)=p^1(1-\lambda^2)^{2/2} . \quad (4.45)$$

For $k=2$ and $n=1$

$$f(p,\lambda)=f(p)f(\lambda)=p^2(1-\lambda^2)^{1/2} . \quad (4.46)$$

For $k=2$ and $n=2$

$$f(p,\lambda)=f(p)f(\lambda)=p^2(1-\lambda^2)^{2/2} . \quad (4.47)$$

For $k=3$ and $n=2$

$$f(p,\lambda)=f(p)f(\lambda)=p^3(1-\lambda^2)^{2/2} . \quad (4.48)$$

This thesis aims to find conditions and restrictions on S_{21} to achieve sufficient amplitude and desired phase responses over a bandwidth.

4.2.1 One unit element and one lumped element

Constant coefficient values are $g_{10}=1$ and $h_{10}=0$. Coefficient matrices and equations are defined as

$$Mg = \begin{bmatrix} g_{00} & g_{01} \\ 1 & g_{11} \end{bmatrix} , \quad (4.49)$$

$$Mh = \begin{bmatrix} h_{00} & h_{01} \\ 0 & h_{11} \end{bmatrix} , \quad (4.50)$$

$$g_{11} = (1 + h_{11})^{\frac{1}{2}} , \quad (4.51)$$

$$g_{01} = g_{00} * g_{11} - h_{00} * h_{11} , \quad (4.52)$$

$$h_{00} = g_{00} * m1 , \quad (4.53)$$

$$h_{01} = g_{01} * m2 . \quad (4.54)$$

For series capacitor and unit element, $m1$ is equal to 1, and $m2$ equals 1.

For unit element and shunt inductor, $m1$ is equal to -1, and $m2$ is equal to 1.

For shunt inductor and unit element, m1 and m2 are equal to -1.

For unit element and series capacitor, m1 equals 1, and m2 equals -1.

4.2.2 One unit element and two lumped elements

Constant coefficient values are $g_{20}=1$, $h_{20}=0$, $g_{01}=0$, and $h_{01}=0$. Coefficient matrices and equations are defined as

$$M_g = \begin{bmatrix} g_{00} & 0 \\ g_{10} & g_{11} \\ 1 & g_{21} \end{bmatrix}, \quad (4.55)$$

$$M_h = \begin{bmatrix} h_{00} & 0 \\ h_{10} & h_{11} \\ 0 & h_{21} \end{bmatrix}, \quad (4.56)$$

$$g_{10} = (2 * g_{00} + h_{10}^2)^{\frac{1}{2}}, \quad (4.57)$$

$$g_{21} = (1 + h_{21})^{\frac{1}{2}}, \quad (4.58)$$

$$g_{11} = g_{21} * g_{10} - h_{21} * h_{10}, \quad (4.59)$$

$$h_{11} = g_{11} * m1, \quad (4.60)$$

$$h_{00} = g_{00} * m1. \quad (4.61)$$

For m1=1, the order of the components in the network is a series capacitor, unit element, and shunt inductor.

For m1=-1, the order of the components in the network is a shunt inductor, unit element, and series capacitor.

4.2.3 Two unit elements and one lumped element

Constant coefficient values are $g_{10}=1$, $h_{10}=0$. Coefficient matrices and equations are defined as

$$M_g = \begin{bmatrix} g_{00} & g_{01} & g_{02} \\ 1 & g_{11} & g_{12} \end{bmatrix}, \quad (4.62)$$

$$M_h = \begin{bmatrix} h_{00} & h_{01} & h_{02} \\ 0 & h_{11} & h_{12} \end{bmatrix}, \quad (4.63)$$

$$g_{01} = g_{00} * g_{11} - h_{00} * h_{11}, \quad (4.64)$$

$$h_{01} = 2 * h_{12} \frac{g_{00} - m1 * h_{00}}{g_{11} - m1 * h_{11}}, \quad (4.65)$$

$$g_{02} = \frac{g_{01} * g_{12} - h_{01} * h_{12}}{g_{11} - m1 * h_{11}}, \quad (4.66)$$

$$h_{11} = g_{11} * m1, \quad (4.67)$$

$$h_{02} = g_{02} * m1. \quad (4.68)$$

For $m1=1$, the order of the components in the network is a unit element, shunt inductor, and unit elements.

For $m1=-1$, the order of the components in the network is a unit element, series capacitor, and unit elements.

4.2.4 Two unit elements and two lumped elements

Constant coefficient values are $g_{20}=1$, $h_{20}=0$, $g_{02}=0$, and $h_{02}=0$. Coefficient matrices and equations are defined as

$$M_g = \begin{bmatrix} g_{00} & g_{01} & 0 \\ g_{10} & g_{11} & g_{12} \\ 1 & g_{21} & g_{22} \end{bmatrix}, \quad (4.69)$$

$$M_h = \begin{bmatrix} h_{00} & h_{01} & 0 \\ h_{10} & h_{11} & h_{12} \\ 0 & h_{21} & h_{22} \end{bmatrix}, \quad (4.70)$$

$$g_{11} = g_{21} * g_{10} - h_{21} * h_{10}, \quad (4.71)$$

$$h_{11} = h_{22} \frac{g_{10} - m2 * h_{10}}{g_{21} - m2 * h_{21}} + h_{00} \frac{g_{21} - m2 * h_{21}}{g_{10} - m2 * h_{10}}, \quad (4.72)$$

$$g_{12} = \frac{g_{11} * g_{22} - h_{11} * h_{22}}{g_{21} - m2 * h_{21}}, \quad (4.73)$$

$$g_{01} = \frac{g_{00} * g_{11} - h_{00} * h_{11}}{g_{10} - m2 * h_{10}}, \quad (4.74)$$

$$h_{11} = g_{11} * m1, \quad (4.75)$$

$$h_{01} = g_{01} * m2. \quad (4.76)$$

For $m1=1$ and $m2=1$, the order of the components in the network is a series capacitor, unit element, shunt inductor, and unit element.

For $m1=-1$ and $m2=-1$, the order of the components in the network is a shunt inductor, unit element, series capacitor, and unit element.

For $m1=1$ and $m2=-1$, the order of the components in the network is a unit element, series capacitor, unit element, and shunt inductor.

For $m1=-1$ and $m2=1$, the order of the components in the network is a unit element, shunt inductor, unit element, and series capacitor.

4.2.5 Two unit elements and three lumped elements

Constant coefficients values are $g_{30}=1$, $h_{30}=0$, $g_{02}=0$, $h_{02}=0$, $g_{01}=0$, $h_{01}=0$, $g_{12}=0$, $h_{12}=0$. Coefficient matrixes are defined in equations (4.42-43).

The equations are defined as

$$g_{21} = g_{31} * g_{20} - h_{31} * h_{20} \quad , \quad (4.77)$$

$$h_{21} = h_{10} \frac{g_{31} - m * h_{31}}{g_{20} - m * h_{20}} + h_{32} \frac{g_{20} - m * h_{20}}{g_{31} - m * h_{31}} \quad , \quad (4.78)$$

$$g_{22} = \frac{g_{21} * g_{32} - h_{21} * h_{32}}{g_{31} - m * h_{31}} \quad , \quad (4.79)$$

$$g_{11} = \frac{g_{10} * g_{21} - h_{20} * h_{21} - g_{31}g_{00} + h_{31}h_{00}}{g_{20} - m * h_{20}} \quad , \quad (4.80)$$

$$h_{11} = g_{11} * m \quad , \quad (4.81)$$

$$h_{22} = g_{22} * m \quad . \quad (4.82)$$

For $m=1$, the order of the components in the network is a shunt inductor, unit element, series capacitor, unit element, and shunt capacitor.

For $m= -1$, the order of the components in the network is a series capacitor, unit element, shunt inductor, unit element, and series capacitor.

4.3 LPPSN via Shunt Capacitors Separated by UE

In literature, low-pass lossless two-port networks via shunt capacitors separated by unit element were studied in [32]. This thesis consists of five different configurations of low pass via mixed element networks as phase shifters. Some equations are derived for one lumped element and one unit element, two lumped elements and one unit element, one lumped element and two unit elements, two lumped elements and two unit elements, three lumped elements, and two unit elements. These equations are used to calculate the unknown coefficients of $g(p,\lambda)$ and $h(p,\lambda)$.

For three capacitors and two distributed elements, the coefficient matrix of g polynomial (M_g) is defined as

$$M_g = \begin{bmatrix} 1 & g_{01} & g_{02} \\ g_{10} & g_{11} & g_{12} \\ 0 & g_{21} & g_{22} \\ 0 & 0 & g_{32} \end{bmatrix} . \quad (4.83)$$

For three capacitors and two distributed elements, the coefficient matrix of h polynomial (M_h) is defined as

$$M_h = \begin{bmatrix} 0 & h_{01} & h_{02} \\ h_{10} & h_{11} & h_{12} \\ 0 & h_{21} & h_{22} \\ 0 & 0 & h_{32} \end{bmatrix} . \quad (4.84)$$

Unknown parameters in g and h are g_{10} , g_{11} , g_{21} , and h_{10} , h_{11} , h_{21} .

The last column represents lumped elements ($\lambda=0$), and the first row represents distributed elements ($p=0$) in M_g and M_h .

f polynomial is written from equation (35).

For $n=1$, $k=1,2$

$$f(p,\lambda) = f(p)f(\lambda) = (1-\lambda^2)^{2/2} = (1-\lambda^2) . \quad (4.85)$$

For $n=2$, $k=1,2,3$

$$f(p,\lambda) = f(p)f(\lambda) = (1-\lambda^2)^{2/2} = (1-\lambda^2) . \quad (4.86)$$

This thesis aims to find conditions and restrictions on S_{21} parameters to achieve the maximum amplitude and desired phase response over bandwidth.

4.3.1 One unit element and one shunt capacitor

Constant coefficient values are $g_{00}=1$, $h_{00}=0$. Coefficient matrices and equations are defined as

$$M_g = \begin{bmatrix} 1 & g_{01} \\ g_{10} & g_{11} \end{bmatrix}, \quad (4.87)$$

$$M_h = \begin{bmatrix} 0 & h_{01} \\ h_{10} & h_{11} \end{bmatrix}, \quad (4.88)$$

$$g_{10} = \frac{g_{11}}{g_{01} - m_1 * h_{01}}, \quad (4.89)$$

$$h_{11} = g_{11} * m_2, \quad (4.90)$$

$$h_{10} = g_{10} * m_1. \quad (4.91)$$

The value of m_1 is always equal to -1.

For $m_2=1$, the order of the components in the network is shunt capacitor and unit element.

For $m_2=-1$, the order of the components in the network is a unit element and shunt capacitor.

4.3.2 One unit element and two shunt capacitors

Constant coefficient values are $g_{00}=1$, $h_{00}=0$, $g_{20}=0$, $h_{20}=0$. Coefficient matrices and equations are defined as

$$M_g = \begin{bmatrix} 1 & g_{01} \\ g_{10} & g_{11} \\ 0 & g_{21} \end{bmatrix}, \quad (4.92)$$

$$M_h = \begin{bmatrix} 0 & h_{01} \\ h_{10} & h_{11} \\ 0 & h_{21} \end{bmatrix}, \quad (4.93)$$

$$g_{10} = \frac{g_{11}}{g_{01} - m_1 * h_{01}}, \quad (4.94)$$

$$h_{10} = g_{10} * m1 \quad , \quad (4.95)$$

$$h_{21} = g_{21} * m2 \quad . \quad (4.96)$$

The values of m1 and m2 are equal to -1.

The order of components is shunt capacitor, unit element, and shunt capacitor in network.

4.3.3 Two unit elements and one shunt capacitor

Constant coefficient values are $g_{00}=1$, $h_{00}=0$. Coefficient matrices and equations are defined as

$$M_g = \begin{bmatrix} 1 & g_{01} & g_{02} \\ g_{10} & g_{11} & g_{12} \end{bmatrix} , \quad (4.97)$$

$$M_h = \begin{bmatrix} 0 & h_{01} & h_{02} \\ h_{10} & h_{11} & h_{12} \end{bmatrix} , \quad (4.98)$$

$$g_{11} = g_{02} * (g_{01} * g_{12} - h_{01} * h_{12}) - h_{02}^2 \frac{g_{12} - m1 * h_{12}}{g_{01} - m1 * h_{01}} , \quad (4.99)$$

$$h_{11} = \frac{g_{11} * g_{02} + h_{01} * h_{12} - g_{01} * g_{12}}{h_{02}} , \quad (4.100)$$

$$g_{10} = \frac{g_{11}}{g_{01} - m1 * h_{01}} , \quad (4.101)$$

$$h_{10} = g_{10} * m1 \quad , \quad (4.102)$$

$$h_{12} = g_{12} * m2 \quad . \quad (4.103)$$

The m1 and m2 are equal to -1 and +1, respectively.

The order of components is a unit element, shunt capacitor, and unit element in the network.

4.3.4 Two unit elements and two shunt capacitors

Constant coefficient values are $g_{00}=1$, $h_{00}=0$, $g_{02}=0$, $h_{02}=0$. Coefficient matrices and equations are defined as

$$M_g = \begin{bmatrix} 1 & g_{01} & g_{02} \\ g_{10} & g_{11} & g_{12} \\ 0 & g_{21} & g_{22} \end{bmatrix}, \quad (4.104)$$

$$M_h = \begin{bmatrix} 0 & h_{01} & h_{02} \\ h_{10} & h_{11} & h_{12} \\ 0 & h_{21} & h_{22} \end{bmatrix}, \quad (4.105)$$

$$\alpha = g_{12} - m_1 * h_{12}, \quad (4.106)$$

$$\beta = g_{01} - m_1 * h_{01}, \quad (4.107)$$

$$g_{11} = g_{02} * (g_{01} * g_{12} - h_{01} * h_{12}) - h_{02}^2 \frac{\alpha}{\beta} + h_{02}^2 \frac{(\beta) \left(\frac{g_{02} * h_{22}}{h_{02}} - g_{22} \right)}{\alpha}, \quad (4.108)$$

$$h_{11} = \frac{g_{11} * g_{02} + h_{01} * h_{12} - g_{01} * g_{12}}{h_{02}}, \quad (4.109)$$

$$g_{21} = \frac{g_{11} * g_{22} - h_{11} * h_{22}}{g_{12} - m_1 * h_{12}}, \quad (4.110)$$

$$g_{10} = \frac{g_{11}}{g_{01} - m_1 * h_{01}}, \quad (4.111)$$

$$h_{10} = g_{10} * m_1, \quad (4.112)$$

$$h_{22} = g_{22} * m_2, \quad (4.113)$$

$$h_{21} = g_{21} * m_3. \quad (4.114)$$

The values of m_1 and m_3 are always equal to -1.

For $m_2=1$, the order of the components in the network is a unit element, shunt capacitor, unit element, and shunt capacitor.

For $m_2=-1$, the order of the components in the network is a shunt capacitor and unit element, shunt capacitor, and unit element.

4.3.5 Two unit elements and three shunt capacitors

Constant coefficients values are $g_{00}=1$, $h_{00}=0$, $g_{20}=0$, $h_{20}=0$, $g_{30}=0$, $h_{30}=0$, $g_{31}=0$,

$h_{31}=0$. Coefficient matrices are defined in equations (4.82-83).

The equations are defined as

$$\alpha = g_{12} - m1 * h_{12} \quad , \quad (4.115)$$

$$\beta = g_{01} - m1 * h_{01} \quad , \quad (4.116)$$

$$g_{11} = g_{02} * (g_{01} * g_{12} - h_{01} * h_{12}) - h_{02}^2 \frac{\alpha}{\beta} + h_{02}^2 \frac{(\beta) \left(\frac{g_{02} * h_{22}}{h_{02}} - g_{22} \right)}{\alpha} \quad , \quad (4.117)$$

$$h_{11} = \frac{g_{11} * g_{02} + h_{01} * h_{12} - g_{01} * g_{12}}{h_{02}} \quad , \quad (4.118)$$

$$g_{21} = \frac{g_{11} * g_{22} + h_{01} * h_{32} - g_{01} * g_{32} - h_{11} * h_{22}}{g_{12} - m1 * h_{12}} \quad , \quad (4.119)$$

$$g_{10} = \frac{g_{11}}{g_{01} - m1 * h_{01}} \quad , \quad (4.120)$$

$$h_{10} = g_{10} * m1 \quad , \quad (4.121)$$

$$h_{32} = g_{32} * m2 \quad , \quad (4.122)$$

$$h_{21} = g_{21} * m1 \quad . \quad (4.123)$$

The values of m1 and m2 are always equal to -1.

The order of components in the network is shunt capacitor, unit element, shunt capacitor, unit element, and shunt capacitor.

4.4 HPPSN via Series Capacitors Separated by UE

The lossless ladder network with series capacitors separated by transmission line is going to be studied in this thesis by using scattering parameters described with two-variable, canonic polynomials $g(p,\lambda)$, $h(p,\lambda)$, $f(p,\lambda)$ [34].

The row and column for the representation of distributed and lumped elements must be defined individually in M_g and M_h so that the equations to calculate unknown coefficients. M_g and M_h are figured out from equations (3.36-37).

This thesis aims to find conditions and restrictions on S_{21} parameter to achieve the maximum amplitude and desired phase response over the wanted bandwidth.

The equations are used to calculate the unknown coefficients with independent coefficients. The equations are defined and written in subsections of this section. The equations are defined in subsections for all networks.

4.4.1 One series capacitor and one unit element

Constant coefficients are $g_{10}=1$, $h_{10}=0$. The last column represents the lumped elements, and the last row represents the unit element. In this column and row, the coefficients are defined as independent parameters. The coefficients g_{00} and h_{00} are defined as unknown parameters.

The coefficient matrices and equations are defined as

$$M_g = \begin{bmatrix} g_{00} & g_{01} \\ 1 & g_{11} \end{bmatrix}, \quad (4.124)$$

$$M_h = \begin{bmatrix} h_{00} & h_{01} \\ 0 & h_{11} \end{bmatrix}, \quad (4.125)$$

$$g_{00} = \frac{g_{01}}{g_{11} - m^2 * h_{11}}, \quad (4.126)$$

$$h_{00} = g_{00} * m2 , \quad (4.127)$$

$$h_{01} = g_{01} * m1 . \quad (4.128)$$

The value of m2 is always +1.

For m2=1, the order of the components in the network is a series capacitor and unit element.

For m2= -1, the order of the components in the network is a unit element and series capacitor.

4.4.2 Two series capacitors and one unit element

Constant coefficients are $g_{20}=1$, $h_{20}=0$, $g_{00}=1$, $h_{00}=0$. The last column represents the lumped elements, and the last row represents the unit element. In this column and row, the coefficients are defined as independent parameters. The coefficients g_{10} and h_{10} are defined as unknown parameters.

The coefficient matrices and equations are defined as

$$M_g = \begin{bmatrix} 0 & g_{01} \\ g_{10} & g_{11} \\ 1 & g_{21} \end{bmatrix} , \quad (4.129)$$

$$M_h = \begin{bmatrix} 0 & h_{01} \\ h_{10} & h_{11} \\ 0 & h_{21} \end{bmatrix} , \quad (4.130)$$

$$g_{10} = \frac{g_{11}}{g_{21} - m2 * h_{21}} , \quad (4.131)$$

$$h_{10} = g_{10} * m2 , \quad (4.132)$$

$$h_{01} = g_{01} * m1 . \quad (4.133)$$

The values of m_1 and m_2 are always equal to +1. The order of the components in the network is a series capacitor, unit element, and series capacitor.

4.4.3 One series capacitor and two unit elements

Constant coefficient values are $g_{10}=1$, $h_{10}=0$, The last column represents the lumped elements, and the last row represents the unit element. In this column and row, the coefficients are defined as independent parameters. The coefficients g_{01} , g_{02} and h_{01} , h_{02} are defined as unknown parameters.

The coefficient matrices and equations are defined as

$$M_g = \begin{bmatrix} g_{00} & g_{01} & g_{02} \\ 1 & g_{11} & g_{12} \end{bmatrix}, \quad (4.134)$$

$$M_h = \begin{bmatrix} h_{00} & h_{01} & h_{02} \\ 0 & h_{11} & h_{12} \end{bmatrix}, \quad (4.135)$$

$$g_{01} = g_{12} * (g_{02} * g_{11} - h_{02} * h_{11}) - h_{12}^2 \frac{g_{02} - m_2 * h_{02}}{g_{11} - m_2 * h_{11}}, \quad (4.136)$$

$$h_{01} = \frac{g_{01} * g_{12} + h_{02} * h_{11} - g_{02} * g_{11}}{h_{12}}, \quad (4.137)$$

$$g_{00} = \frac{g_{01}}{g_{11} - m_2 * h_{11}}, \quad (4.138)$$

$$h_{02} = g_{02} * m_1, \quad (4.139)$$

$$h_{00} = g_{00} * m_2. \quad (4.140)$$

The value of m_1 is -1, and m_2 is equal to +1. The order of the components in the network is a unit element, series capacitor, and unit element.

4.4.4 Two series capacitors and two unit elements

Constant coefficients are $g_{20}=1$, $h_{20}=0$, $g_{00}=0$, $h_{00}=0$. The last column represents the lumped elements, and the last row represents unit elements. In this column and row, the coefficients are defined as independent parameters. The coefficients g_{10} , g_{11} , g_{01} and h_{10} , h_{11} , h_{01} are defined as unknown parameters.

The coefficient matrices and equations are defined as

$$M_g = \begin{bmatrix} 0 & g_{01} & g_{02} \\ g_{10} & g_{11} & g_{12} \\ 1 & g_{21} & g_{22} \end{bmatrix}, \quad (4.141)$$

$$M_h = \begin{bmatrix} 0 & h_{01} & h_{02} \\ h_{10} & h_{11} & h_{12} \\ 0 & h_{21} & h_{22} \end{bmatrix}, \quad (4.142)$$

$$\alpha = g_{12} - m_2 * h_{12}, \quad (4.143)$$

$$\beta = g_{21} - m_2 * h_{21}, \quad (4.144)$$

$$g_{11} = g_{22} * (g_{21} * g_{12} - h_{21} * h_{12}) - h_{22}^2 \frac{\alpha}{\beta} + h_{22}^2 \frac{(\beta) \left(\frac{g_{22} * h_{02}}{h_{22}} - g_{02} \right)}{\alpha}, \quad (4.145)$$

$$h_{11} = \frac{g_{11} * g_{22} + h_{21} * h_{12} - g_{21} * g_{12}}{h_{22}}, \quad (4.146)$$

$$g_{01} = \frac{g_{11} * g_{02} - h_{11} * h_{02}}{g_{12} - m_2 * h_{12}}, \quad (4.147)$$

$$g_{10} = \frac{g_{11}}{g_{21} - m_3 * h_{21}}, \quad (4.148)$$

$$h_{02} = g_{02} * m_1, \quad (4.149)$$

$$h_{01} = g_{01} * m_2, \quad (4.150)$$

$$h_{10} = g_{10} * m_3. \quad (4.151)$$

The values of m_2 and m_3 are always equal to +1.

For $m_1=1$, the order of the components in the network is a series capacitor, unit element, series capacitor, and unit element

For $m_1=-1$, the order of the components in the network is a unit element, series capacitor, unit element, and series capacitor.

4.4.5 Three series capacitors and two unit elements

Constant coefficients are $g_{30}=1$, $h_{30}=0$, $g_{00}=0$, $g_{10}=0$, $g_{01}=0$, $h_{10}=0$, $h_{00}=0$, $h_{01}=0$. The last column represents the lumped elements, and the last row represents the unit elements. In this column and row, the coefficients are defined as independent parameters. The coefficients g_{20} , g_{11} , g_{21} and h_{20} , h_{11} , h_{21} are defined as unknown parameters.

The coefficient matrices and equations are defined as

$$M_g = \begin{bmatrix} 0 & 0 & g_{02} \\ 0 & g_{11} & g_{12} \\ g_{20} & g_{21} & g_{22} \\ 1 & g_{31} & g_{32} \end{bmatrix}, \quad (4.152)$$

$$M_h = \begin{bmatrix} 0 & 0 & h_{02} \\ 0 & h_{11} & h_{12} \\ h_{20} & h_{21} & h_{22} \\ 0 & h_{31} & h_{32} \end{bmatrix}, \quad (4.153)$$

$$\alpha = g_{22} - m_2 * h_{22}, \quad (4.154)$$

$$\beta = g_{31} - m_2 * h_{31}, \quad (4.155)$$

$$g_{21} = g_{32} * (g_{31} * g_{22} - h_{31} * h_{22}) - h_{32}^2 \frac{\alpha}{\beta} + h_{32}^2 \frac{(\beta) \left(\frac{g_{32} * h_{12}}{h_{32}} - g_{12} \right)}{\alpha}, \quad (4.156)$$

$$h_{21} = \frac{g_{21} * g_{32} + h_{22} * h_{31} - g_{22} * g_{31}}{h_{32}}, \quad (4.157)$$

$$g_{11} = \frac{g_{12} * g_{21} - h_{21} * h_{12} - g_{02} * g_{31} + h_{02} * h_{21}}{g_{22} - m_2 * h_{22}}, \quad (4.158)$$

$$g_{20} = \frac{g_{21}}{g_{31} - m_2 * h_{31}}, \quad (4.159)$$

$$h_{02} = g_{02} * m_1, \quad (4.160)$$

$$h_{11} = g_{11} * m_2, \quad (4.161)$$

$$h_{20} = g_{20} * m_2. \quad (4.162)$$

The values of m_1 and m_2 are always equal +1.

The order of the components in a high-pass network is a series capacitor, unit network, series capacitor, unit network, and series capacitor.



5. COMPONENT VALUE CALCULATIONS

Networks can be defined with transfer scattering parameters in terms of two independent variables (p, λ) and are shown as

$$T(p, \lambda) = \frac{1}{f(p, \lambda)} \begin{bmatrix} \sigma g(-p, -\lambda) & h(p, \lambda) \\ \sigma h(-p, -\lambda) & g(p, \lambda) \end{bmatrix}, \quad (5.1)$$

$$T_{12} = \frac{h(p, \lambda)}{f(p, \lambda)}, T_{11} = \frac{\sigma g(-p, -\lambda)}{f(p, \lambda)}, T_{22} = \frac{g(p, \lambda)}{f(p, \lambda)}, T_{21} = \frac{\sigma h(-p, -\lambda)}{f(p, \lambda)}. \quad (5.2)$$

Transfer scattering parameters are used to define networks containing only lumped elements are shown as [37,38]

$$T(p) = \frac{1}{f(p)} \begin{bmatrix} \sigma g(-p) & h(p) \\ \sigma h(-p) & g(p) \end{bmatrix}, \quad (5.3)$$

$$T_{12} = \frac{h(p)}{f(p)}, T_{11} = \frac{\sigma g(-p)}{f(p)}, T_{22} = \frac{g(p)}{f(p)}, T_{21} = \frac{\sigma h(-p)}{f(p)}. \quad (5.4)$$

The transfer scattering parameters are used to define networks containing only distributed elements are shown as [31]

$$T(\lambda) = \frac{1}{f(\lambda)} \begin{bmatrix} \sigma g(-\lambda) & h(\lambda) \\ \sigma h(-\lambda) & g(\lambda) \end{bmatrix}, \quad (5.6)$$

$$T_{12} = \frac{h(\lambda)}{f(\lambda)}, T_{11} = \frac{\sigma g(-\lambda)}{f(\lambda)}, T_{22} = \frac{g(\lambda)}{f(\lambda)}, T_{21} = \frac{\sigma h(-\lambda)}{f(\lambda)}. \quad (5.7)$$

Transfer scattering parameters are also defined with the same polynomials $g(p, \lambda)$, $h(p, \lambda)$ and $f(p, \lambda)$ like as scattering parameters in Section 4.

Lumped and distributed elements' values are calculated via transfer scattering parameters. Transfer scattering matrices for networks via mixed elements are defined as

$$T(p, \lambda) = T_e(p) T_{RN}(p, \lambda). \quad (5.8)$$

$T_e(p)$ define the transfer scattering matrix of the first lumped element in the network in equation (5.8). $g(p)$ and $h(p)$ polynomials can be defined according to the type of network and lumped element.

$$T(p,\lambda) = T_e(\lambda) T_{RN}(p, \lambda) \quad . \quad (5.9)$$

$T_e(\lambda)$ define the transfer scattering matrix of the first distributed component in the network via equation (5.9).

After calculating the value of the first lumped element from the current coefficient matrices of the network, the transfer scattering parameter of this lumped element $T_e(p)$ is extracted from the current transfer scattering matrix $T(p,\lambda)$. The remaining transfer scattering matrix can be calculated as

$$T(p,\lambda)T_e(p)^{-1} = T_{RN1}(p, \lambda) \quad . \quad (5.10)$$

Unit element value can be calculated according to coefficient matrices within the first remaining transfer scattering parameters. The second lumped element can be calculated after the second remaining transfer scattering parameter $T_{RN2}(p,\lambda)$ is calculated, after the extraction of the transfer scattering parameter of the unit element $T(\lambda)$ from the first remaining transfer scattering parameter $T_{RN1}(p,\lambda)$ and defined as

$$T_{RN1}(p, \lambda)T_e(\lambda)^{-1} = T_{RN2}(p, \lambda) \quad . \quad (5.11)$$

5.1 HPN via Series Capacitors Separated by UE

The network in Figure 5.1 has three series capacitors separated by unit elements that can be defined with two independent variables (p, λ) transfer scattering parameters as equation (5.1) [37]. The transfer scattering parameters define the networks with only lumped elements shown in equation (5.3-4). The transfer scattering parameters determine the networks which only contain distributed elements, as shown in equation (5.6-7).

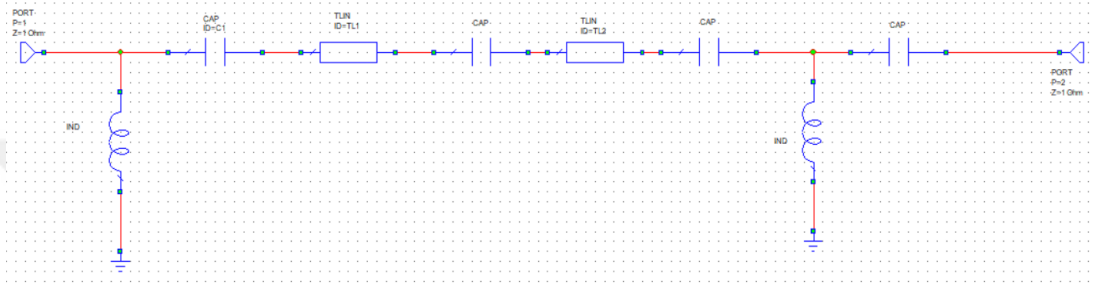


Figure 5.1 HPN via series capacitors separated by UE

The first element of the network is a series capacitor, so $\sigma = h_{0n_\lambda}/g_{0n_\lambda}$ is equal to one. n_λ determine the number of distributed elements in the network.

The value of the first capacitor can be calculated from coefficient matrices in equation (4.152-153) and defined as

$$C_1 = \frac{g_{1n_\lambda} - \sigma h_{1n_\lambda}}{g_{1n_\lambda} + \sigma h_{1n_\lambda}} \quad (5.11)$$

For calculation of the second component value, the coefficient matrices M_g^{RN1} and M_h^{RN1} are defined as

$$h_{x,y}^{RN1} = h_{x+1,y} + \frac{1}{2C_1} (h_{x+2,y} - g_{x+2,y}), \quad (5.12)$$

$$g_{x,y}^{RN1} = g_{x+1,y} + \frac{1}{2C_1} (h_{x+2,y} - g_{x+2,y}). \quad (5.13)$$

x values are $0, 1, \dots, (n_p-1)$. n_p is the number of lumped elements, and y values are $0, 1, \dots, n_\lambda$ in equations (5.12-13).

The second component is a unit element. The characteristic impedance of the unit element is calculated as

$$Z_1 = \frac{(g_{np,0} + g_{np,1} + \dots + g_{np,n\lambda}) + (h_{np,0} + h_{np,1} + \dots + h_{np,n\lambda})}{(g_{np,0} + g_{np,1} + \dots + g_{np,n\lambda}) - (h_{np,0} + h_{np,1} + \dots + h_{np,n\lambda})} . \quad (5.14)$$

The characteristic impedance can also be calculated using the study methods [40].

For calculation of the third component value, coefficient matrices M_g^{RN2} and M_h^{RN2} are defined as

$$h_{x,y}^{RN2} = h_{x,y}^{RN1} + \frac{1}{2Z_1} (h_{x,y-1}^{RN1} + g_{x,y-1}^{RN1}) + \frac{Z_1}{2} (h_{x,y-1}^{RN1} - g_{x,y-1}^{RN1}) , \quad (5.15)$$

$$g_{x,y}^{RN2} = g_{x,y}^{RN1} - \frac{1}{2Z_1} (h_{x,y-1}^{RN1} + g_{x,y-1}^{RN1}) + \frac{Z_1}{2} (h_{x,y-1}^{RN1} - g_{x,y-1}^{RN1}) , \quad (5.16)$$

x values are 0, 1, ..., (n_p-1). n_p is the number of lumped elements. y values are 0, 1, ..., n_λ - 1 in equations (5.15-16)

The second lumped element value is calculated as

$$C_2 = \frac{g_{1n\lambda-1} - \sigma h_{1n\lambda-1}}{g_{1n\lambda-1} + \sigma h_{1n\lambda-1}} . \quad (5.17)$$

Third and last remaining transfer scattering parameter can be calculated like the first remaining transfer scattering parameter calculation in equation (5.12-13). The last lumped element and distributed element can be calculated via the last remaining transfer scattering parameters

5.2 LPN via Shunt Capacitors Separated with UE

The calculation of capacitor values is defined in the study [35]. The network in Figure 5.2 has three shunt capacitors separated by unit elements that can be defined with two independent variables transfer scattering parameters in equation (5.1). Transfer scattering parameters are used to determine the network with only lumped elements shown in equation (5.3-4). Transfer scattering parameters are used to define the network that contains only distributed elements, as shown in equation (5.6-7).

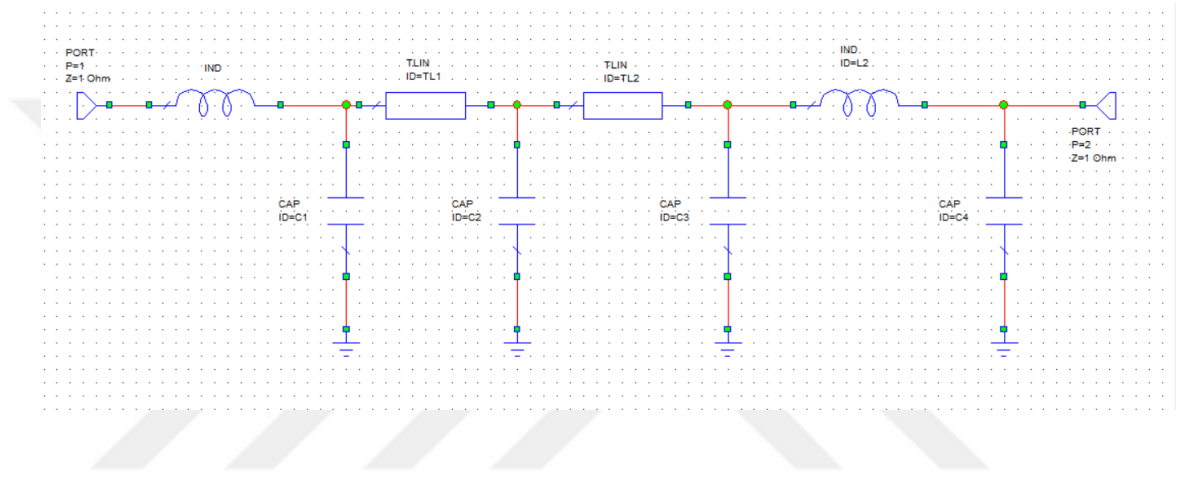


Figure 5.2 LPN via shunt capacitors separated by UE

The first element of the network is a shunt capacitor, so $\sigma = h_{n_p n_\lambda} / g_{n_p n_\lambda}$ is equal to -1. n_λ determines the number of distributed elements in the network. n_p determines the number of lumped elements in the network.

The value of the capacitor can be calculated as

$$C_1 = \frac{g_{n_p n_\lambda} + \sigma h_{n_p n_\lambda}}{g_{n_p-1, n_\lambda} - \sigma h_{n_p-1, n_\lambda}}. \quad (5.18)$$

For calculation of the second component value, the coefficient matrices M_g^{RN1} and M_h^{RN1} are defined as

$$h_{x,y}^{RN1} = h_{x,y} + \frac{C_1}{2} (h_{x-1,y} + g_{x-1,y}), \quad (5.19)$$

$$g_{x,y}^{RN1} = g_{x,y} - \frac{C_1}{2} (h_{x-1,y} + g_{x-1,y}). \quad (5.20)$$

x is equal to $0, 1, \dots, n_p-1$ and y is equal to $0, 1, \dots, n_\lambda$ in equations (5.19-20).

The second component is a unit element. The characteristic impedance of the unit element is calculated as

$$Z_1 = \frac{(g_{0,0} + g_{0,1} + \dots + g_{0,n\lambda}) + (h_{0,0} + h_{0,1} + \dots + h_{0,n\lambda})}{(g_{0,0} + g_{0,1} + \dots + g_{0,n\lambda}) - (h_{0,0} + h_{0,1} + \dots + h_{0,n\lambda})} . \quad (5.21)$$

After the characteristic impedance of the unit element is calculated, equations (5.15-16) are used to calculate the second remaining transfer scattering parameter. Then, the second lumped element value can be calculated.

The value of the second capacitor can be calculated as

$$C_2 = \frac{g_{n_{p-1},n_{\lambda-1}} + \sigma_2 h_{n_{p-1},n_{\lambda-1}}}{g_{n_{p-2},n_{\lambda-1}} - \sigma_2 h_{n_{p-2},n_{\lambda-1}}} , \quad (5.22)$$

$$\sigma_2 = \frac{g_{n_{p-1},n_{\lambda-1}}}{h_{n_{p-1},n_{\lambda-1}}} . \quad (5.23)$$

The third and last remaining transfer scattering parameter can be calculated as

$$h_{x,y}^{RN3} = h_{x,y} + \frac{C_2}{2} (h_{x-1,y} + g_{x-1,y}) , \quad (5.24)$$

$$g_{x,y}^{RN3} = g_{x,y} - \frac{C_2}{2} (h_{x-1,y} + g_{x-1,y}) . \quad (5.25)$$

x value is assigned with $0, 1, \dots, n_{p-2}$ and y value is assigned with $0, 1, \dots, n_{\lambda-2}$ in equations (5.24-25).

The last unit element value can be calculated as

$$Z_2 = \frac{(g_{0,0} + g_{0,1} + \dots + g_{0,n_{\lambda-1}}) + (h_{0,0} + h_{0,1} + \dots + h_{0,n_{\lambda-1}})}{(g_{0,0} + g_{0,1} + \dots + g_{0,n_{\lambda-1}}) - (h_{0,0} + h_{0,1} + \dots + h_{0,n_{\lambda-1}})} . \quad (5.26)$$

The total capacitor value can be calculated as

$$C_T = \frac{g_{n_{p-2},0} + \sigma_T h_{n_{p-2},0}}{g_{n_{p-3},0} - \sigma_T h_{n_{p-3},0}} . \quad (5.27)$$

$\sigma_T = h_{n_{p-2},0}/g_{n_{p-2},0}$ is equal to -1 in equation (5.27).

The last lumped element value can be calculated as

$$C_3 = C_T - C_1 - C_2 \quad . \quad (5.28)$$

5.3 HPN via Series Capacitors and Shunt Inductors Separated by UE

The network in Figure 5.3 has two capacitors and one inductor or two inductors, and one capacitor separated by unit elements defined with two independent variables transfer scattering parameters in equation (5.1). The transfer scattering parameters are used to determine the networks with only lumped elements shown in equation (5.3-4). The transfer scattering parameters are used to describe the networks with only distributed elements shown in equation (5.6-7).

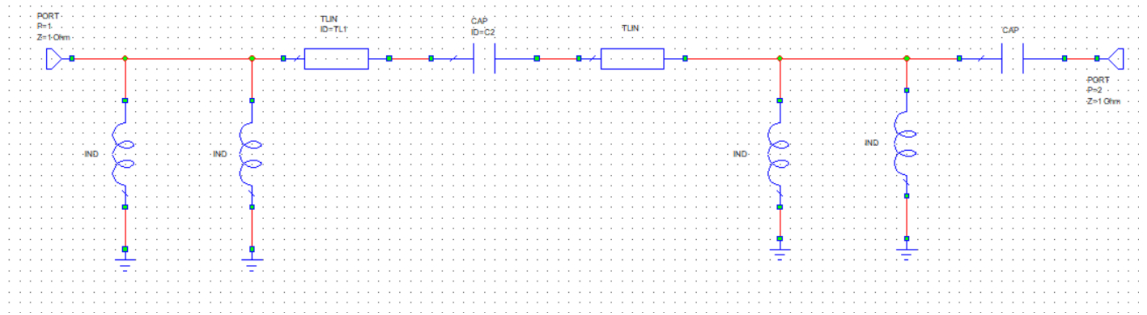


Figure 5.3 HPN via series capacitors and shunt inductors separated by UE

If the first element of the network is a series capacitor, $\sigma = h_{00}/g_{00}$ is equal to 1. If the first element of the network is a shunt inductor, $\sigma = h_{00}/g_{00}$ is equal to -1. n_λ represents the number of distributed elements in the networks. n_p represents the number of lumped elements in the networks.

The value of the first component can be calculated as

$$C_1 = \frac{g_{10} - \sigma h_{10}}{g_{00} + \sigma h_{00}} \quad . \quad (5.29)$$

If the first component is a series capacitor, the coefficient matrices M_g^{RN1} and M_h^{RN1} are defined as

$$h_{x,y}^{RN1} = h_{x+1,y} + \frac{1}{2C_1} (h_{x+2,y} - g_{x+2,y}) , \quad (5.30)$$

$$g_{x,y}^{RN1} = g_{x+1,y} + \frac{1}{2C_1} (h_{x+2,y} - g_{x+2,y}) . \quad (5.31)$$

x is $0,1,\dots,n_p-1$ and y is $0,1,\dots,n_\lambda$ in equations (5.30-31).

If the first component is a shunt inductor, the coefficient matrices M_g^{RN1} and M_h^{RN1} are defined as

$$h_{x,y}^{RN1} = h_{x+1,y} + \frac{1}{2L_1} (h_{x+2,y} + g_{x+2,y}) , \quad (5.32)$$

$$g_{x,y}^{RN1} = g_{x+1,y} - \frac{1}{2L_1} (h_{x+2,y} + g_{x+2,y}) . \quad (5.33)$$

x is $0,1,\dots,n_p-2$ and y is $0,1,\dots,n_\lambda-2$ in equations (5.32-33).

If the second component is a unit element, the characteristic impedance of the unit element is calculated as

$$Z_1 = \frac{(g_{np-1,0} + g_{np-1,1} + \dots + g_{np-1,n_\lambda}) + (h_{np-1,0} + h_{np-1,1} + \dots + h_{np-1,n_\lambda})}{(g_{np-1,0} + g_{np-1,1} + \dots + g_{np-1,n_\lambda}) - (h_{np-1,0} + h_{np-1,1} + \dots + h_{np-1,n_\lambda})} . \quad (5.34)$$

After the characteristic impedance of the unit element is calculated, equations (5.15-16) are used to calculate the second remaining transfer scattering parameter. Then, the second lumped element value can be calculated.

The value of the capacitor or inductor can be calculated as

$$C_2 = \frac{g_{10} - \sigma_2 h_{10}}{g_{00} + \sigma_2 h_{00}} , \quad (5.35)$$

$$\sigma_2 = \frac{g_{00}}{h_{00}} . \quad (5.36)$$

The third remaining transfer scattering matrices are calculated with equation (5.30-31) if the second lumped element is a series capacitor. The third remaining transfer scattering matrices are calculated with equations (5.32-33) if the second lumped element is a shunt inductor.

The fourth component is a unit element. The characteristic impedance of the unit element is calculated as

$$Z_2 = \frac{(g_{np-2,0} + g_{np-2,1} + \dots + g_{np-1,n\lambda}) + (h_{np-2,0} + h_{np-2,1} + \dots + h_{np-2,n\lambda})}{(g_{np-2,0} + g_{np-2,1} + \dots + g_{np-2,n\lambda}) - (h_{np-2,0} + h_{np-2,1} + \dots + h_{np-2,n\lambda})}. \quad (5.37)$$

The last lumped element is calculated as

$$C_3 = \frac{g_{10} - \sigma h_{10}}{g_{00} + \sigma h_{00}}, \quad (5.38)$$

$$\sigma_2 = \frac{g_{00}}{h_{00}}. \quad (5.39)$$

5.4 LPN via Shunt Capacitors and Series Inductors Separated by UE

The network in Figure 5.4 has two capacitors and one inductor or two inductors, and one capacitor separated by unit elements that can be defined with two independent variables transfer scattering parameters in equation (5.1). The transfer scattering parameters are used to define the networks with only lumped elements shown in equation (5.3-4). The transfer scattering parameters are used to define the networks with only distributed elements shown in equation (5.6-7).

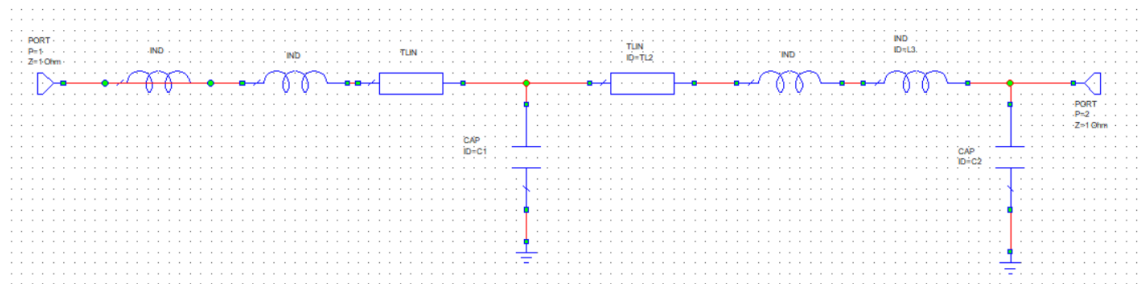


Figure 5.4 LPN via shunt capacitors and series inductors separated by UE

If the first element of the network is a series inductor, $\sigma = h_{n_p 0}/g_{n_p 0}$ is equal to 1. If the first element of the network is a shunt capacitor, $\sigma = h_{n_p 0}/g_{n_p 0}$ is equal to -1. n_λ defines the number of distributed elements in the network. n_p determines the number of lumped elements in the network.

The value of the capacitor or inductor can be calculated as

$$C_1 = \frac{g_{n_p 0} + \sigma h_{n_p 0}}{g_{n_p-1,0} - \sigma h_{n_p-1,0}} . \quad (5.40)$$

If the first component is a shunt capacitor, the coefficient matrices M_g^{RN1} and M_h^{RN1} are calculated as

$$h_{x,y}^{RN1} = h_{x,y} + \frac{C_1}{2} (h_{x-1,y} + g_{x-1,y}) , \quad (5.41)$$

$$g_{x,y}^{RN1} = g_{x,y} - \frac{C_1}{2} (h_{x-1,y} + g_{x-1,y}) . \quad (5.42)$$

x is $0, 1, \dots, n_p-1$ and y is $0, 1, \dots, n_\lambda$ in equations (5.41-42).

If the first component is a series inductor, the coefficient matrices M_g^{RN1} and M_h^{RN1} are calculated as

$$h_{x,y}^{RN1} = h_{x,y} + \frac{C_1}{2} (h_{x-1,y} - g_{x-1,y}) , \quad (5.43)$$

$$g_{x,y}^{RN1} = g_{x,y} + \frac{C_1}{2} (h_{x-1,y} - g_{x-1,y}) . \quad (5.44)$$

x is $0, 1, \dots, n_p-2$ and y is $0, 1, \dots, n_\lambda - 2$ in equations (5.43-44).

The second component is a unit element. The characteristic impedance of the unit element is calculated as

$$Z_1 = \frac{(g_{0,0} + g_{0,1} + \dots + g_{0,n_\lambda}) + (h_{0,0} + h_{0,1} + \dots + h_{0,n_\lambda})}{(g_{0,0} + g_{0,1} + \dots + g_{0,n_\lambda}) - (h_{0,0} + h_{0,1} + \dots + h_{0,n_\lambda})} . \quad (5.45)$$

After the characteristic impedance of unit element is calculated, equations (5.15-16) are used to calculate second remaining transfer scattering parameter. Then, the second lumped element value can be calculated.

The value of the capacitor or inductor can be calculated as

$$C_2 = \frac{g_{n_p-1,0} + \sigma_2 h_{n_p-1,0}}{g_{n_p-2,0} - \sigma_2 h_{n_p-2,0}}, \quad (5.46)$$

$$\sigma_2 = \frac{g_{n_p-1,0}}{h_{n_p-1,0}}. \quad (5.47)$$

The third remaining transfer scattering parameters are calculated with equation (5.41-42) if the second lumped element is a shunt capacitor. The third remaining transfer scattering matrices are calculated with equation (5.43-44) if the second lumped element is a series inductor.

The last distributed element value can be defined as

$$Z_2 = \frac{(g_{0,0} + g_{0,1} + \dots + g_{0,n\lambda-1}) + (h_{0,0} + h_{0,1} + \dots + h_{0,n\lambda-1})}{(g_{0,0} + g_{0,1} + \dots + g_{0,n\lambda-1}) - (h_{0,0} + h_{0,1} + \dots + h_{0,n\lambda-1})}. \quad (5.48)$$

The value of the capacitor or inductor can be calculated as

$$C_3 = \frac{g_{n_p-2,0} + \sigma_3 h_{n_p-2,0}}{g_{n_p-3,0} - \sigma_3 h_{n_p-3,0}}, \quad (5.49)$$

$$\sigma_3 = \frac{g_{n_p-2,0}}{h_{n_p-2,0}}. \quad (5.50)$$

6. OPTIMIZATION PROCESS

Optimization process is executed within MATLAB [45] to calculate accurate component values for a desired transducer power gain and phase response in networks. The nonlinear least square method is used for the optimization process. The algorithm in the method is Levenberg-Marquardt [16].

$$f(x) = \min[[F_1(x) + F_2(x) + \dots + F_d(x)]^2] . \quad (6.1)$$

In equation (6.1), $f(x)$ represents the total error that d is the number of the normalized frequency intervals defined at the beginning of the process. The error $F(x)$ is the difference between desired value (TPG) and the calculated one (TPG_C). The calculation process of TPG_C is described as

$$\text{TPG}_C = \frac{(1 - S_G)(1 - S_L)|f(p, \lambda)|}{|g(p, \lambda) - h(p, \lambda)S_G + \alpha S_L h(-p, -\lambda) - \alpha S_G g(-p, -\lambda)|^2} . \quad (6.2)$$

Reflection from generator impedance is defined as

$$S_G = \frac{Z_g - 1}{Z_g + 1} . \quad (6.3)$$

Reflection from load impedance is defined as

$$S_L = \frac{Z_L - 1}{Z_L + 1} . \quad (6.4)$$

Z_g and Z_L are impedance of generator and load impedance in equations (6.3-4), respectively. The total error of transducer power gain (TPG_{error}) can be shown as

$$TPG_{error} = \left[\sum_{k=1}^l (TPG - TPG_{C(k)})^2 \right] . \quad (6.5)$$

In equation (6.5), l is the maximum number of angular frequency intervals. The value of l is selected as 10 for high-pass and low-pass networks for only TPG optimization. TPG in the equation (6.5) is equal to 0.98, and $TPG_{C(k)}$ determines a matrix with one row and ten columns and represents the calculated value of TPG for each angular frequency value.

The total error of transducer power gain (TPG_{error}) and phase ($Phase_{error}$) are used in the optimization of transducer power gain and phase response in lossless two-port high / low pass network as phase shifters, respectively and are described as

$$TPG_{error} = \left[\sum_{k=1}^l (|f(p(k), \lambda(k))| - |g(p(k), \lambda(k))|)^2 \right] , \quad (6.6)$$

$$Phase_{error} = \sum_{k=1}^l \left(\frac{\Lambda}{2} - \angle g(p(k), \lambda(k)) \right)^2 . \quad (6.7)$$

The total error ($Total_error$) in design is calculated as

$$Total_error = TPG_{error} + Phase_{error} . \quad (6.8)$$

In equation (6.6-8), l is the maximum number of angular frequency values. The value of l are selected as 20 for the high-pass and low-pass networks in the optimization process.

$|f(p, \lambda)|$ and $|g(p, \lambda)|$ are matrices with one row and twenty columns showing the magnitude of $f(p, \lambda)$ and $g(p, \lambda)$ polynomials. The magnitude of $|g(p, \lambda)|$ should be equal to the magnitude of $|f(p, \lambda)|$ for the optimization process of TPG.

The restrictions are determined according to S_{21} , as seen in equation (4.7). S_{21} represents the power transformation rate from generator impedance to load impedance. $f(p, \lambda)$ polynomials are given in equations (4.5-6). Λ represents desired phase response. The low-pass network provides negative half, and the high-pass network compensates positive half of the phase response. The difference in phase responses of each network provides desired phase response.

For a low-pass network, the total error of transducer power gain is calculated as

$$TPG_{error} = \sum_{k=1}^1 \left((1 - \lambda(k)^2)^{\frac{n}{2}} - |g(p(k), \lambda(k))| \right)^2, \quad (6.9)$$

For a low-pass network, the total error of phase response is calculated as

$$Phase_{error} = \sum_{k=1}^1 \left(\frac{\Lambda}{2} - \angle g(p(k), \lambda(k)) \right)^2, \quad (6.10)$$

The total error (Total_error) in design is calculated as in equation (6.8). n represents the number of the unit element in equation (6.9).

For the high-pass network, equation (6.6) is changed as $f(p, \lambda)$ described in equations (4.44-48).

If there is only one lumped element in a high-pass network, $|f(p, \lambda)|$ is equal to $w(1-\lambda^2)^{n/2}$ in equation (6.11), and $\angle g(p, \lambda)$ (phase) should be equal to $90^\circ - \Lambda/2$ in equation (6.12). The total phase error and TPG in optimization are calculated as

$$TPG_{error} = \sum_{k=1}^1 \left(w(k)(1 - \lambda(k)^2)^{\frac{n}{2}} - |g(p(k), \lambda(k))| \right)^2, \quad (6.11)$$

$$Phase_{error} = \sum_{k=1}^1 \left(90^\circ - \frac{\Lambda}{2} - \angle g(p(k), \lambda(k)) \right)^2. \quad (6.12)$$

The total error (Total_error) in design is calculated as in equation (6.8). If there are two lumped elements in a high-pass network, $|f(p, \lambda)|$ is equal to $w^2(1-\lambda^2)^{n/2}$ in equation (6.13), and $\angle g(p, \lambda)$ should be equal to $180^\circ - \Lambda/2$ in equation (6.14). The total error of phase and TPG in optimization is written as

$$TPG_{error} = \sum_{k=1}^1 \left(w^2(k)(1 - \lambda(k)^2)^{\frac{n}{2}} - |g(p(k), \lambda(k))| \right)^2, \quad (6.13)$$

$$Phase_{error} = \sum_{k=1}^1 \left(180^\circ - \frac{\Lambda}{2} - \angle g(p(k), \lambda(k)) \right)^2, \quad (6.14)$$

The total error (Total_error) in design is calculated as in equation (6.8). If there are three lumped elements in a high-pass network, $|f(p, \lambda)|$ is equal to $w^3(1-\lambda^2)^{n/2}$ in equation (6.15) and $\angle g(p, \lambda)$ should be equal to $-90^\circ - \Lambda/2$ in equation (6.16). The total error of phase and TPG in optimization is written as

$$TPG_{error} = \sum_{k=1}^1 \left(w^3(k)(1 - \lambda(k)^2)^{\frac{n}{2}} - |g(p(k), \lambda(k))| \right)^2, \quad (6.15)$$

$$Phase_{error} = \sum_{k=1}^1 \left(-90^\circ - \frac{\Lambda}{2} - \angle g(p(k), \lambda(k)) \right)^2, \quad (6.16)$$

The total error (Total_error) in design is calculated as in equation (6.8).

The command line in MATLAB represents as

$$Y = \text{lsqnonlin}(\text{func}, v, \text{lowb}, \text{upperb}, \text{options}) \quad (6.17)$$

In equation (6.17), func is a function of the optimization process used to calculate the independent coefficients of M_h . v matrix contains the independent coefficients of M_h and transmission line delay of the unit element. lowb and upperb are the lower bound and upper bound of these values in Y matrix that can be between negative and positive infinity. The optimization options are Max Iteration, Max Function Evaluation, Step Tolerance, and Function Tolerance [47].

Step 1

Values of independent coefficients of $h(p,\lambda)$ and transmission delay of the unit elements are assigned randomly between 0 and 1, and the non-linear least square method options are determined in Matlab.

Step 2

Independent variables of $g(p,0)$ and $g(0,\lambda)$ are calculated via equations (3.33) and (3.34), respectively. Later, other dependent coefficient variables are calculated.

Step 3

Transducer power gain is calculated via equations (6.2-4). The total error of transducer power gain at each frequency value is calculated via equations (6.5) for the high-pass and low-pass networks.

For the phase optimization process, the total error at each angular frequency value is calculated via equations (6.11) for the low-pass networks. The total error is calculated via equations (6.12-20) for the high-pass networks.

If the differences between the next calculated error and the current one are less than the designated total error in Matlab options (Function Tolerance) or the difference between the current variables and the next calculated ones in v matrix is less than designated ones in Matlab options (Step Tolerance), the optimization process is ended. Then, the process continues with Step 5. Otherwise, continue with Step 4.

Step 4

If differences in both conditions are not less than the designated ones in Matlab options (Step or Function Tolerance), independent variables and time delay are calculated with the help of the Levenberg- Marquardt algorithm, and the process return to step 2. The process won't return to step 2, if the iteration number in Matlab exceeds the maximum function evaluation number defined in Matlab options in Step 1. The optimization process is ended with an overdraft of the maximum function evaluation number, and the process continues with Step 5.

Step 5

According to optimization values of the independent coefficients of $h(p, \lambda)$ and the time delay of the unit elements, the independent variables of $g(p, 0)$ and $g(0, \lambda)$ are calculated via equations (3.33) and (3.34), respectively. Later, other dependent coefficient variables are calculated.

After calculating $g(p, \lambda)$ and $h(p, \lambda)$ coefficients, the value of lumped and distributed components are calculated.

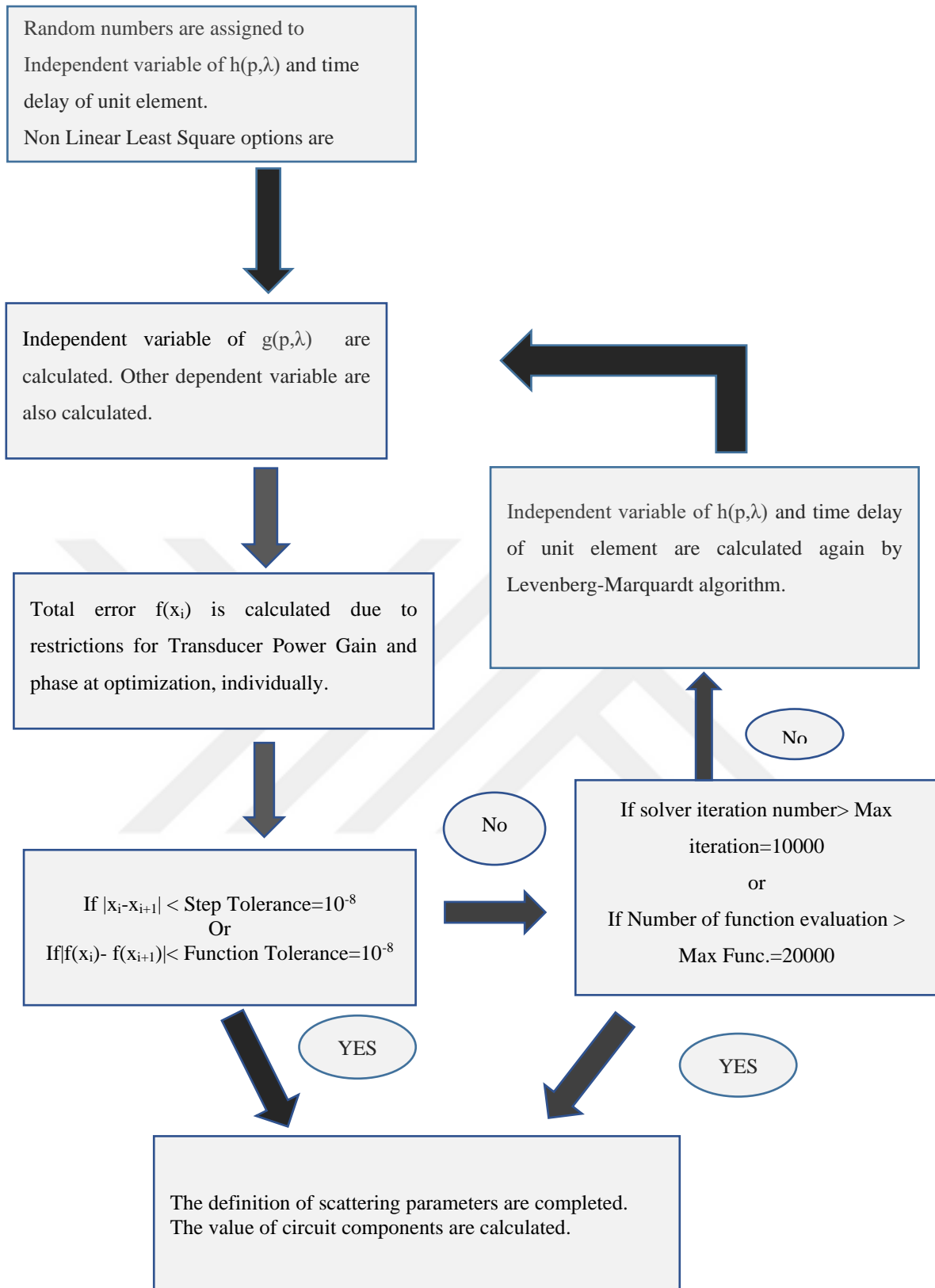


Figure 6.1 The calculation process of circuit component values

7. HIGH-PASS AND LOW-PASS NETWORKS

There are four different types of networks described in this Section. All the low-pass circuits have three parts. The first part has a resistance, and a series inductor called generated impedance. The second part has a network via shunt capacitors separated by unit elements or series inductors and shunt capacitors separated by unit elements. The last part is the load impedance which contains a series inductor, shunt capacitor, and shunt resistance.

All high pass circuits have three parts. The first part has resistance with a shunt inductor called generated impedance. The second part is a network via series capacitors separated by unit elements or shunt inductors and series capacitors separated by unit elements. The last part is the load impedance which contains a shunt inductor with a series capacitor and resistance.

7.1 HPN via Series Capacitors Separated by UE

In Figure 7.1, the circuit has three lumped and two-unit elements. The normalized generated impedance has a series resistance (1Ω) and a shunt inductor ($1H$). The normalized load impedance has a shunt inductor ($1H$), a series capacitor ($2F$), and series resistance (1Ω).

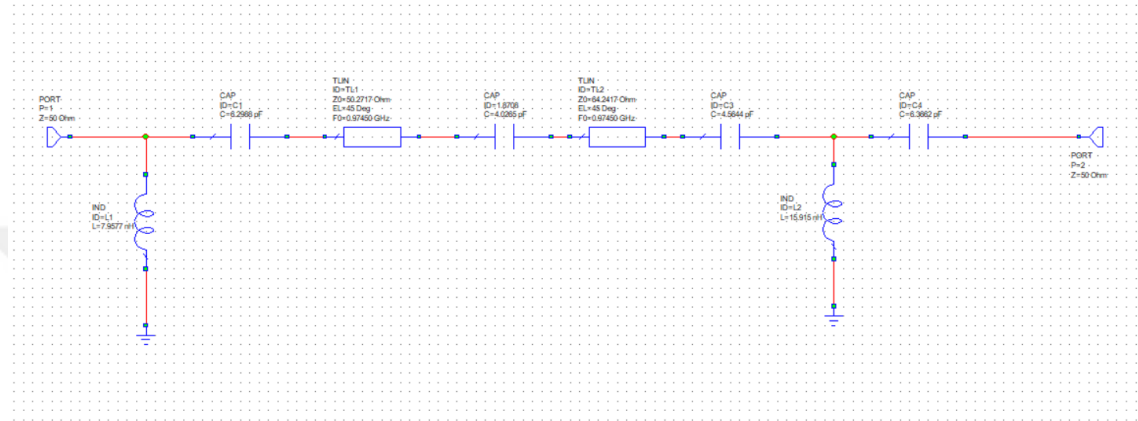


Figure 7.1 Synthesis of HPN via series capacitor separated by UE

The scattering parameters in equations (3.26-3.27) are defined with two independent variables (p, λ) g, h, f polynomials as shown in equations (3.32-35).

Random variables are assigned to independent coefficients of $h(p, \lambda)$ and transmission delay of the unit element. These values are optimized with the Non-Linear Least Square method in Matlab. Constant values are $h_{30}=0$ and $g_{30}=1$.

The normalized angular frequency (ωH) values are between one and two, with 0.1 intervals used in the optimization process. ωH is written as

$$\omega H = 1:0.1:2 .$$

v matrix represents randomly assigned independent coefficients and transmission delay of unit element and written as

$$v = [0.7513 \ 0.2558 \ 0.5060 \ 0.6991 \ 0.5909 \ 0.9593] .$$

With v matrix, the independent coefficients of $g(p, \lambda)$ (last column- $g_{02}, g_{12}, g_{22}, g_{32}$) are calculated via equations (3.33) for lumped elements and via equation (3.34) for unit element (last row- g_{32}, g_{31}, g_{30}). Roots of $g(p)$ and $g(\lambda)$ polynomials are chosen in left half plane because these polynomials are Hurwitz.

After this calculation, dependent coefficients in matrices of $g(p, \lambda)$ and $h(p, \lambda)$ polynomials are calculated with equation (4.154-162). Scattering parameters are used to calculate transducer power gain with equations (6.2-4).

The optimization process is executed as described in steps in Section 6 to get satisfactory results as

$$Y = [-0.2477 \ 0.1850 \ -0.0182 \ 0.1 \ 0.2587 \ 0.8059] .$$

Y matrix contains independent coefficients of $h(p, \lambda)$ and transmission delay of the unit element, respectively. The transmission delay value of the unit element is 0.8059. The equations (3.33-3.34) are used to calculate the independent coefficients of $g(p, \lambda)$ ($g_{02}, g_{12}, g_{22}, g_{32}, g_{31}, g_{30}$).

The coefficient matrices of $g(p, \lambda)$ and $h(p, \lambda)$ are written as

$$M_h = \begin{bmatrix} 0 & 0 & 0.1 \\ 0 & 0.6839 & -0.0182 \\ 0.9966 & -0.1913 & 0.1850 \\ 0 & 0.2587 & -0.2477 \end{bmatrix} ,$$

$$M_g = \begin{bmatrix} 0 & 0 & 0.1 \\ 0 & 0.6839 & 0.3776 \\ 0.9966 & 1.7669 & 0.8962 \\ 1 & 2.0316 & 1.0302 \end{bmatrix} .$$

Via equation (3.35), $f(p, \lambda)$ is defined as

$$f(p, \lambda) = p^3(1 - \lambda^2)^{\frac{2}{2}} .$$

The values of lumped elements and distributed elements are calculated via equations in Subsection 5.1.

The first component is a capacitor in Figure 7.1, and the value of the capacitor can be calculated as

$$C_1 = \frac{g_{12} - \sigma h_{12}}{g_{02} + \sigma h_{02}} = \frac{0.3776 - 1 * (-0.0182)}{0.1 + 1 * 0.1} = 1.9768 ,$$

$$\sigma = \frac{g_{02}}{h_{02}} = 1 .$$

The second component in the network is calculated with coefficient matrices in the first remaining transfer scattering parameters. For the second component value calculation, the coefficient of the matrix M_g^{RN1} and M_h^{RN1} of the first remaining transfer scattering parameters are calculated via equations (5.12-13)

$$h_{0,0}^{RN1} = h_{0+1,0} + \frac{1}{2 * C_1} (h_{0+2,0} - g_{0+2,0}) = 0 + \frac{1}{2 * 1.9768} (0.9966 - 0.9966) = 0 ,$$

$$h_{1,0}^{RN1} = h_{1+1,0} + \frac{1}{2 * C_1} (h_{1+2,0} - g_{1+2,0}) = 0.9966 + \frac{1}{2 * 1.9768} (0 - 1) = 0.7178 ,$$

$$h_{2,0}^{RN1} = h_{2+1,0} + \frac{1}{2 * C_1} (h_{2+2,0} - g_{2+2,0}) = 0 + \frac{1}{2 * 1.9768} (0 - 0) = 0 ,$$

$$h_{0,1}^{RN1} = h_{0+1,1} + \frac{1}{2 * C_1} (h_{0+2,1} - g_{0+2,1})$$

$$= 0.6839 + \frac{1}{2 * 1.9768} (-0.1913 - 1.7669) = 0.1390 ,$$

$$h_{1,1}^{RN1} = h_{1+1,1} + \frac{1}{2 * C_1} (h_{1+2,1} - g_{1+2,1}) = -0.1913 + \frac{1}{2 * 1.9768} (0.2587 - 2.0316)$$

$$= -0.6846 ,$$

$$h_{2,1}^{RN1} = h_{2+1,1} + \frac{1}{2 * C_1} (h_{2+2,1} - g_{2+2,1}) = 0.2587 + \frac{1}{2 * 1.9768} (0 - 0) = 0.2587 ,$$

$$h_{0,2}^{RN1} = h_{0+1,2} + \frac{1}{2 * C_1} (h_{0+2,2} - g_{0+2,2})$$

$$= -0.0182 + \frac{1}{2 * 1.9768} (0.1850 - 0.8962) = 0.0986 ,$$

$$h_{1,2}^{RN1} = h_{1+1,2} + \frac{1}{2 * C_1} (h_{1+2,2} - g_{1+2,2}) = 0.1850 + \frac{1}{2 * 1.9768} (-0.2477 - 1.0302)$$

$$= 0.8294 ,$$

$$\begin{aligned} h_{2,2}^{RN1} &= h_{2+1,2} + \frac{1}{2 * C_1} (h_{2+2,2} - g_{2+2,2}) = -0.2477 + \frac{1}{2 * 1.9768} (0 - 0) \\ &= -0.2477 , \end{aligned}$$

$$\begin{aligned} g_{0,0}^{RN1} &= g_{0+1,0} + \frac{1}{2 * C_1} (h_{0+2,0} - g_{0+2,0}) = 0 + \frac{1}{2 * 1.9768} (0.9966 - 0.9966) \\ &= 0 , \end{aligned}$$

$$\begin{aligned} g_{1,0}^{RN1} &= g_{1+1,0} + \frac{1}{2 * C_1} (h_{1+2,0} - g_{1+2,0}) = 0.9966 + \frac{1}{2 * 1.9768} (0 - 1) \\ &= 0.7178 , \end{aligned}$$

$$\begin{aligned} g_{2,0}^{RN1} &= g_{2+1,0} + \frac{1}{2 * C_1} (h_{2+2,0} - g_{2+2,0}) = 1 + \frac{1}{2 * 1.9768} (0 - 0) \\ &= 1 , \end{aligned}$$

$$\begin{aligned} g_{0,1}^{RN1} &= g_{0+1,1} + \frac{1}{2 * C_1} (h_{0+2,1} - g_{0+2,1}) \\ &= 0.6839 + \frac{1}{2 * 1.9768} (-0.1913 - 1.7669) = 0.139 , \end{aligned}$$

$$\begin{aligned} g_{1,1}^{RN1} &= g_{1+1,1} + \frac{1}{2 * C_1} (h_{1+2,1} - g_{1+2,1}) = 1.7669 + \frac{1}{2 * 1.9768} (0.2587 - 2.0316) \\ &= 1.2736 , \end{aligned}$$

$$g_{2,1}^{RN1} = g_{2+1,1} + \frac{1}{2 * C_1} (h_{2+2,1} - g_{2+2,1}) = 2.0316 + \frac{1}{2 * 1.9768} (0 - 0) = 2.0316 ,$$

$$\begin{aligned} g_{0,2}^{RN1} &= g_{0+1,2} + \frac{1}{2 * C_1} (h_{0+2,2} - g_{0+2,2}) = 0.6839 + \frac{1}{2 * 1.9768} (0.1850 - 0.8962) \\ &= 0.4580 , \end{aligned}$$

$$\begin{aligned} g_{1,2}^{RN1} &= g_{1+1,2} + \frac{1}{2 * C_1} (h_{1+2,2} - g_{1+2,2}) \\ &= 0.8962 + \frac{1}{2 * 1.9768} (-0.2472 - 1.0302) = 0.5406 , \end{aligned}$$

$$g_{2,2}^{RN1} = g_{2+1,2} + \frac{1}{2 * C_1} (h_{2+2,2} - g_{2+2,2}) = 1.0302 + \frac{1}{2 * 1.9768} (0 - 0) = 1.0302 ,$$

$$M_g^{RN1} = \begin{bmatrix} 0 & g_{01} & g_{02} \\ g_{10} & g_{11} & g_{12} \\ 1 & g_{21} & g_{22} \end{bmatrix} = \begin{bmatrix} 0 & 0.1390 & 0.4580 \\ 0.7178 & 1.2736 & 0.5406 \\ 1 & 2.0316 & 1.0302 \end{bmatrix} ,$$

$$M_h^{RN1} = \begin{bmatrix} 0 & h_{01} & h_{02} \\ h_{10} & h_{11} & h_{12} \\ 0 & h_{21} & h_{22} \end{bmatrix} = \begin{bmatrix} 0 & 0.1390 & 0.0986 \\ 0.7184 & -0.6846 & 0.8294 \\ 0 & 0.2587 & -0.2477 \end{bmatrix} .$$

The second component is a unit element. The characteristic impedance of first unit element is calculated as

$$\begin{aligned} Z_1 &= \frac{(g_{20} + g_{21} + g_{22}) + (h_{20} + h_{21} + h_{22})}{(g_{20} + g_{21} + g_{22}) - (h_{20} + h_{21} + h_{22})} \\ &= \frac{(1 + 2.0316 + 1.0302) + (0 + 0.2587 - 0.2477)}{(1 + 2.0316 + 1.0302) - (0 + 0.2587 - 0.2477)} \\ &= 1.0054 \text{ ,} \end{aligned}$$

For the third component value calculation, the matrix coefficients M_g^{RN2} and M_h^{RN2} are calculated via equations (5.15-16) and calculated as

$$\begin{aligned} h_{0,0}^{RN2} &= h_{0,0}^{RN1} + \frac{1}{2Z_1}(h_{0,0-1}^{RN1} + g_{0,0-1}^{RN1}) + \frac{Z_1}{2}(h_{0,0-1}^{RN1} - g_{0,0-1}^{RN1}) \\ &= 0 + \frac{1}{2 * 1.0054}(0 + 0) + \frac{1.0054}{2}(0 - 0) = 0 \text{ ,} \\ h_{10}^{RN2} &= h_{10}^{RN1} + \frac{1}{2Z_1}(h_{1,0-1}^{RN1} + g_{1,0-1}^{RN1}) + \frac{Z_1}{2}(h_{1,0-1}^{RN1} - g_{1,0-1}^{RN1}) \\ &= 0.7184 + \frac{1}{2 * 1.0054}(0 + 0) + \frac{1.0054}{2}(0 - 0) = 0.7184 \text{ ,} \\ h_{20}^{RN2} &= h_{20}^{RN1} + \frac{1}{2Z_1}(h_{2,0-1}^{RN1} + g_{2,0-1}^{RN1}) + \frac{Z_1}{2}(h_{2,0-1}^{RN1} - g_{2,0-1}^{RN1}) \\ &= 0 + \frac{1}{2 * 1.0054}(0 + 0) + \frac{1.0054}{2}(0 - 0) = 0 \text{ ,} \\ h_{0,1}^{RN2} &= h_{0,1}^{RN1} + \frac{1}{2Z_1}(h_{0,1-1}^{RN1} + g_{0,1-1}^{RN1}) + \frac{Z_1}{2}(h_{0,1-1}^{RN1} - g_{0,1-1}^{RN1}) \\ &= 0.1390 + \frac{1}{2 * 1.0054}(0 + 0) + \frac{1.0054}{2}(0 - 0) = 0.1390 \text{ ,} \\ h_{11}^{RN2} &= h_{11}^{RN1} + \frac{1}{2Z_1}(h_{1,1-1}^{RN1} + g_{1,1-1}^{RN1}) + \frac{Z_1}{2}(h_{1,1-1}^{RN1} - g_{1,1-1}^{RN1}) \\ &= -0.6846 + \frac{1}{2 * 1.0054}(0.7184 + 0.7178) + \frac{1.0054}{2}(0.7184 - 0.7178) \\ &= 0.0299 \text{ ,} \\ h_{21}^{RN2} &= h_{21}^{RN1} + \frac{1}{2Z_1}(h_{2,1-1}^{RN1} + g_{2,1-1}^{RN1}) + \frac{Z_1}{2}(h_{2,1-1}^{RN1} - g_{2,1-1}^{RN1}) \\ &= 2.0316 + \frac{1}{2 * 1.0054}(0 + 1) + \frac{1.0054}{2}(0 - 1) = 0.2533 \text{ ,} \\ g_{0,0}^{RN2} &= g_{0,0}^{RN1} - \frac{1}{2Z_1}(h_{0,0-1}^{RN1} + g_{0,0-1}^{RN1}) + \frac{Z_1}{2}(h_{0,0-1}^{RN1} - g_{0,0-1}^{RN1}) \\ &= 0 - \frac{1}{2 * 1.0054}(0 + 0) + \frac{1.0054}{2}(0 - 0) = 0 \text{ ,} \end{aligned}$$

$$\begin{aligned}
g_{1,0}^{RN2} &= g_{1,0}^{RN1} - \frac{1}{2Z_1}(h_{1,0-1}^{RN1} + g_{1,0-1}^{RN1}) + \frac{Z_1}{2}(h_{1,0-1}^{RN1} - g_{1,0-1}^{RN1}) \\
&= 0.7178 - \frac{1}{2 * 1.0054}(0 + 0) + \frac{1.0054}{2}(0 - 0) = 0.7178 , \\
g_{2,0}^{RN2} &= g_{2,0}^{RN1} - \frac{1}{2Z_1}(h_{2,0-1}^{RN1} + g_{2,0-1}^{RN1}) + \frac{Z_1}{2}(h_{2,0-1}^{RN1} - g_{2,0-1}^{RN1}) \\
&= 1 - \frac{1}{2 * 1.0054}(0 + 0) + \frac{1.0054}{2}(0 - 0) = 1 , \\
g_{0,1}^{RN2} &= g_{0,1}^{RN1} - \frac{1}{2Z_1}(h_{0,1-1}^{RN1} + g_{0,1-1}^{RN1}) + \frac{Z_1}{2}(h_{0,1-1}^{RN1} - g_{0,1-1}^{RN1}) \\
&= 0.1390 - \frac{1}{2 * 1.0054}(0 + 0) + \frac{1.0054}{2}(0 - 0) = 0.1390 , \\
g_{1,1}^{RN2} &= g_{1,1}^{RN1} - \frac{1}{2Z_1}(h_{1,1-1}^{RN1} + g_{1,1-1}^{RN1}) + \frac{Z_1}{2}(h_{1,1-1}^{RN1} - g_{1,1-1}^{RN1}) \\
&= 1.2736 - \frac{1}{2 * 1.0054}(0.7184 + 0.7178) + \frac{1.0054}{2}(0.7184 - 0.7178) = 0.5597 , \\
g_{2,1}^{RN2} &= g_{2,1}^{RN1} - \frac{1}{2Z_1}(h_{2,1-1}^{RN1} + g_{2,1-1}^{RN1}) + \frac{Z_1}{2}(h_{2,1-1}^{RN1} - g_{2,1-1}^{RN1}) \\
&= 2.0316 - \frac{1}{2 * 1.0054}(0 + 1) + \frac{1.0054}{2}(0 - 1) = 1.0316 , \\
M_g^{RN2} &= \begin{bmatrix} 0 & g_{01} \\ g_{10} & g_{11} \\ 1 & g_{21} \end{bmatrix} = \begin{bmatrix} 0 & 0.1390 \\ 0.7178 & 0.5597 \\ 1 & 1.0316 \end{bmatrix} , \\
M_h^{RN2} &= \begin{bmatrix} 0 & h_{01} \\ h_{10} & h_{11} \\ 1 & h_{21} \end{bmatrix} = \begin{bmatrix} 0 & 0.1390 \\ 0.7184 & 0.0299 \\ 0 & 0.2533 \end{bmatrix} .
\end{aligned}$$

The second lumped element is calculated via the coefficient matrices M_g^{RN2} and M_h^{RN2} at the second remaining transfer scattering parameters and calculated as

$$\begin{aligned}
C_2 &= \frac{g_{11} - \sigma_2 h_{11}}{g_{01} + \sigma_2 h_{01}} = \frac{0.5597 - (1)(0.0299)}{0.1390 + (1)(0.1390)} = 1.2649 , \\
\sigma_2 &= \frac{g_{01}}{h_{01}} = 1 .
\end{aligned}$$

The calculation of the total capacitor value in network is as follows

$$\begin{aligned}
C_T &= \frac{g_{30} - \sigma_4 h_{30}}{g_{20} + \sigma_4 h_{20}} = \frac{1 - (1) * 0}{0.9966 + (1)(0.9966)} = 0.5017 , \\
\sigma_4 &= \frac{g_{20}}{h_{20}} = 1 .
\end{aligned}$$

The characteristic impedance of last unit element is calculated as

$$Z_2 = \frac{(g_{20} + g_{21}) + (h_{20} + h_{21})}{(g_{20} + g_{21}) - (h_{20} + h_{21})} = \frac{(1 + 1.0316) + (0 + 0.2533)}{(1 + 1.0316) - (0 + 0.2533)} = 1.2848 .$$

The third lumped element value is calculated as

$$\frac{1}{C_T} = \frac{1}{C_1} + \frac{1}{C_2} + \frac{1}{C_3} ,$$

$$\frac{1}{0.5017} = \frac{1}{1.9768} + \frac{1}{1.2649} + \frac{1}{C_3} ,$$

$$C_3 = 1.4340 .$$

The normalized lumped and unit element values are $C_1=1.9768$, $C_2=1.2649$, $C_3=1.4340$, and $Z_1=1.0054$, $Z_2=1.1848$, respectively. Denormalization frequency is $f_{\text{norm}}=1$ GHz, and denormalization resistance is $R_{\text{norm}}=50\Omega$.

Denormalized capacitor (C_{nb}) values are calculated as

$$C_{nb} = \frac{C}{2 * \pi * f_{\text{norm}} * R_{\text{norm}}} . \quad (7.1)$$

Denormalized capacitors values (C_{nb}) are calculated as with equation (7.1)

$$C_{n1} = \frac{C_1}{2 * \pi * 10^9 * 50} = \frac{1.9768}{2 * \pi * 10^9 * 50} = 6.1988\text{pF} ,$$

$$C_{n2} = \frac{C_2}{2 * \pi * 10^9 * 50} = \frac{1.2649}{2 * \pi * 10^9 * 50} = 4.0265 \text{ pF} ,$$

$$C_{n3} = \frac{C_3}{2 * \pi * 10^9 * 50} = \frac{1.4340}{2 * \pi * 10^9 * 50} = 4.5644\text{pF} .$$

b represents the order of the denormalized capacitor values in the network in equation (7.1).

Denormalized inductor (L_n) value is calculated as

$$L_n = \frac{L * R_{\text{norm}}}{2 * \pi * f_{\text{norm}}} . \quad (7.2)$$

Denormalized inductor value in generator impedance is calculated as

$$L_{ng} = \frac{L * R_{norm}}{2 * \pi * f_{norm}} = \frac{1 * 50}{2 * \pi * 10^9} = 7.9577 \text{ nH} .$$

Denormalized inductor value in load impedance is calculated as

$$L_{nL} = \frac{L * R_{norm}}{2 * \pi * f_{norm}} = \frac{2 * 50}{2 * \pi * 10^9} = 15.915 \text{ nH} .$$

Denormalized capacitor value in load impedance is calculated as

$$C_{nL} = \frac{C}{2 * \pi * 10^9 * 50} = \frac{2}{2 * \pi * 10^9 * 50} = 6.3662 \text{ pF} .$$

Denormalization resistance and denormalized characteristics impedance of unit element (Z_n) is calculated as

$$Z_n = Z * R_{norm} . \quad (7.3)$$

Denormalization resistance (Z_{ng}) in generator impedance is calculated as

$$Z_{ng} = Z * R_{norm} = 1 * 50 = 50 \Omega .$$

Denormalization resistance (Z_{nL}) in load impedance is calculated as

$$Z_{nL} = Z * R_{norm} = 1 * 50 = 50 \Omega .$$

Denormalization characteristic impedance of first unit element (Z_{u1}) and second unit element (Z_{u2}) in the network are calculated as

$$Z_{u1} = Z_1 * R_{norm} = 1.0054 * 50 = 50.2717 \Omega ,$$

$$Z_{u2} = Z_2 * R_{norm} = 1.2848 * 50 = 64.2417 \Omega .$$

The simulation with these denormalization values is executed in Microwave Office Tool. TLIN is used for unit elements in Microwave Office Tool. Electrical length is 45° in TLIN.

As seen in Figure 7.1, the circuit is simulated in Microwave Office Tool [50]. The response of transducer power gain from the generator to load impedance is presented in Figure 7.2, which is 0.98 at 1 GHz.

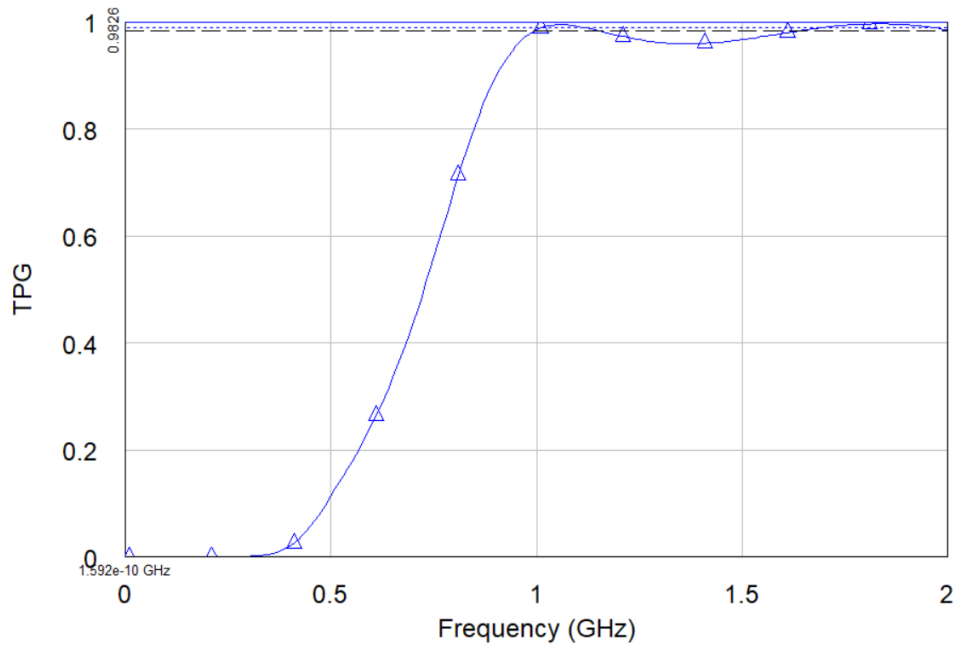


Figure 7.2 TPG response of HPN via series capacitors separated by UE

7.2 LPN via Shunt Capacitors Separated by UE

In Figure 7.3, the circuit has three lumped elements and two-unit elements. The normalized generated impedance has a resistance (1Ω) and series inductor ($1H$). The normalized load impedance has a series inductor ($2H$), a shunt capacitor ($1F$), and shunt resistance (1Ω).

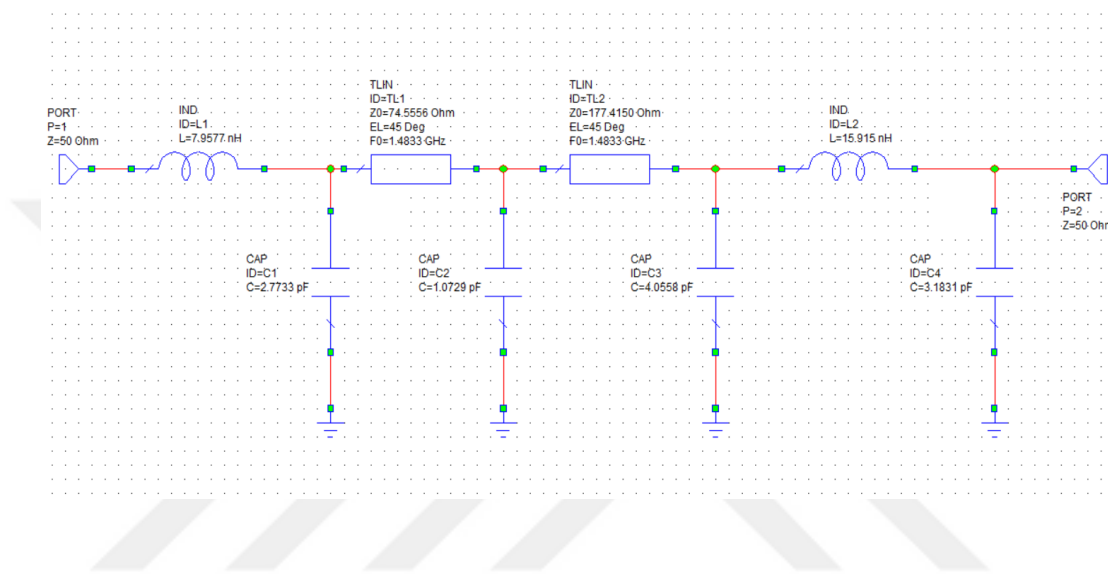


Figure 7.3 Synthesis of LPN via shunt capacitors separated by UE

The scattering parameters in equations (3.26-3.27) are defined with two independent variables (p, λ) g, h, f polynomials as shown in equations (3.32-35).

Random variables are assigned to independent coefficients ($h_{02}, h_{12}, h_{22}, h_{32}, h_{01}$) of $h(p, \lambda)$ and transmission delay of the unit element. These values are optimized with Non-Linear Least Square method in Matlab. Constant values are $h_{00}=0$ and $g_{00}=1$.

The values of normalized angular frequency (WL) values are from zero to one with 0.1 intervals used in the optimization process and written as

$$WL=0:0.1:1 .$$

Values in v matrix are assigned with random variables between 0 and 1 that the values are the independent coefficients of $h(p,\lambda)$ and transmission delay of the unit element, respectively. The values in v matrix are written as

$$v=[0.8147 \ 0.9058 \ 0.1270 \ 0.9134 \ 0.6324 \ 0.0975] .$$

With these parameters, the independent coefficient variables of $g(p, \lambda)$ ($g_{02}, g_{12}, g_{22}, g_{32}, g_{01}$) are calculated via equations (3.33) for lumped elements (last column- $g_{02}, g_{12}, g_{22}, g_{32}$) and via equation (3.34) for unit element(first row- g_{02}, g_{01}, g_{00}). Roots of $g(p)$ and $g(\lambda)$ polynomials are chosen in left half plane because the polynomials are strictly Hurwitz.

The optimization process is executed as described in Figure 6.1 to get optimized results as

$$Y=[-0.9899 \ 0.3593 \ -0.8074 \ -0.9797 \ 2.0435 \ 0.5295] .$$

Y matrix contains optimization results of independent coefficients of $h(p,\lambda)$ and transmission delay of the unit element, respectively The transmission delay value of the unit element is 0.5295. The equations (3.33-3.34) are used to calculate the independent coefficients of $g(p,\lambda)$ ($g_{02}, g_{12}, g_{22}, g_{32}, g_{01}$).

After this calculation, dependent variables in coefficient matrices of $g(p,\lambda)$ and $h(p,\lambda)$ are calculated with equation (4.115-123). Scattering parameters are used to calculate transducer power gain with equations (6.2-4).

The coefficient matrices of $g(p, \lambda)$ and $h(p, \lambda)$ are written as

$$M_h = \begin{bmatrix} 0 & 2.0435 & -0.9797 \\ -1.2413 & 0.6685 & -0.8074 \\ 0 & -3.7782 & 0.3593 \\ 0 & 0 & -0.9899 \end{bmatrix} ,$$

$$M_g = \begin{bmatrix} 1 & 2.9959 & 1.3999 \\ 1.2413 & 6.2552 & 2.5908 \\ 0 & 3.7782 & 1.9131 \\ 0 & 0 & 0.9899 \end{bmatrix} .$$

Normalized lumped and distributed elements values are calculated as described in Subsection 5.2. The component values are $C_1=0.8713$, $C_2=0.3371$, $C_3=1.2742$, $Z_1=1.4911$, $Z_2=3.5483$. The normalized frequency of the unit element in Microwave Office Tool is 0.2361.

Denormalized lumped element values at 1 GHz are calculated via equation (7.1). Denormalized distributed element values are calculated via equation (7.3). Denormalized lumped and unit element values are $C_1=2.7733$ pF, $C_2=1.0729$ pF, $C_3=4.0558$ pF and $Z_1=74.5556\Omega$, $Z_2=177.4150\Omega$, respectively. Denormalization resistance and denormalized lumped element values at generator impedance are $Z=50\Omega$, $L=7.9577$ nH via equation (7.2). Denormalization resistance and denormalized lumped elements values in load impedance are $Z=50\Omega$, $L=15.915$ nH via equation (7.2), and $C=3.1831$ pF.

The simulation is executed with denormalization component values as seen in Figure 7.3 with Microwave Office Tool at 1 GHz. The response of transducer power gain from the generator to load impedance is presented in Figure 7.4, which is 0.9415 at 1 GHz.

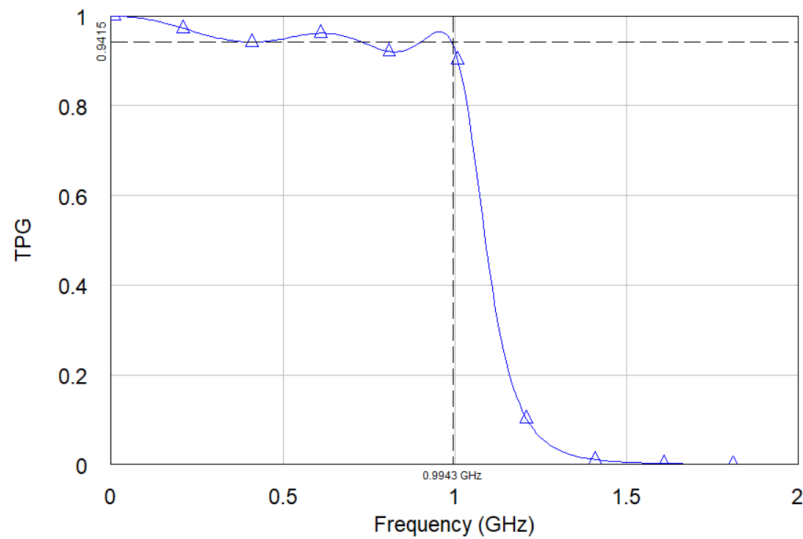


Figure 7.4 TPG response of LPN via shunt capacitors separated by UE

7.3 LPN via Series Inductors and Shunt Capacitors Separated by UE

In this part, the circuit has three lumped elements and two-unit elements, as seen in Figure 7.5. The normalized generated impedance has a resistance (1Ω) and series inductor ($1H$). The normalized load impedance has a series inductor ($2H$), a shunt capacitor ($1F$), and shunt resistance (1Ω).

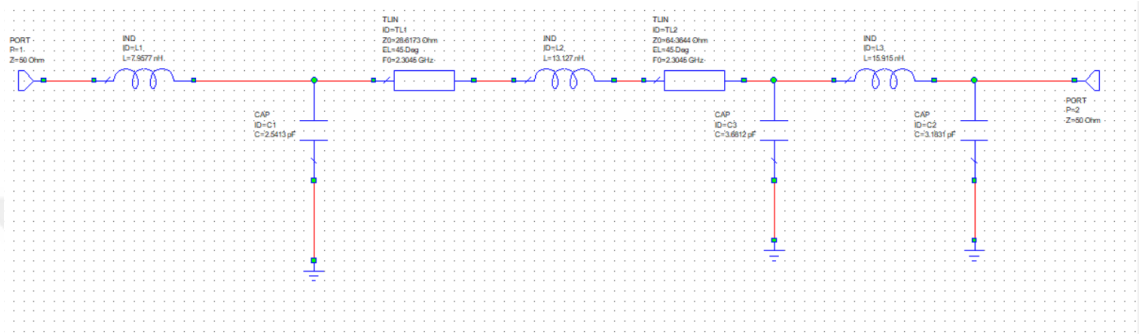


Figure 7.5 Synthesis of LPN via shunt capacitors and series inductors separated by UE

The two independent variable scattering parameters are calculated via equations (3.26-3.27) and $g(p,\lambda)$, $h(p,\lambda)$, and $f(p,\lambda)$, polynomials are shown in equations (3.32-35).

Random variables are assigned to independent coefficients (h_{02} , h_{10} , h_{20} , h_{30} , h_{01}) of $h(p,\lambda)$ polynomials and transmission delay of the unit element. These values are optimized with Non-Linear Least Square method in Matlab. Constant values are $h_{00}=0$ and $g_{00}=1$.

The normalized angular frequency (WL) values are between zero to one with 0.1 intervals in the optimization process. WL is defined as

$$WL=0:0.1:1 .$$

Values in v matrix are assigned with random variables between 0 and 1 that the values are the independent coefficients of $h(p,\lambda)$ and transmission delay of the unit element, respectively. The values in v matrix are written as

$$v=[0.6892 \ 0.7482 \ 0.4505 \ 0.2838 \ 0.2290 \ 0.9133] .$$

With these parameters, the independent coefficients of $g(p,\lambda)$ ($g_{02}, g_{00}, g_{10}, g_{20}, g_{30}, g_{01}$) are calculated via equations (3.33) for lumped elements (first column- $g_{00}, g_{10}, g_{20}, g_{30}$) and equation (3.34) for unit element (first row- g_{02}, g_{01}, g_{00}). Roots of $g(p)$ and $g(\lambda)$ polynomials are chosen in left half plane because these polynomials are strictly Hurwitz.

The optimization process is going to be repeated as described in Section 6 to get optimized values as

$$Y = [-0.7621 \ 0.2949 \ -0.1529 \ -0.7023 \ -0.3322 \ 0.3408] .$$

Y matrix contains independent coefficients of $h(p,\lambda)$ and transmission delay of the unit element, respectively. The transmission delay value of the unit element is 0.3408. The equations (3.33-3.34) are used to calculate the independent variables of $g(p,\lambda)$ ($g_{02}, g_{10}, g_{20}, g_{30}, g_{01}$). g_{00} is equal to one, and h_{00} is equal to zero.

After this calculation, dependent coefficients in matrix of $g(p,\lambda)$ and $h(p,\lambda)$ are calculated via equation (4.35-41). Scattering parameters are used to calculate transducer power gain via equations (6.2-4). The coefficient matrices of $g(p, \lambda)$ and $h(p, \lambda)$ polynomials are written as

$$M_h = \begin{bmatrix} 0 & -0.3322 & -0.9023 \\ -0.1529 & -0.4679 & -2.5976 \\ 0.2949 & -3.0376 & 0 \\ -0.7621 & 0 & 0 \end{bmatrix} ,$$

$$M_g = \begin{bmatrix} 1 & 2.1918 & 1.3469 \\ 1.8025 & 3.9 & 2.5976 \\ 1.6128 & 3.0376 & 0 \\ 0.7621 & 0 & 0 \end{bmatrix} .$$

Normalized lumped and distributed elements values are calculated as described in Subsection 5.4. The normalized components values are $C_1=0.7989$, $C_2=1.6496$, $C_3=1.1565$, $Z_1=0.5723$, $Z_2=1.2873$. The normalized frequency of the unit element in Microwave Office Tool is 0.3669.

Denormalized capacitor value according to 1 GHz is calculated via equation (7.1), and denormalized inductor value are calculated with equation (7.2). The Denormalized distributed element value is calculated with equation (7.3). Denormalized lumped element values and denormalized distributed element values are $C_1=2.5413\text{pF}$, $L_2=13.127\text{nH}$,

$C_3=3.6812\text{pF}$ and $Z_1=28.6123\Omega$, $Z_2=64.3644\Omega$, respectively. Denormalization resistance and denormalized lumped element values in generator impedance are $Z=50\Omega$ and $L=7.9577\text{nH}$ via equation (7.2), respectively. Denormalization resistance and denormalized lumped element values at load impedance are $Z=50\Omega$ and $L=15.915\text{nH}$ via equation (7.2), $C=3.1831\text{ pF}$, respectively.

The simulation is executed with denormalized component values, as seen in Figure 7.5 at Microwave Office Tool. The response of transducer power gain from the generator to load impedance is presented in Figure 7.6, which is 0.92 at 1 GHz.

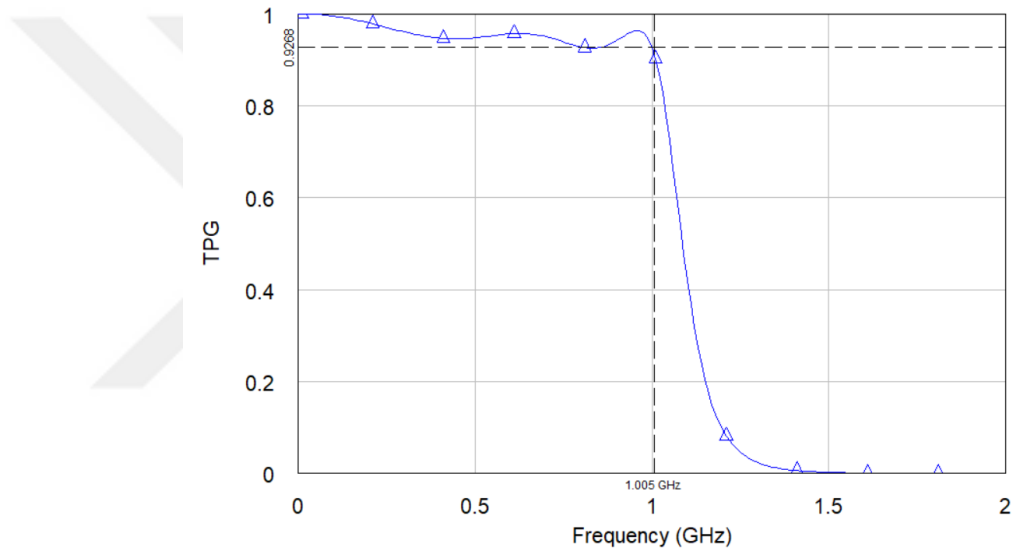


Figure 7.6 TPG of LPN via shunt capacitors and series inductors separated by UE

7.4 HPN via Shunt Inductors and Series Capacitors Separated by UE

In Figure 7.7, the circuit has three lumped elements and two-unit elements. The normalized generated impedance has a resistance, and load impedance has a series capacitor (2H), a shunt inductor (2F), and shunt resistance (1Ω).

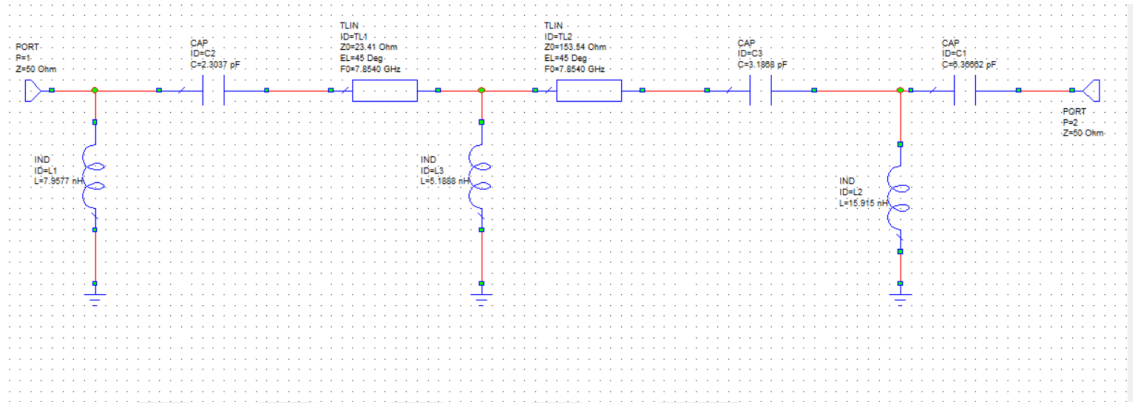


Figure 7.7 Synthesis of HPN via SC and SHI separated by UE

Two independent variable scattering parameters are written via equations (3.26-3.27), and $g(p,\lambda)$, $h(p,\lambda)$, and $f(p,\lambda)$ polynomials are shown via equations (3.32-3.35).

Random variables are assigned to independent coefficients (h_{31} , h_{10} , h_{20} , h_{30} , h_{32}) of $h(p,\lambda)$ and transmission delay of unit element. These values are optimized with Non-Linear Least Square method in Matlab. Constant values are $h_{00}=0$ and $g_{00}=1$.

The normalized angular frequency (WH) values are between one to two with 0.1 intervals for optimization. WL is written as

$$WL=1:0.1:2 .$$

Values in v matrix are assigned with random variables between 0 and 1. The parameters are the independent coefficients of $h(p,\lambda)$ and transmission delay of the unit element, respectively. The values in v matrix are written as

$$v=[0.1068 \ 0.6538 \ 0.4962 \ 0.7791 \ 0.7150 \ 0.9037] .$$

With v matrix, the independent coefficients of $g(p, \lambda)$ ($g_{32}, g_{00}, g_{10}, g_{20}, g_{30}, g_{31}$) are calculated via equations (3.33) for lumped elements (first column- $g_{00}, g_{10}, g_{20}, g_{30}$) and equation (3.34) for unit element (last row- g_{32}, g_{31}, g_{30}) Roots of $g(p)$ and $g(\lambda)$ polynomials are chosen in left half plane because these polynomials are strictly Hurwitz.

The optimization process is going to be repeated as described in Section 6 to get optimized values as

$$Y = [-3.2020 \ 0.5394 \ 0.4235 \ 0.2936 \ 1.0583 \ 0.1] .$$

Y matrix contains independent coefficients of $h(p, \lambda)$ and transmission delay of the unit element, respectively. The transmission delay value of the unit element is 0.1. The equations (3.33-3.34) are used to calculate the independent variables of $g(p, \lambda)$ ($g_{31}, g_{10}, g_{20}, g_{30}, g_{32}$).

After this calculation, equations (4.69-76) are used to calculate the dependent coefficients of $g(p, \lambda)$ and $h(p, \lambda)$ polynomials and scattering parameters. Transducer power gain is calculated with equation (6.2-4).

The coefficient matrices of $g(p, \lambda)$ and $h(p, \lambda)$ are written as

$$M_h = \begin{bmatrix} 1.0583 & 0 & 0 \\ 0.2936 & 5.3106 & 0 \\ 0.4235 & -1.5246 & 5.7089 \\ 0 & 0.5294 & -3.2020 \end{bmatrix} ,$$

$$M_g = \begin{bmatrix} 1.0583 & 0 & 0 \\ 1.8255 & 5.3106 & 0 \\ 1.9571 & 5.6429 & 5.7089 \\ 1 & 3 & 3.3546 \end{bmatrix} .$$

Normalized lumped and distributed elements values are calculated as described in Subsection 5.3. The normalized components values are $C_1=0.7237$, $C_2=0.6520$, $C_3=1.0021$ and $Z_1=0.4684$, $Z_2=3.0710$. The normalized frequency of the unit element in Microwave Office Tool is 1.2504.

Denormalized capacitor value at 1 GHz is calculated with equation (7.1), and denormalized inductor value is calculated with equation (7.2). Denormalized distributed element value is calculated with equation (7.3). Denormalized lumped element values and denormalized distributed element values are $C_1=2.3037\text{pF}$, $L_2=5.1888\text{nH}$, $C_3=3.1868\text{pF}$ and $Z_1=23.41\Omega$, $Z_2=153.54\Omega$ respectively. Denormalization resistance and denormalized lumped element values in generator impedance are $Z=50\Omega$ and $L=7.9577\text{nH}$ via equation (7.2), respectively. Denormalization resistance and denormalized lumped element values at load impedance are $Z=50\Omega$ and $L=15.915\text{nH}$ via equation (7.2), $C=3.1831\text{ pF}$, respectively.

The simulation is executed with denormalized component values, as seen in Figure 7.7 at Microwave Office Tool. The transducer power gain from the generator to load impedance is presented in Figure 7.8, which is 0.98 at 1 GHz

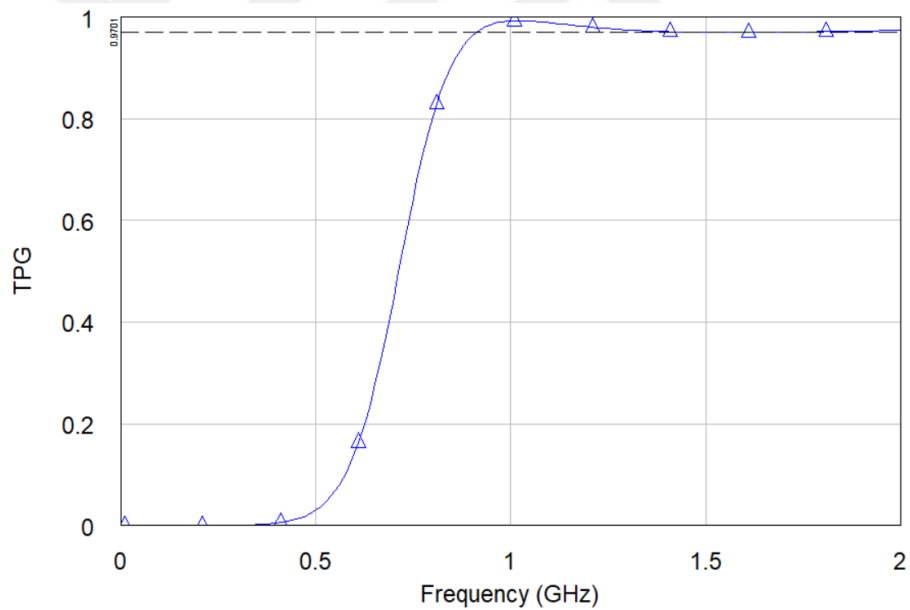


Figure 7.8 TPG of HPN via series capacitors and shunt inductors separated by UE

8. PHASE SHIFTER NETWORKS

There are two main phase shifter networks. One of the phase shifter networks contains series capacitors separated by unit elements for high-pass and shunt capacitors separated by unit elements for low-pass. The other network consists of capacitors and inductors as lumped elements separated by unit elements. The positive half of desired phase response is provided from the high-pass network, and the negative half of desired phase response is obtained from the low-pass network. Generator and load impedance contains only resistances.

8.1 PSN via Shunt or Series Capacitors Separated by UE

In Figure 8.1, the circuit has three lumped elements and two-unit elements. Normalized generated impedance has a resistance (1Ω), and normalized load impedance has a resistance (1Ω).

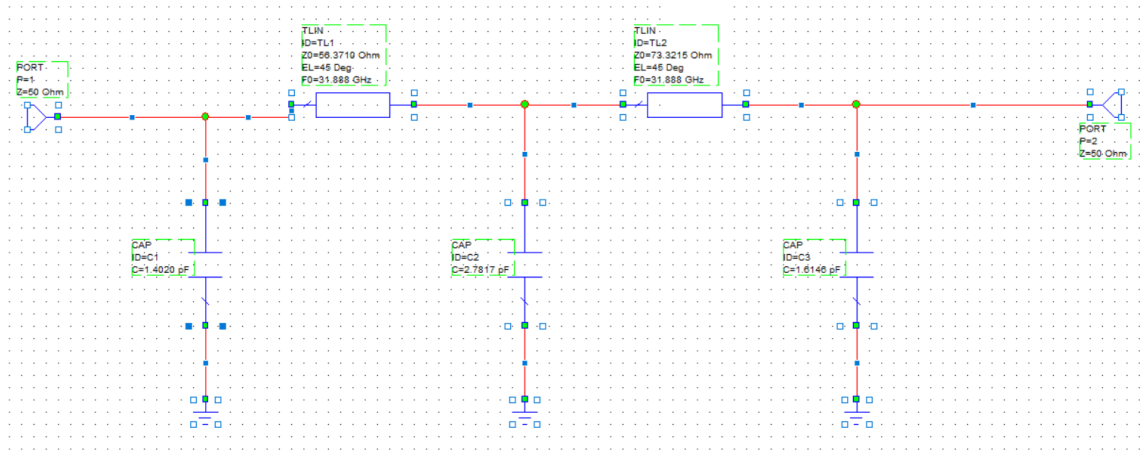


Figure 8.1 LPPSN via shunt capacitors separated by UE

Two independent variable scattering parameters are defined in equations (3.26-3.27). $g(p,\lambda)$, $h(p,\lambda)$, and $f(p,\lambda)$ polynomials are defined in equations (3.32-37).

Independent coefficients (h_{02} , h_{12} , h_{22} , h_{32} , h_{01}) of $h(p,\lambda)$ and transmission delay of the unit element are assigned with random numbers at the beginning of the optimization process. The constant values are $h_{00}=0$ and $g_{00}=1$. The method in the optimization process is Non-Linear Least Square Method and executed in Matlab. The maximum transducer power gain response is equal to 1, and the magnitude of S_{21} should also be equal to 1. With this conditions and equation (3.27), $|f(p,\lambda)| / |g(p,\lambda)|$ should be equal to 1.

Normalized angular frequency (WL) values are between 0.95 to 1.05 with 0.01 intervals at 1 GHz for the optimization process and are written as

$$WL=0.95:0.01:1.05 .$$

The independent coefficients of $h(p,\lambda)$ and transmission delay of the unit element are between 0 and 1, respectively. v matrix is written as

$$v=[0.1818 \ 0.2638 \ 0.1455 \ 0.1361 \ 0.8693 \ 0.5797] .$$

With v matrix, the independent coefficients of $g(p,\lambda)$ (g_{02} , g_{12} , g_{22} , g_{32} , g_{01}) are calculated via equations (3.33) for lumped elements (last column- g_{02} , g_{12} , g_{22} , g_{32}) and equations (3.34) for unit element (first row- g_{02} , g_{01} , g_{00}). Roots of $g(p)$ and $g(\lambda)$ polynomials are chosen in left half plane because the polynomials are strictly Hurwitz.

The optimization process is going to be repeated as described in Section 6. Boundaries of initial values in matrix v is defined as lower bound (lowb) and upper bound (upperb)

$$Lowb=[-\text{Inf} \ -\text{Inf} \ -\text{Inf} \ -\text{Inf} \ -\text{Inf} \ 0.01] ,$$

$$upperb=[-0.01 \ \text{Inf} \ \text{Inf} \ \text{Inf} \ \text{Inf} \ \text{Inf}] .$$

The total error is calculated via equation (6.7) to get optimized values as

$$Y=[-0.1614 \ 0.0482 \ 0.2232 \ -0.2659 \ 0.5125 \ 0.0246] .$$

Y matrix contains independent coefficients of $h(p,\lambda)$ and transmission delay of the unit element, respectively. The transmission delay value of the unit element is 0.1. Equations (3.33-3.34) are used to calculate independent variables of $g(p,\lambda)$ ($g_{02}, g_{12}, g_{22}, g_{32}, g_{01}$). g_{00} is equal to one. After this calculation, equations (4.115-123) are used for the calculation of dependent coefficients of $g(p,\lambda)$ and $h(p,\lambda)$ polynomials and scattering parameters.

The coefficient matrix of $g(p,\lambda)$ and $h(p,\lambda)$ are written as

$$M_h = \begin{bmatrix} 0 & 0.5125 & -0.2659 \\ -0.9108 & -0.0615 & 0.2232 \\ 0 & -0.8317 & 0.0482 \\ 0 & 0 & -0.1614 \end{bmatrix},$$

$$M_g = \begin{bmatrix} 1 & 2.0814 & 1.0348 \\ 0.9108 & 2.3625 & 1.2216 \\ 0 & 0.8317 & 0.6846 \\ 0 & 0 & 0.1614 \end{bmatrix}.$$

Normalized lumped and distributed element values are calculated via equations in Subsection 5.2. The normalized components values are $C_1=0.4404$, $C_2=0.8739$, $C_3=0.5072$ and $Z_1=1.1274$, $Z_2=1.4664$.

Denormalized capacitor values at 100 GHz are calculated via equation (7.1). Denormalized inductor values are calculated via equation (7.2). Denormalized distributed element values are calculated via equation (7.3). Denormalized lumped element values and denormalized distributed element values are $C_1=1.4020$ pF, $C_2=2.7817$ pF, $C_3=1.6146$ pF, and $Z_1=56.3710 \Omega$, $Z_2=73.3215 \Omega$, respectively. Denormalized generator impedance is $Z=50\Omega$. Denormalized load impedance is $Z=50 \Omega$. The normalized frequency of the unit element in Microwave Office Tool is 31.888 GHz.

Denormalized capacitor values at 100 GHz are calculated via equation (7.1). Denormalized inductor values are calculated via equation (7.2). Denormalized distributed element values are calculated via equation (7.3). Denormalized lumped element values and denormalized distributed element values are $C_1=0.2804$ pF, $C_2=0.55634$ pF, $C_3=0.32292$ pF and $Z_1=56.3710 \Omega$, $Z_2=73.3215 \Omega$, respectively. Denormalized generator impedance is $Z=50\Omega$. Denormalized load impedance is $Z=50 \Omega$. The normalized frequency of the unit element in Microwave Office Tool is 159.44 GHz.

Denormalized capacitor values at 100 GHz are calculated via equation (7.1). Denormalized inductor values are calculated via equation (7.2). Denormalized distributed element values are calculated via equation (7.3). Denormalized lumped element values and denormalized distributed element values are $C_1=0.14020$ pF, $C_2=0.27817$ pF, $C_3=0.16146$ pF and $Z_1=56.3710$ Ω , $Z_2=73.3215$ Ω , respectively. Denormalized generator impedance is $Z=50\Omega$. Denormalized load impedance is $Z=50$ Ω . The normalized frequency of unit elements in Microwave Office Tool is 318.88 GHz.

Denormalized capacitor values at 100 GHz are calculated via equation (7.1). Denormalized inductor values are calculated via equation (7.2). Denormalized distributed element values are calculated via equation (7.3). Denormalized lumped element values and denormalized distributed element values are $C_1=0.0701$ pF, $C_2=0.13908$ pF, $C_3=0.08073$ pF and $Z_1=56.3710$ Ω , $Z_2=73.3215$ Ω , respectively. Denormalized generator impedance is $Z=50\Omega$. Denormalized load impedance is $Z=50$ Ω . The normalized frequency of the unit element in Microwave Office Tool is 637.75 GHz.

Denormalized capacitor values at 100 GHz are calculated via equation (7.1). Denormalized inductor values are calculated via equation (7.2). Denormalized distributed element values are calculated via equation (7.3). Denormalized lumped element values and denormalized distributed element values are $C_1=0.056080$ pF, $C_2=0.11127$ pF, $C_3=0.064584$ pF and $Z_1=56.3710$ Ω , $Z_2=73.3215$ Ω , respectively. Denormalized generator impedance is $Z=50\Omega$. Denormalized load impedance is $Z=50$ Ω . The normalized frequency of the unit element in Microwave Office Tool is 797.19 GHz.

Denormalized capacitor values at 100 GHz are calculated via equation (7.1). Denormalized inductor values are calculated via equation (7.2). Denormalized distributed element values are calculated via equation (7.3). Denormalized lumped element values and denormalized distributed element values are $C_1=0.046733$ pF, $C_2=0.092723$ pF, $C_3=0.053820$ pF and $Z_1=56.3710$ Ω , $Z_2=73.3215$ Ω , respectively. Denormalized generator impedance is $Z=50\Omega$. Denormalized load impedance is $Z=50$ Ω . The normalized frequency of the unit element in Microwave Office Tool is 956.63 GHz.

Denormalized capacitor values at 100 GHz are calculated via equation (7.1). Denormalized inductor values are calculated via equation (7.2). Denormalized distributed element values are calculated via equation (7.3). Denormalized lumped element values and denormalized distributed element values are $C_1=0.014020$ pF, $C_2=0.027817$ pF, $C_3=0.016146$ pF and $Z_1=56.3710$ Ω , $Z_2=73.3215$ Ω , respectively. Denormalized generator impedance is $Z=50\Omega$. Denormalized load impedance is $Z=50$ Ω . The normalized frequency of the unit element in Microwave Office Tool is 3188.8 GHz.

In Figure 8.2, the circuit has three lumped and two unit elements. Normalized generated impedance has a resistance (1Ω), and normalized load impedance has a resistance (1Ω).

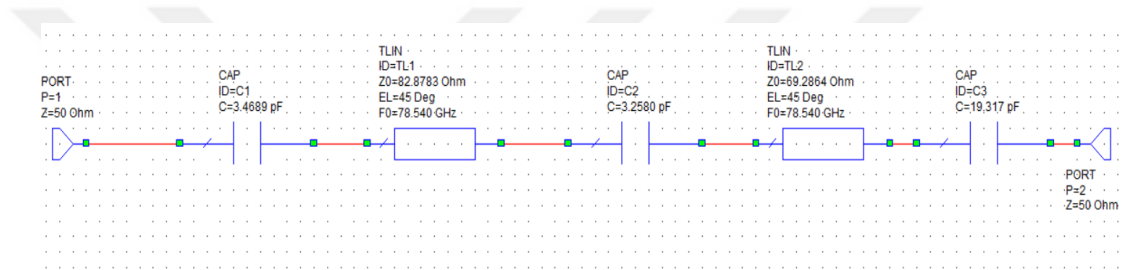


Figure 8.2 HPPSN via series capacitors separated by UE

The scattering parameters are defined in equations (3.26-3.27). $g(p,\lambda)$, $h(p,\lambda)$, and $f(p,\lambda)$ polynomials are written in equations (3.32-37).

Independent coefficients (h_{02} , h_{12} , h_{22} , h_{32} , h_{31}) of $h(p,\lambda)$ and transmission delay of the unit element are assigned with random numbers at the beginning of the optimization process. The constant values are $h_{30}=0$ and $g_{30}=1$. The method in the optimization process is Non-Linear Least Square Method and executed in Matlab. The maximum transducer power gain is equal to 1, and the magnitude of S_{21} equals 1. Via these conditions and equation (3.27), $|f(p,\lambda)| / |g(p,\lambda)|$ should be equal to 1.

The normalized angular frequency (WL) values are between 0.95 and 1.05 with 0.01 interval and are written as

$$WL=0.95:0.01:1.05 .$$

The independent coefficients of $h(p,\lambda)$ and transmission delay of the unit element are between 0 and 1, respectively. v matrix is written as

$$v=[0.1818 \ 0.2638 \ 0.1455 \ 0.1361 \ 0.8693 \ 0.5797] \ .$$

Independent coefficients of $g(p, \lambda)$ ($g_{02}, g_{12}, g_{22}, g_{32}, g_{31}$) are calculated via equations (3.33) for lumped elements (last column- $g_{02}, g_{12}, g_{22}, g_{32}$) and equation (3.34) for unit element(last row- g_{32}, g_{31}, g_{30}). Roots of $g(p)$ and $g(\lambda)$ polynomials are chosen in left half plane because these polynomials are strictly Hurwitz.

The optimization process is going to be repeated as described in Section 6. Boundaries of initial values in matrix v are defined as lower bound (lowb) and upper bound (upperb)

$$\text{Lowb}=[-\text{Inf} \ -\text{Inf} \ -\text{Inf} \ 0.01 \ -\text{Inf} \ 0.01] \ ,$$

$$\text{upperb}=[\text{Inf} \ \text{Inf} \ \text{Inf} \ \text{Inf} \ \text{Inf} \ \text{Inf}] \ .$$

The total error of transducer power gain and phase are calculated via equation (6.10) to get optimized results as

$$Y=[0.1801 \ 0.2694 \ 0.1601 \ 0.0322 \ 0.8593 \ 0.5797] \ .$$

Y matrix contains independent coefficients of $h(p,\lambda)$ and transmission delay of the unit element, respectively. The transmission delay value of the unit element is 0.1707. The equations (3.33-3.34) are used to calculate independent coefficients of $g(p,\lambda)$ ($g_{32}, g_{12}, g_{22}, g_{32}, g_{31}$). g_{30} is equal to one.

After this calculation, equations (4.141-151) are used to calculate the dependent coefficients of $g(p,\lambda)$ and $h(p,\lambda)$ polynomials and scattering parameters.

The coefficient matrices of $g(p, \lambda)$ and $h(p, \lambda)$ polynomials are written as

$$M_g = \begin{bmatrix} 0 & 0 & 0.0322 \\ 0 & 0.4287 & 0.2302 \\ 1.0297 & 1.3643 & 0.6948 \\ 1 & 2.1841 & 1.0161 \end{bmatrix} \ ,$$

$$M_h = \begin{bmatrix} 0 & 0 & 0.0322 \\ 0 & 0.4287 & 0.1601 \\ 1.0297 & 0.5565 & 0.2694 \\ 1 & 0.8592 & 0.1801 \end{bmatrix} \ .$$

Normalized lumped and distributed elements values are calculated via equations in Subsection 5.1. The normalized components values are $C_1=1.0898$, $C_2=1.0235$, $C_3=6.0687$, and $Z_1=1.1274$, $Z_2=1.4664$. The normalized frequency of the unit element in Microwave Office Tool is 12.5035.

Denormalized capacitor values at 1 GHz are calculated with equation (7.1). Denormalized inductor values are calculated via equation (7.2). Denormalized distributed element values are calculated via equation (7.3). Denormalized lumped element values and denormalized distributed element values are $C_1=3.4689$ pF, $C_2=3.2580$ pF, $C_3=19.317$ pF, and $Z_1=56.3710$ Ω , $Z_2=73.3215$ Ω , respectively. Denormalized generator impedance is $Z=50\Omega$. Denormalized load impedance is $Z=50\Omega$. The normalized frequency of the unit element in Microwave Office Tool is 78.540 GHz.

Desired phase response (90°) is provided from these circuits, as seen in Figure 8.1 and Figure 8.2. The results are given in Figure 8.3. The phase performance of high-pass and low-pass networks is sufficient, with -0.1 error around 1 GHz over 10% bandwidth (89.9° at 0.95 GHz and 90.00° at 1.05 GHz).

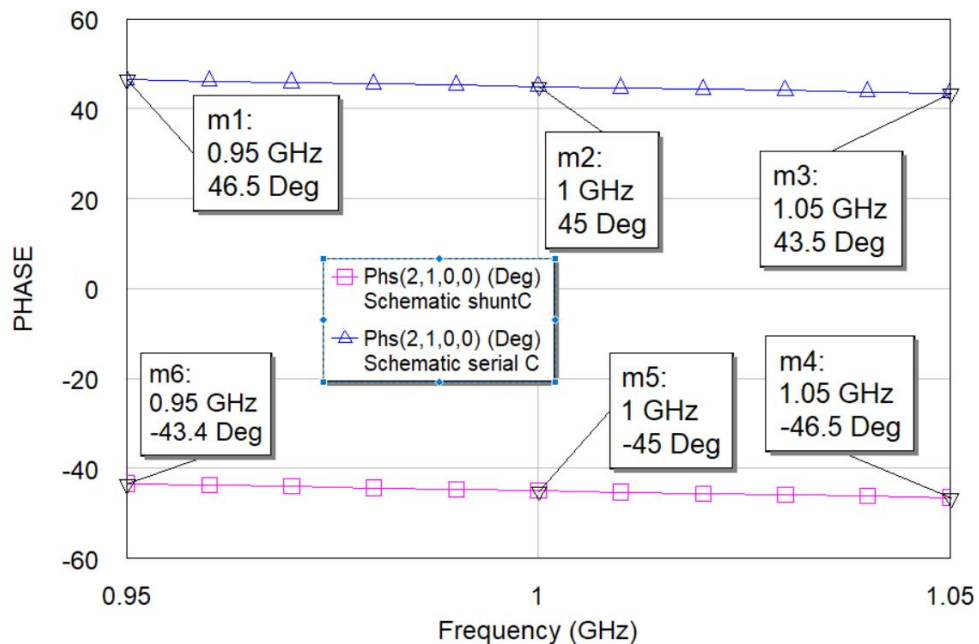


Figure 8.3 PRN via series capacitors or shunt capacitors separated by UE at 1 GHz

Transducer power gain responses of high-pass and low-pass networks are given in Figure 8.4. Transducer power gain is between 0.5889 and 0.5421 in low pass networks over 10% bandwidth, and transducer power gain is between 0.4615 and 0.5123 in high pass networks over 10% bandwidth for 1 GHz.

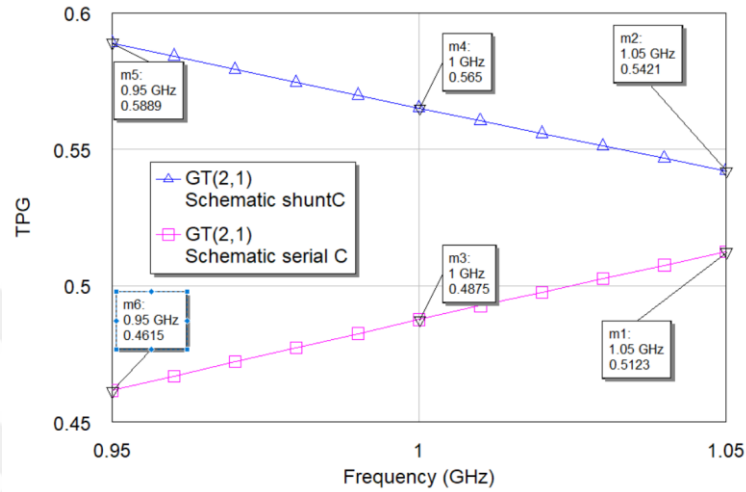


Figure 8.4 TPG of the network via SC or SHC separated by UE at 1 GHz

Denormalized capacitor values at 5 GHz are calculated with equation (7.1). Denormalized inductor values are calculated via equation (7.2). Denormalized distributed element values are calculated via equation (7.3). Denormalized lumped element values and denormalized distributed element values are $C_1=0.69378$ pF, $C_2=0.65161$ pF, $C_3=3.8635$ pF, and $Z_1=56.3710$ Ω , $Z_2=73.3215$ Ω , respectively. Denormalized generator impedance is $Z=50\Omega$. Denormalized load impedance is $Z=50\Omega$. The normalized frequency of the unit element in Microwave Office Tool is 392.70 GHz.

Desired phase response (90^0) results are given in Figure 8.5 at 5 GHz. The phase performance of high-pass and low-pass networks is sufficient, with -0.1 error around 90^0 at 5GHz over 10% bandwidth (89.9^0 at 4.75 GHz and 90.00^0 at 5.25 GHz).

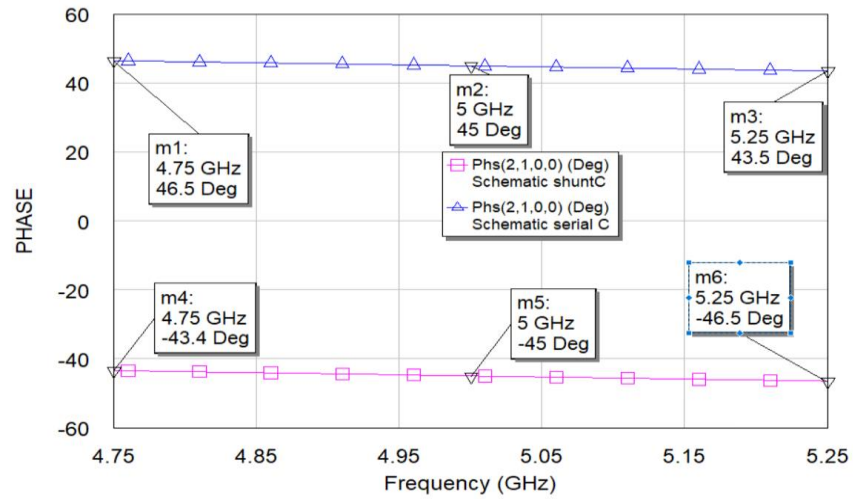


Figure 8.5 PRN via series capacitors or shunt capacitors separated by UE at 5 GHz

Transducer power gain responses of high-pass and low-pass networks are given in Figure 8.6. Transducer power gain is between 0.5889 and 0.5421 in low pass networks over 10% bandwidth, and transducer power gain changes between 0.4615 and 0.5123 in high pass networks over 10% bandwidth for 5 GHz.

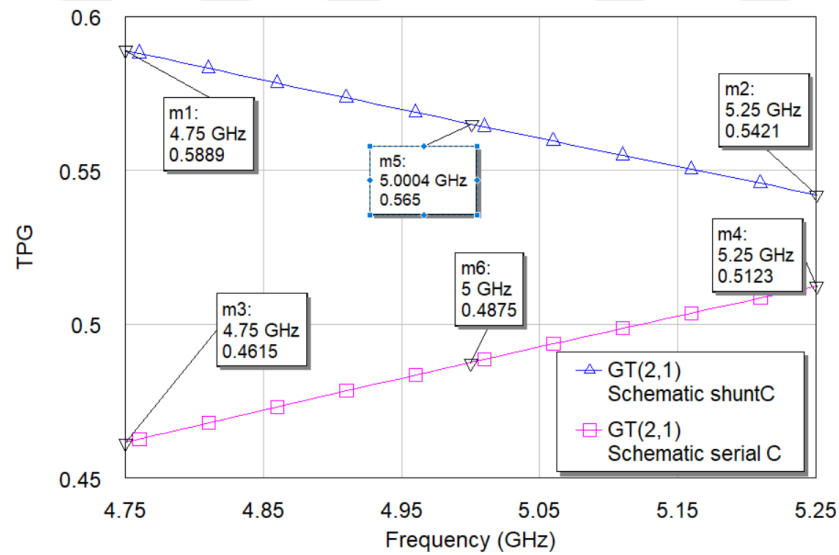


Figure 8.6 TPG of the network via SC or SHC separated by UE at 5 GHz

Denormalized capacitor values at 10 GHz are calculated with equation (7.1). Denormalized inductor values are calculated via equation (7.2). Denormalized distributed element values are calculated via equation (7.3). Denormalized lumped element values and denormalized distributed element values are $C_1=0.34689$ pF, $C_2=0.32580$ pF, $C_3=1.9317$ pF, and $Z_1=56.3710 \Omega$, $Z_2=73.3215 \Omega$, respectively. Denormalized generator impedance is $Z=50\Omega$. Denormalized load impedance is $Z=50\Omega$. The normalized frequency of the unit element in Microwave Office Tool is 785.40 GHz.

Desired phase response (90°) results are given with + 1.4 error in Figure 8.7 at 10 GHz. The phase performance of high-pass and low-pass networks is sufficient, with -0.2 and +0.2 errors around 91.4° at 10 GHz over 10% bandwidth (91.2° at 9.5 GHz and 91.6° at 10.5 GHz).

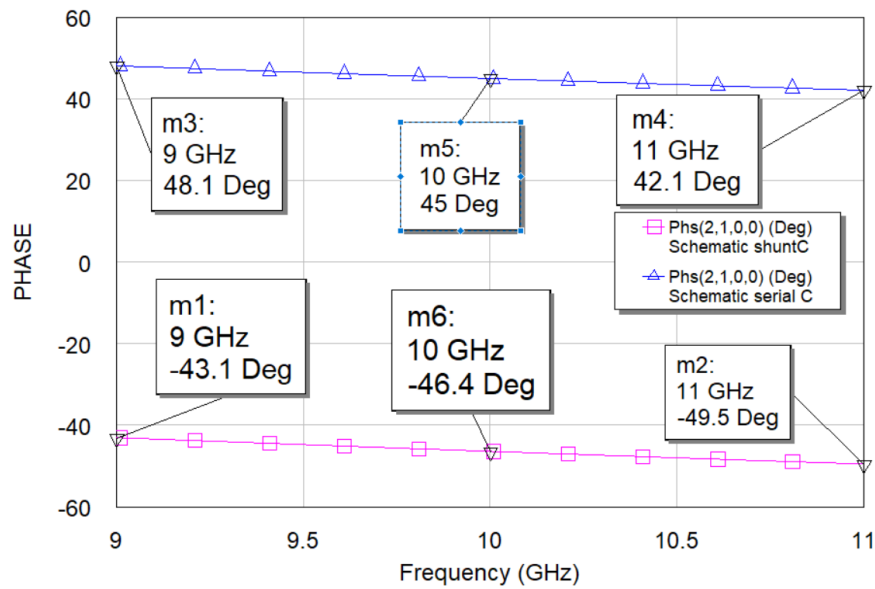


Figure 8.7 PRN via series capacitors or shunt capacitors separated by UE at 10 GHz

Transducer power gain responses of high-pass and low-pass networks are given in Figure 8.8. Transducer power gain is between 0.6245 and 0.536 in low pass networks over 10% bandwidth, and transducer power gain is between 0.4344 and 0.534 in high pass networks over 10% bandwidth for 10 GHz.

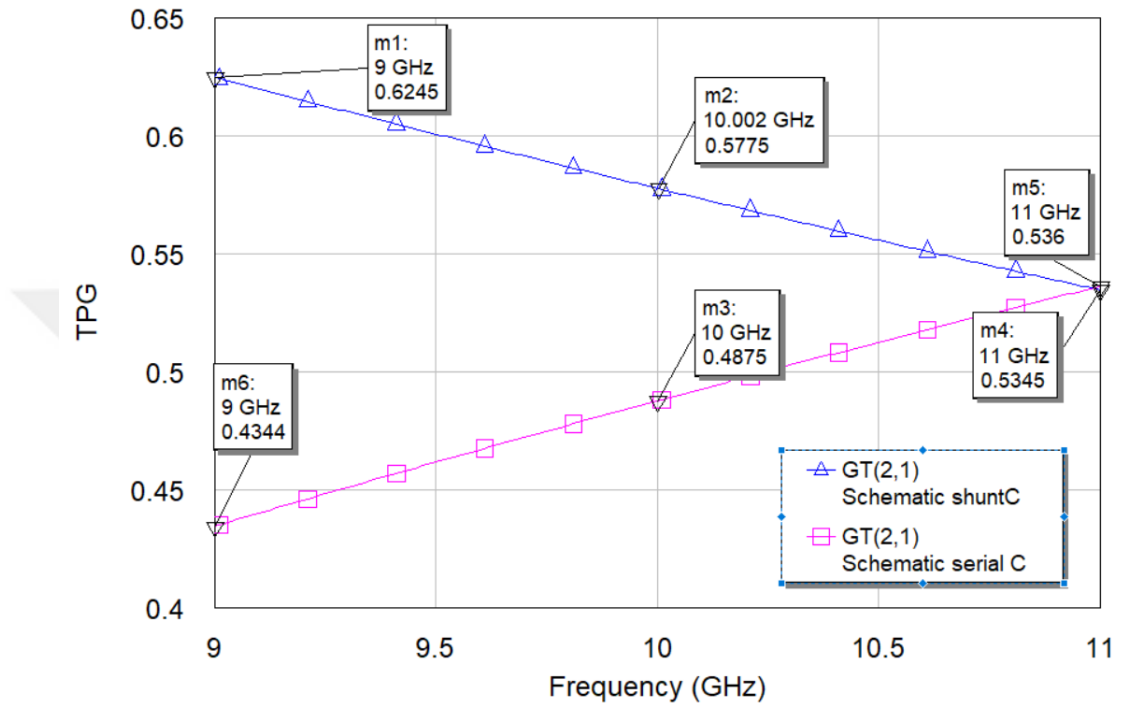


Figure 8.8 TPG of the network via SC or SHC separated by UE at 10 GHz

Denormalized capacitor values at 20 GHz are calculated with equation (7.1). Denormalized inductor values are calculated via equation (7.2). Denormalized distributed element values are calculated via equation (7.3). Denormalized lumped element values and denormalized distributed element values are $C_1=0.17344$ pF, $C_2=0.16290$ pF, $C_3=0.96586$ pF, and $Z_1=56.3710 \Omega$, $Z_2=73.3215 \Omega$, respectively. Denormalized generator impedance is $Z=50\Omega$. Denormalized load impedance is $Z=50\Omega$. The normalized frequency of the unit element in Microwave Office Tool is 1570.8 GHz.

Desired phase response (90^0) results are given with - 0.1 error in Figure 8.9 at 20 GHz. The phase performance of high-pass and low-pass networks is sufficient with + 0.1 error around 89.9^0 over 10% bandwidth at 20 GHz (89.9^0 at 19 GHz, 90.00^0 at 21 GHz).

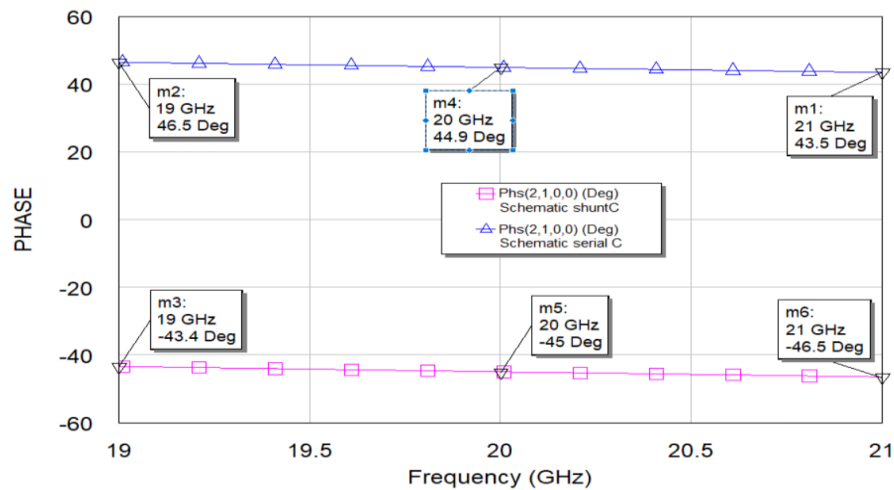


Figure 8.9 PRN via series capacitors or shunt capacitors separated by UE at 20 GHz

Transducer power gain responses of high-pass and low-pass networks are given in Figure 8.10. Transducer power gain is between 0.5889 and 0.5421 in low pass networks over 10% bandwidth, and transducer power gain is between 0.4615 and 0.5123 in high pass networks over 10% bandwidth at 20 GHz.

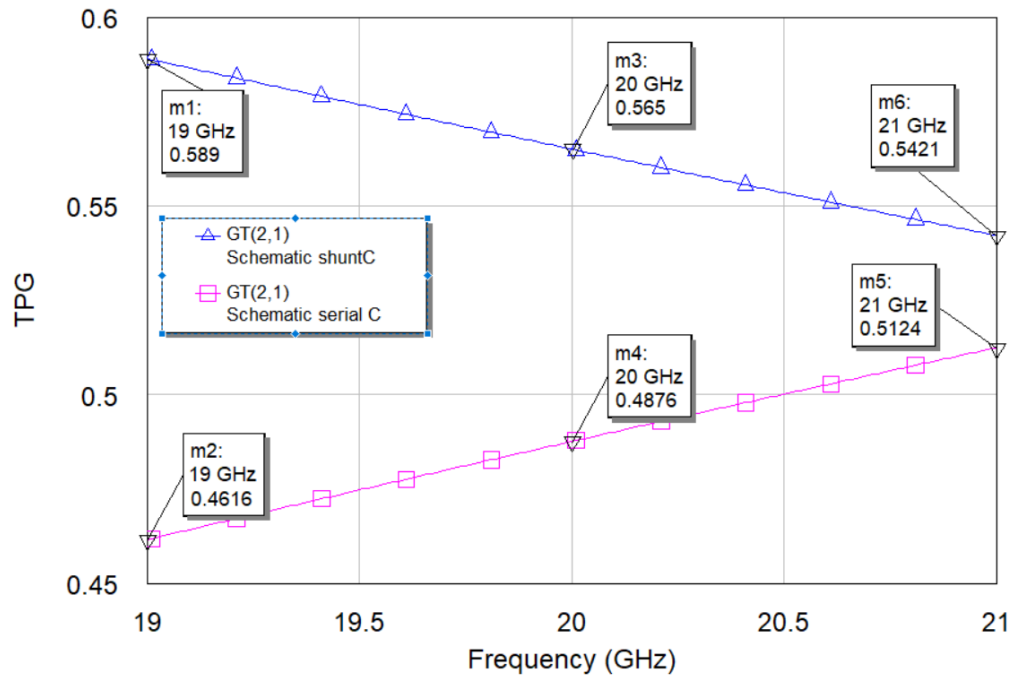


Figure 8.10 TPG of the network via SC or SHC separated by UE at 20 GHz

Denormalized capacitor values at 25 GHz are calculated with equation (7.1). Denormalized inductor values are calculated via equation (7.2). Denormalized distributed element values are calculated via equation (7.3). Denormalized lumped element values and denormalized distributed element values are $C_1=0.13876\text{pF}$, $C_2=0.13032\text{pF}$, $C_3=0.77269\text{pF}$, and $Z_1=56.3710\ \Omega$, $Z_2=73.3215\ \Omega$, respectively. Denormalized generator impedance is $Z=50\ \Omega$. Denormalized load impedance is $Z=50\ \Omega$. The normalized frequency of the unit element in Microwave Office Tool is 1963.5 GHz.

Desired phase response (90°) results are given with $+0.1$ error in Figure 8.11 at 25 GHz. The phase performance of high-pass and low-pass networks is sufficient, around 90.1° over 10% bandwidth at 25 GHz (90° at 23.75 GHz, 90° at 26.25 GHz).

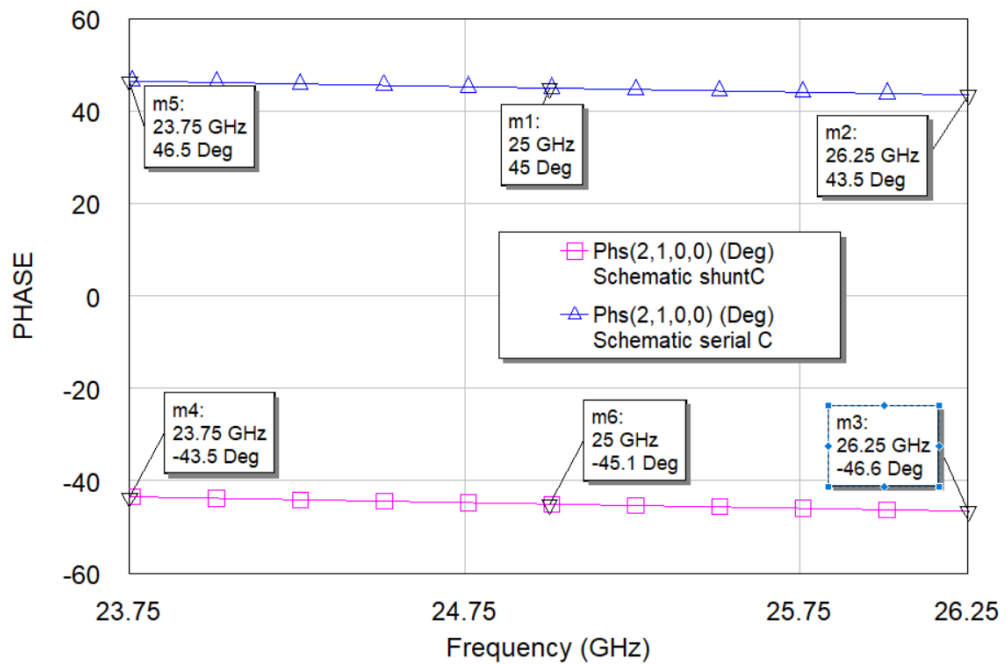


Figure 8.11 PRN via series capacitors or shunt capacitors separated by UE at 25 GHz

Transducer power gain responses of high-pass and low-pass networks are given in Figure 8.12. Transducer power gain is between 0.587 and 0.540 in low pass networks over 10% bandwidth, and transducer power gain is between 0.4615 and 0.5123 in high pass networks over 10% bandwidth at 25 GHz.

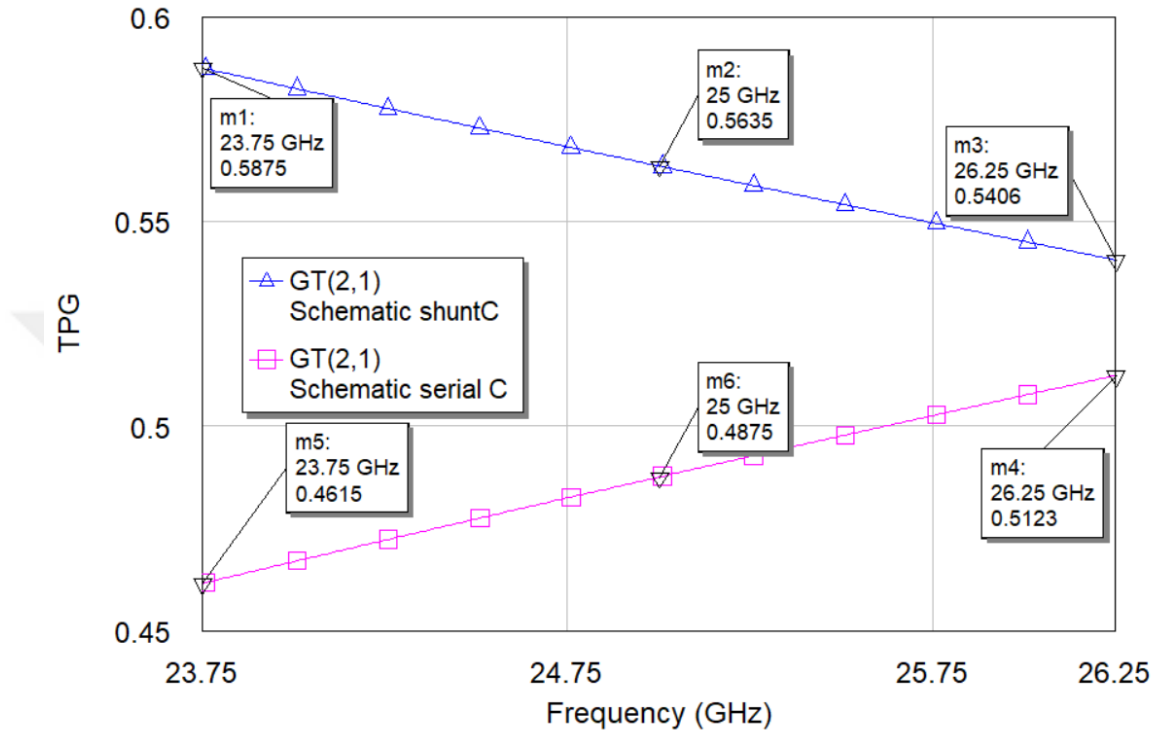


Figure 8.12 TPG of network via SC or SHC separated by UE at 25 GHz

Denormalized capacitor values at 30 GHz are calculated with equation (7.1). Denormalized inductor values are calculated via equation (7.2). Denormalized distributed element values are calculated via equation (7.3). Denormalized lumped element values and denormalized distributed element values are $C_1=0.11563\text{pF}$, $C_2=0.10860\text{pF}$, $C_3=0.64391\text{pF}$, and $Z_1=56.3710\ \Omega$, $Z_2=73.3215\ \Omega$, respectively. Denormalized generator impedance is $Z=50\ \Omega$. Denormalized load impedance is $Z=50\ \Omega$. The normalized frequency of the unit element in Microwave Office Tool is 2356.2 GHz.

Desired phase response (90°) results are given in Figure 8.13 at 30GHz. The phase performance of high-pass and low-pass networks is sufficient around 90° over 10% bandwidth at 30 GHz (90° at 28.5 GHz, 90° at 31.5 GHz).

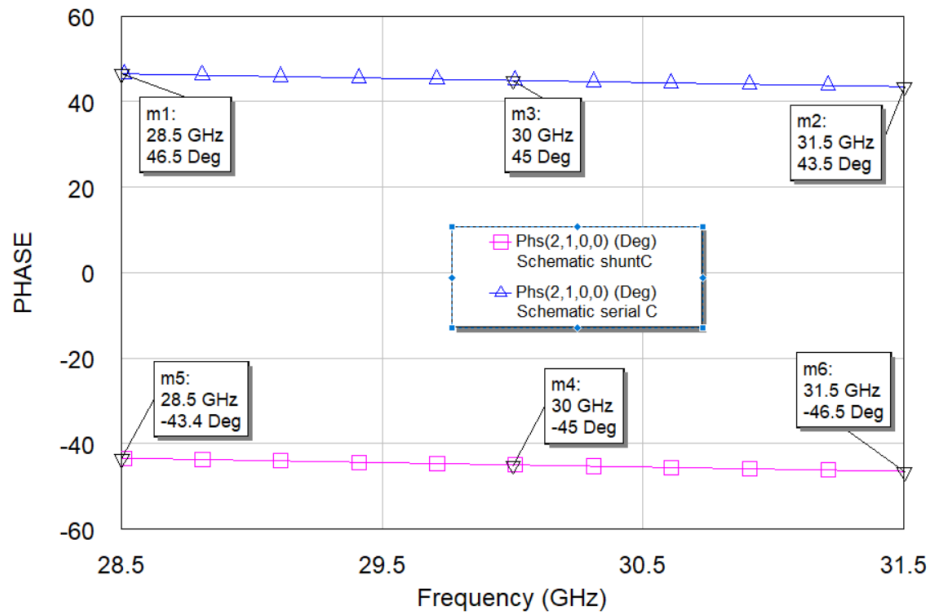


Figure 8.13 PRN via series capacitors or shunt capacitors separated by UE at 30 GHz

Transducer power gain responses of high-pass and low-pass networks are given in Figure 8.14. Transducer power gain is between 0.588 and 0.542 in low pass networks over 10% bandwidth, and transducer power gain is between 0.4615 and 0.5123 in high pass networks over 10% bandwidth at 30 GHz.

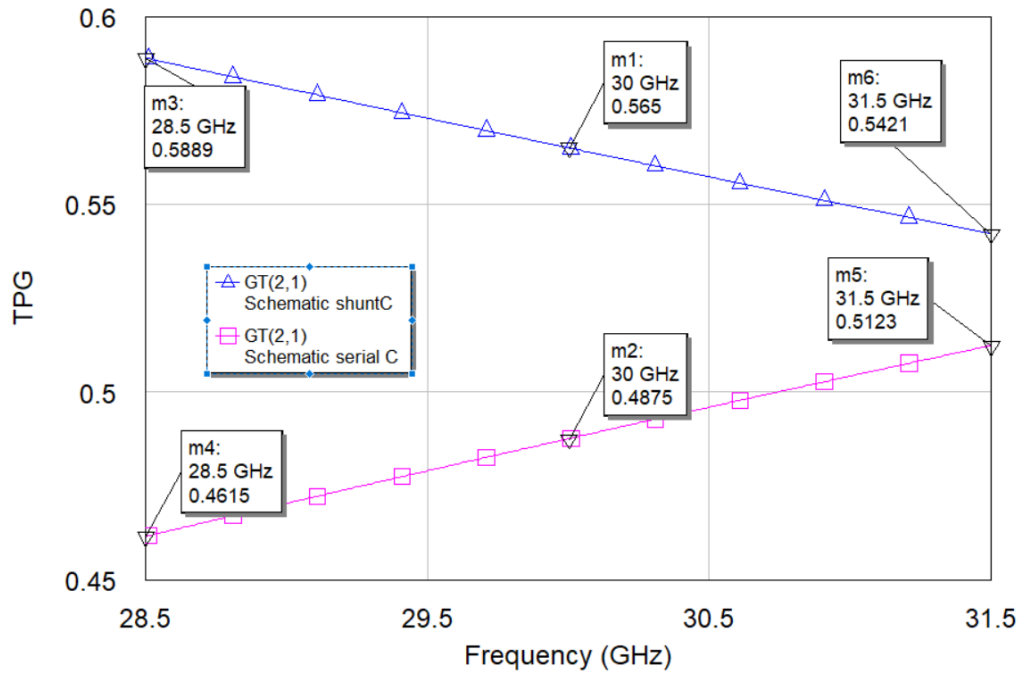


Figure 8.14 TPG of the network via SC or SHC separated by UE at 30 GHz

Denormalized capacitor values at 100 GHz are calculated with equation (7.1). Denormalized inductor values are calculated via equation (7.2). Denormalized distributed element values are calculated via equation (7.3). Denormalized lumped element values and denormalized distributed element values are $C_1=0.034689\text{pF}$, $C_2=0.032580\text{pF}$, $C_3=0.19317\text{pF}$, and $Z_1=56.3710\ \Omega$, $Z_2=73.3215\ \Omega$, respectively. Denormalized generator impedance is $Z=50\ \Omega$. Denormalized load impedance is $Z=50\ \Omega$. The normalized frequency of the unit element in Microwave Office Tool is 7854 GHz.

Desired phase response (90°) results are given in Figure 8.15 at 100 GHz. The phase performance of high-pass and low-pass networks is sufficient, with -0.1 error around 90° over 10% bandwidth at 30 GHz (89.9° at 95 GHz, 90° at 105 GHz).

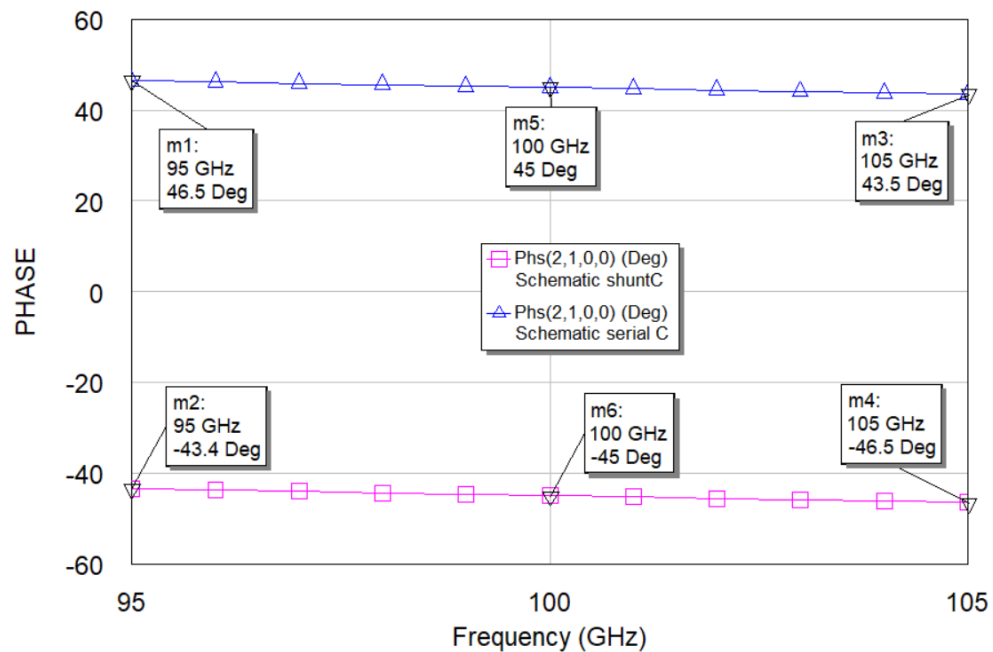


Figure 8.15 PRN via series capacitors or shunt capacitors separated by UE at 100GHz

Transducer power gain responses of high-pass and low-pass networks are given in Figure 8.16. Transducer power gain is between 0.588 and 0.542 in low pass networks over 10% bandwidth, and transducer power gain is between 0.4615 and 0.5123 in high pass networks over 10% bandwidth at 100 GHz.

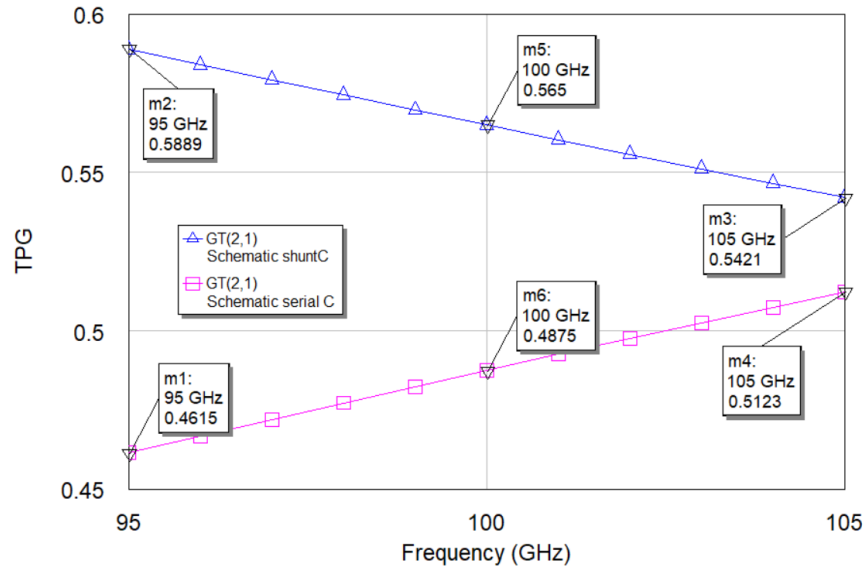


Figure 8.16 TPG of the network via SC or SHC separated by UE at 100 GHz

Results for TPG response of networks at center frequency 1 GHz to 100 GHz are insufficient for long-range coverage areas in communication systems where insertion loss is lower than 2.688 dB for 10% narrowband. For octave band from 0.6 GHz to 1.2 GHz at center 1 GHz, insertion loss is lower than 1.267 dB, as seen in Figure 8.17. Loss of power causes reductions in distance between transmitter and receiver for reliable communication. Because of its low-rate power capability, this type of design can be used indoors or outdoors, like in short-range communication of self-driving cars. Typically, for long-range communication, insertion loss should be less than 10 dB and 20 dB, which means 10 % and 1 % power loss while power is transformed from the generator to load impedance. Although this network provides low-rate power capability, phase responses are sufficient that phase error is $\pm 0.5^\circ$ around 89.94° at 1 GHz for 10% narrowband. For %40 bandwidth, phase response -0.17° at 0.8 GHz and $+ 0.76^\circ$ at 1.2 GHz. The insertion loss is better than 2.055 dB. For octave bandwidth, phase response -0.30° at 0.6 GHz and $+ 0.76^\circ$ at 1.2 GHz. The insertion loss is better than 1.267 dB. As seen in the results,

insertion loss and phase errors increase as bandwidth increases, as seen in Figure 8.19. The low phase error rate provides a high concentration of radiation signal to desired areas with minimum interference. Moreover, concentration on desired areas and minimization of interference increases the 5G smart antenna wireless communication data rate.

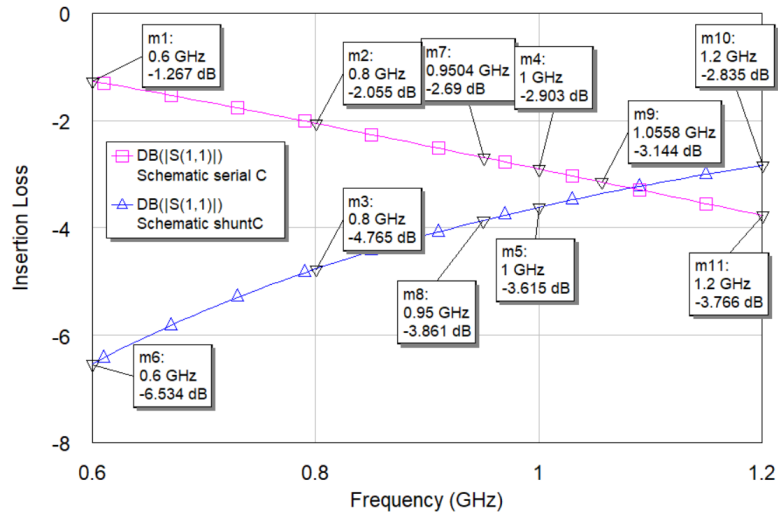


Figure 8.17 Insertion loss of network via SC or SHC separated by UE at 1 GHz

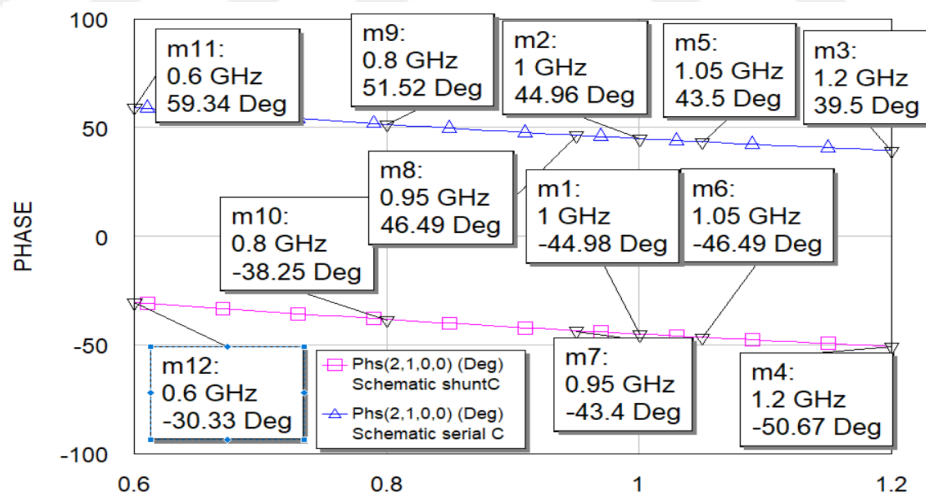


Figure 8.18 PRN via SC or SCH separated by UE over octave bandwidth at 1 GHz

A low-pass and high pass via only lumped elements as 90° phase shifters at three stage T form network and 180° phase shifters are examined, and mathematical equations are defined to calculate component values for desired phase response in the study [21]. Due to these equations, component values for high-pass and low-pass networks are computed at 1 GHz center. Component values for the three-stage T-type high-pass network are $C_1=7.6846$ pF, $L_2=11.254$ nH, and $C_3=7.6847$ pF. The generator and load impedance values are 50Ω . Component values for three stage T-type low-pass network are $L_1=3.2962$ nH, $C_2=2.2508$ pF, and $L_3=3.2962$ nH. The generator and load impedance values are 50Ω . Figure. Phase response and insertion loss of this circuit are indicated in Figure 8.20 and Figure 8.21. This design has a maximum $+0.3^\circ$ phase error around 90° at center 1 GHz for %10 bandwidth, and insertion loss is better than 72.78 dB. This design has $+2.87^\circ$ error at 0.8 GHz, and $+1.89^\circ$ error at 1.2 GHz around 90° at center 1 GHz for %40 bandwidth, and insertion loss is better than 27.47 dB. This design has max $+36.01^\circ$ at 0.6 GHz and $+1.89^\circ$ at 1.2 GHz around 90° at center 1 GHz for octave bandwidth, and insertion loss is better than 27.47 dB.

The design of lossless two-port high/low pass via series capacitors and shunt capacitors separated by unit elements has better phase responses at three different bandwidths. Still, the study's design has better insertion loss rates [36].

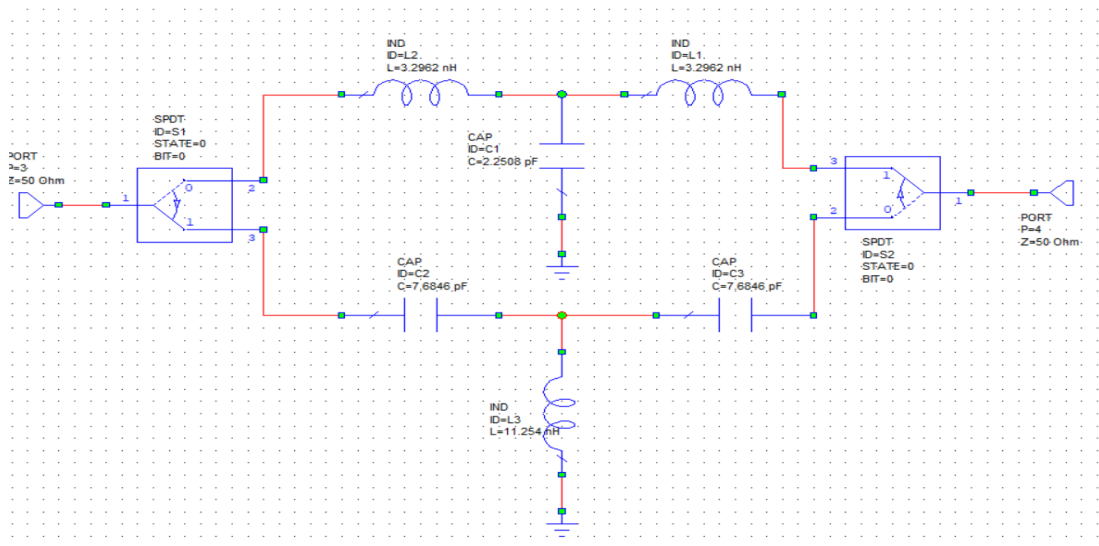


Figure 8.19 High/low pass via lumped elements as 90° phase shifters at 1 GHz

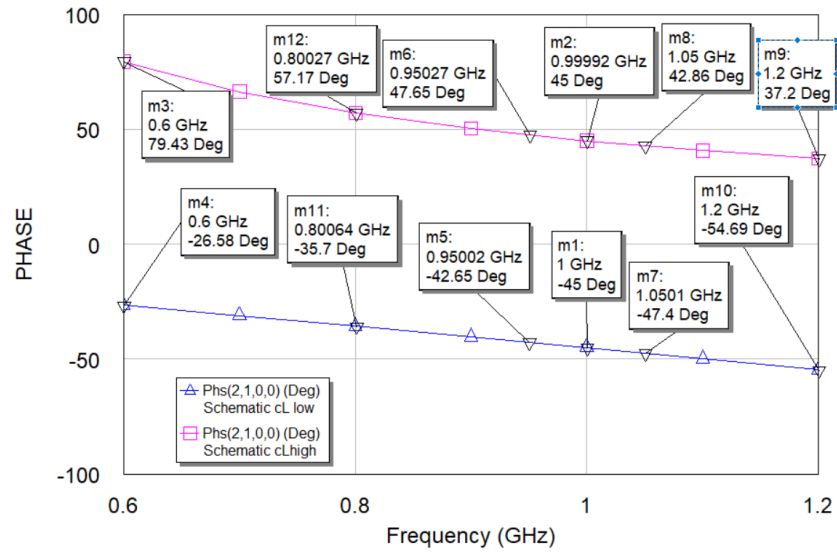


Figure 8.20 PRN via lumped elements over octave bandwidth at 1 GHz

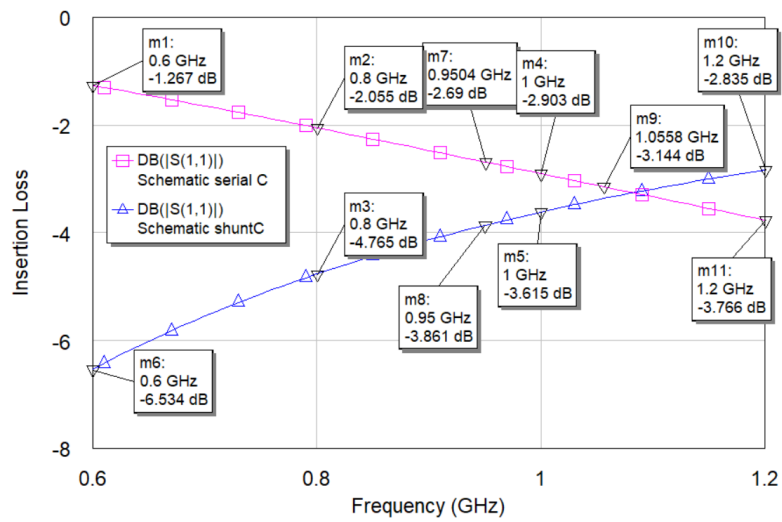


Figure 8.21 ILN via lumped elements over octave bandwidth at 1 GHz

Low/high pass networks via lumped elements as 90° phase shifter is designed ± 2 phase errors with diode switches for octave bandwidth in the study [44].

The design consists of a resonator, two shunt transmission lines, and a reference line in Figure 8.22. Phase variations are $\pm 2^0$ between 2.85 GHz and 7.15 GHz around 90^0 at center 5 GHz. The insertion loss is better than 10 dB at 129 % bandwidth with the additional effect of switch elements in the study [48].

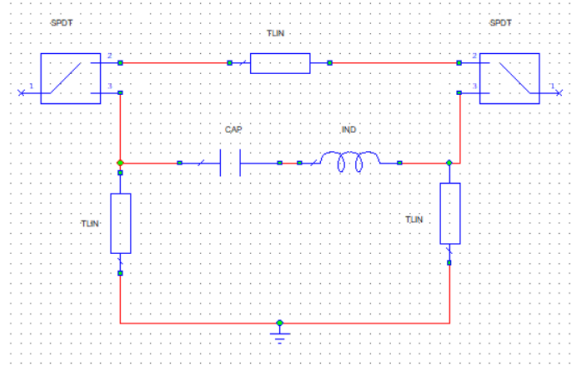


Figure 8.22 A broadband 90^0 phase shifter via series resonator and transmission line

Component values are calculated at 5 GHz center frequency for lossless high/low pass network via series and shunt capacitors separated by transmission lines. The phase response is indicated in Figure 8.23, and insertion loss is shown in Figure 8.24. Phase responses are 89.94^0 at 2.85 GHz and 90.45^0 at 7.15 GHz at 5 GHz, but insertion loss is better than 1.158 dB. As seen, the phase response is better, but insertion loss is higher in lossless high/low pass networks.

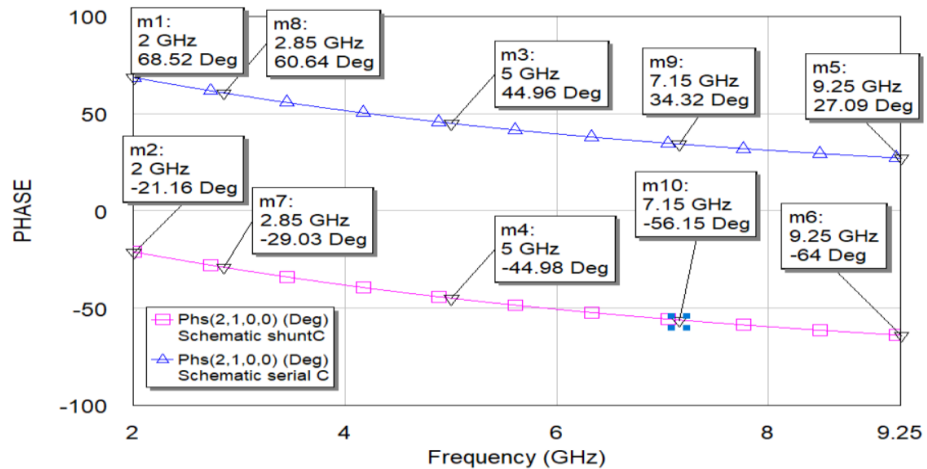


Figure 8.23 PRN via SC or SHC separated by UE over 129% bandwidth at 5 GHz

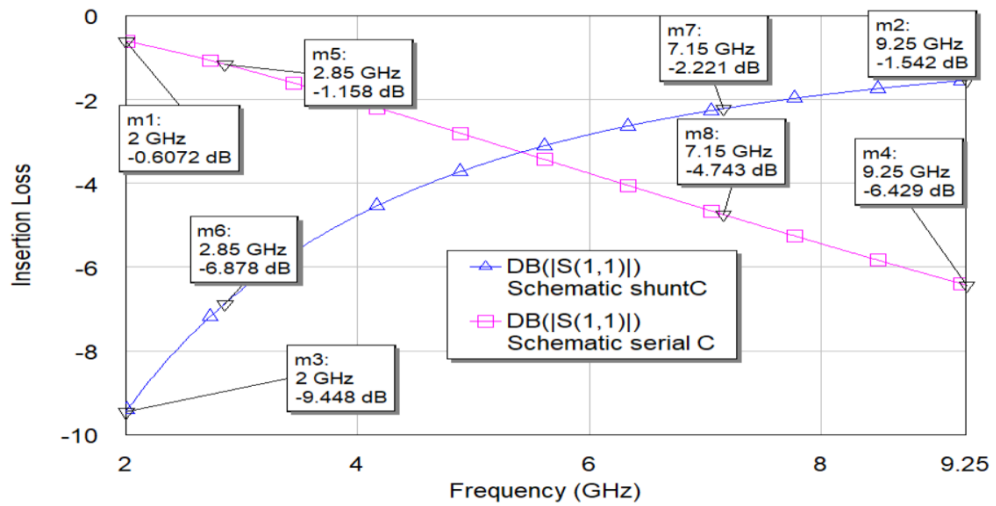


Figure 8.24 ILN via SC or SHC separated by UE over 129% bandwidth at 5 GHz

A Shiffman phase shifter is designed for 90^0 phase shifting at Ku-band (12 GHz to 18 GHz) and contains 4 port networks with a reference line and a coupled line defined time delay in the study [19]. Insertion loss is better than 10 dB, and phase variations are less than -9^0 at 12 GHz and $+11^0$ at 18 GHz.

Denormalized capacitor values at 15 GHz are calculated with equation (7.1) for a high pass network via series and shunt capacitors separated by transmission lines. Denormalized inductor values are calculated via equation (7.2). Denormalized distributed element values are calculated via equation (7.3). Denormalized lumped element values and denormalized distributed element values are $C_1=0.021326\text{pF}$, $C_2=0.21719\text{ pF}$, $C_3=1.2878\text{ pF}$, and $Z_1=82.8783\ \Omega$, $Z_2=69.2864\ \Omega$ in high pass, respectively. Denormalized generator impedance is $Z=50\Omega$. Denormalized load impedance is $Z=50\Omega$. The normalized frequency of the unit element in Microwave Office Tool is 1178.1 GHz.

Denormalized capacitor values at 15 GHz are calculated with equation (7.1) for low pass network via series and shunt capacitors separated by transmission lines. Denormalized inductor values are calculated via equation (7.2). Denormalized distributed element values are calculated via equation (7.3). Denormalized lumped element values and denormalized distributed element values are $C_1=0.093456\text{ pF}$, $C_2=0.18545\text{ pF}$, $C_3=0.10763\text{ pF}$, and $Z_1=56.3710\ \Omega$, $Z_2=73.3215\ \Omega$ in low pass, respectively.

Denormalized generator impedance is $Z=50\Omega$. Denormalized load impedance is $Z=50\Omega$. The normalized frequency of the unit element in Microwave Office Tool is 478.90 GHz.

The phase response of high/low pass lossless two-port network via series capacitors and shunt capacitors separated by transmission line is 90.75 at 12 GHz, 91.22 at 18 GHz, and 91.01 at 15 GHz center frequency in Figure 8.25. The component values Insertion loss is better than 1.936 dB in Figure 8.26 and higher than the study in [19]. In all studies shown in this Subsection 8.1 and Subsection 8.2, this design has fewer variations in narrowband and wideband and higher insertion loss. A decrease in phase variations causes an increment in insertion loss.

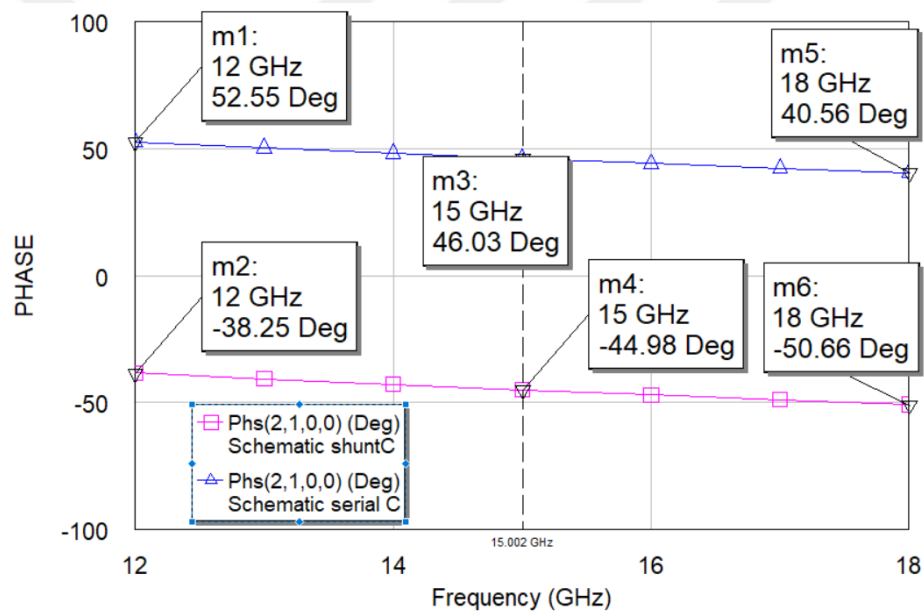


Figure 8.25 PRN via SC or SHC separated by UE over Ku-band at 15 GHz

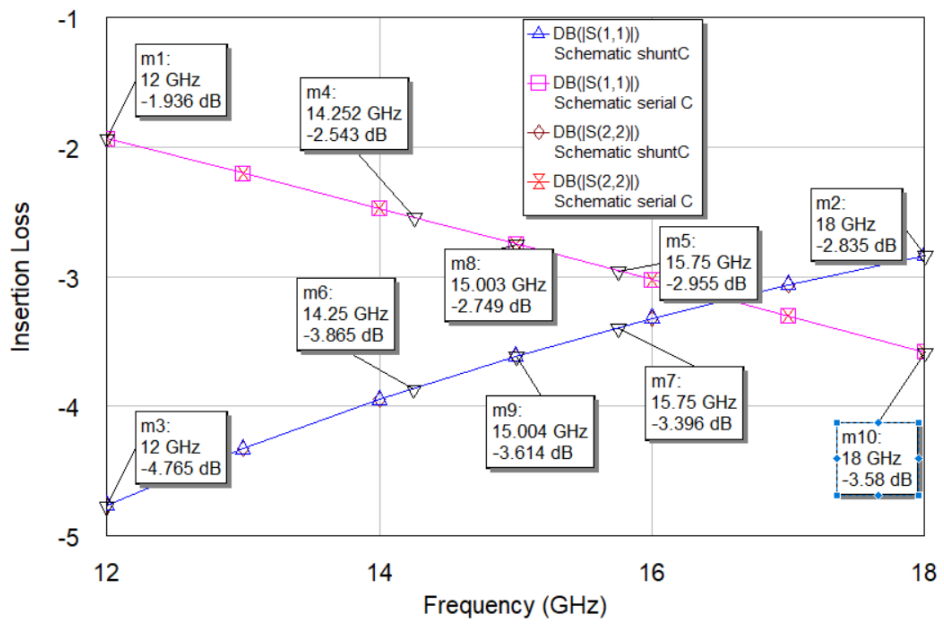


Figure 8.26 ILN via SC or SHC separated by UE over Ku-band at 15 GHz

8.2 PSN via Capacitors and Inductors Separated by UE

In Figure 8.27, the circuit has three lumped elements and two-unit elements. Normalized generated impedance has a resistance (1Ω), and normalized load impedance has a resistance (1Ω).

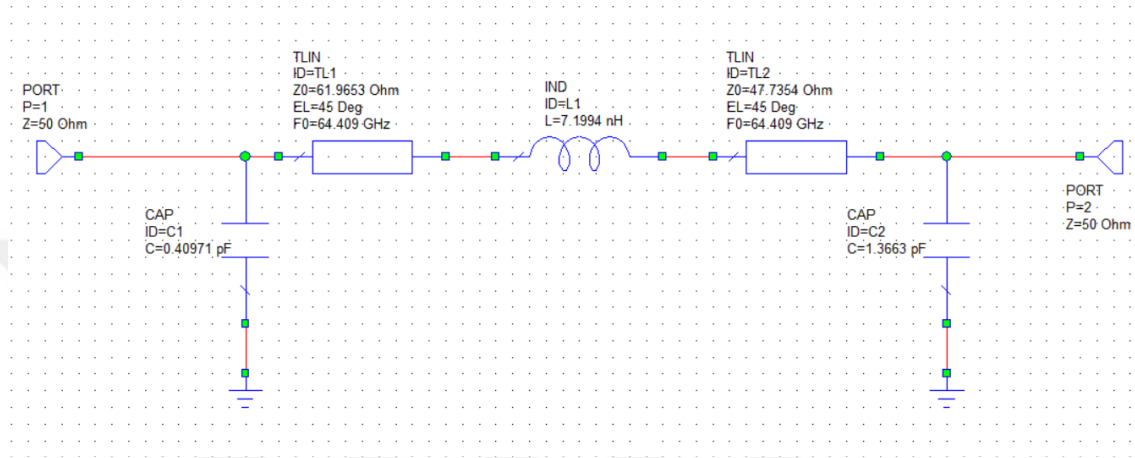


Figure 8.27 LPPSN via mixed lumped elements separated by UE at 1GHz

The scattering parameters are defined in equations (3.26-3.27). $g(p,\lambda)$, $h(p,\lambda)$, and $f(p,\lambda)$ polynomials are written in equations (3.32-37).

Independent coefficients (h_{02} , h_{10} , h_{20} , h_{30} , h_{01}) of $h(p,\lambda)$ and the transmission delay of the unit element are assigned with random numbers. These variables are optimized in Matlab. The constant values are $h_{00}=0$ and $g_{00}=1$. The method of the optimization process is Non-Linear Least Square Method. The maximum transducer power gain is equal to 1, and the magnitude of S_{21} should also be equal to 1. With this condition and equation (3.27), $|f(p,\lambda)| / |g(p,\lambda)|$ should be equal to 1.

The normalized angular frequency (WL) values are between 0.95 and 1.05 with 0.01 intervals in the optimization process and written as

$$WL=0.95:0.01:1.05 .$$

Variables in v matrix are assigned with random values between 0 and 1 that represent independent coefficients of $h(p,\lambda)$ and transmission delay of the unit element, respectively. v matrix is written as

$$v=[0.4314 \ 0.9106 \ 0.1818 \ 0.2638 \ 0.1455 \ 0.1361] \ .$$

With v matrix, independent coefficients of $g(p,\lambda)$ ($g_{02}, g_{10}, g_{20}, g_{30}, g_{01}$) are calculated via equation (3.33) for lumped elements (first column- $g_{00}, g_{10}, g_{20}, g_{30}$) and equation (3.34) for unit element (first row- g_{02}, g_{01}, g_{00}). $g(p)$ and $g(\lambda)$ polynomial roots are chosen in left half plane because the polynomials are strictly Hurwitz.

The optimization process is repeated as described in Section 6. Boundaries of initial values in matrix v are defined as lower bound (lowb) and upper bound (upperb)

$$\text{Lowb}=[-\text{Inf} \ -\text{Inf} \ -\text{Inf} \ -\text{Inf} \ -\text{Inf} \ 0.01] \ ,$$

$$\text{upperb}=[-0.00001 \ \text{Inf} \ \text{Inf} \ \text{Inf} \ \text{Inf} \ \text{Inf}] \ .$$

The total error of phase and transducer power gain is calculated via equation (6.7) to get optimized results as

$$Y=[-0.0250 \ 0.1359 \ 0.1734 \ 0.2639 \ 0.1698 \ 0.0122] \ .$$

Y matrix contains independent coefficients of $h(p,\lambda)$ and transmission delay of the unit element, respectively. The transmission delay value of the unit element is 0.0122. The equations (3.33-3.34) are used to calculate independent variables of $g(p,\lambda)$ ($g_{02}, g_{10}, g_{20}, g_{30}, g_{01}$).

After this calculation, equations (4.35-41) are used to calculate dependent coefficients in $g(p,\lambda)$ and $h(p,\lambda)$ polynomials and scattering parameters.

The coefficient matrix of $g(p,\lambda)$ and $h(p,\lambda)$ are written as

$$M_h = \begin{bmatrix} 0 & 0.1698 & 0.2639 \\ 0.1734 & -0.8769 & -0.5785 \\ -0.1359 & -0.2124 & 0 \\ -0.0250 & 0 & 0 \end{bmatrix},$$

$$M_g = \begin{bmatrix} 1 & 2.0242 & 1.0342 \\ 0.7313 & 1.4509 & 0.5785 \\ 0.2524 & 0.2124 & 0 \\ 0.0250 & 0 & 0 \end{bmatrix}.$$

Normalized lumped and distributed elements values are calculated via equations in Subsection 5.4. The normalized components values are $C_1=0.1287$, $L_2=0.9047$, $C_3=0.4292$ and $Z_1=1.8995$, $Z_2=1.2491$. The normalized frequency of the unit element in Microwave Office Tool is 10.2539.

Denormalized capacitor values at 1 GHz are calculated via equation (7.1). Denormalized inductor values are calculated via equation (7.2). Denormalized distributed element values are calculated via equation (7.3). Denormalized lumped element values and denormalized distributed element values are $C_1=0.40971$ pF, $L_2=7.1994$ nH, $C_3=1.3663$ pF, and $Z_1=1.2393$ Ω , $Z_2=0.9547$ Ω , respectively. Denormalized generator impedance value is $Z=50$ Ω . Denormalized load impedance value is $Z=50$ Ω . The normalized frequency of the unit element in Microwave Office Tool is 64.409 GHz.

Denormalized capacitor values at 1 GHz are calculated via equation (7.1). Denormalized inductor values are calculated via equation (7.2). Denormalized distributed element values are calculated via equation (7.3). Denormalized lumped element values and denormalized distributed element values are $C_1=0.081942$ pF, $L_2=1.4399$ nH, $C_3=0.27325$ pF, and $Z_1=61.9653$ Ω , $Z_2=47.7354$ Ω , respectively. Denormalized generator impedance value is $Z=50\Omega$. Denormalized load impedance value is $Z=50\Omega$. The normalized frequency of the unit element in Microwave Office Tool is 322.04 GHz.

Denormalized capacitor values at 1 GHz are calculated via equation (7.1). Denormalized inductor values are calculated via equation (7.2). Denormalized distributed element values are calculated via equation (7.3). Denormalized lumped element values and denormalized distributed element values are $C_1=0.040971$ pF, $L_2=0.71994$ nH, $C_3=0.31663$ pF, and $Z_1=61.6953$ Ω , $Z_2=47.7354$ Ω , respectively. Denormalized generator

impedance value is $Z=50\Omega$. Denormalized load impedance value is $Z=50\Omega$. The normalized frequency of the unit element in Microwave Office Tool is 644.09 GHz.

Denormalized capacitor values at 1 GHz are calculated via equation (7.1). Denormalized inductor values are calculated via equation (7.2). Denormalized distributed element values are calculated via equation (7.3). Denormalized lumped element values and denormalized distributed element values are $C_1=0.020485$ pF, $L_2=0.35997$ nH, $C_3=0.06831$ pF, and $Z_1=61.9653 \Omega$, $Z_2=47.7354 \Omega$, respectively. Denormalized generator impedance value is $Z=50\Omega$. Denormalized load impedance value is $Z=50\Omega$. The normalized frequency of the unit element in Microwave Office Tool is 1288.26 GHz.

Denormalized capacitor values at 1 GHz are calculated via equation (7.1). Denormalized inductor values are calculated via equation (7.2). Denormalized distributed element values are calculated via equation (7.3). Denormalized lumped element values and denormalized distributed element values are $C_1=0.016388$ pF, $L_2=0.28798$ nH, $C_3=0.054650$ pF, and $Z_1=61.9653 \Omega$, $Z_2=47.7354 \Omega$, respectively. Denormalized generator impedance value is $Z=50\Omega$. Denormalized load impedance value is $Z=50\Omega$. The normalized frequency of the unit element in Microwave Office Tool is 1610.2 GHz.

Denormalized capacitor values at 1 GHz are calculated via equation (7.1). Denormalized inductor values are calculated via equation (7.2). Denormalized distributed element values are calculated via equation (7.3). Denormalized lumped element values and denormalized distributed element values are $C_1=0.013657$ pF, $L_2=0.23998$ nH, $C_3=0.045542$ pF, and $Z_1=61.9653 \Omega$, $Z_2=47.7354 \Omega$, respectively. Denormalized generator impedance value is $Z=50\Omega$. Denormalized load impedance value is $Z=50\Omega$. The normalized frequency of unit elements in Microwave Office Tool is 1932.3 GHz.

Denormalized capacitor values at 100 GHz are calculated via equation (7.1). Denormalized inductor values are calculated via equation (7.2). Denormalized distributed element values are calculated via equation (7.3). Denormalized lumped element values and denormalized distributed element values are $C_1=4.0971$ fF, $L_2=0.071994$ nH, $C_3=13.663$ fF, and $Z_1=61.9653 \Omega$, $Z_2=47.7354 \Omega$, respectively. Denormalized generator

impedance value is $Z=50\Omega$. Denormalized load impedance value is $Z=50\Omega$. The normalized frequency of the unit element in Microwave Office Tool is 6440.9 GHz.

In Figure 8.28, the circuit has three lumped and two-unit elements. The normalized generated impedance has a resistance (1Ω), and the normalized load impedance has a resistance (1Ω).

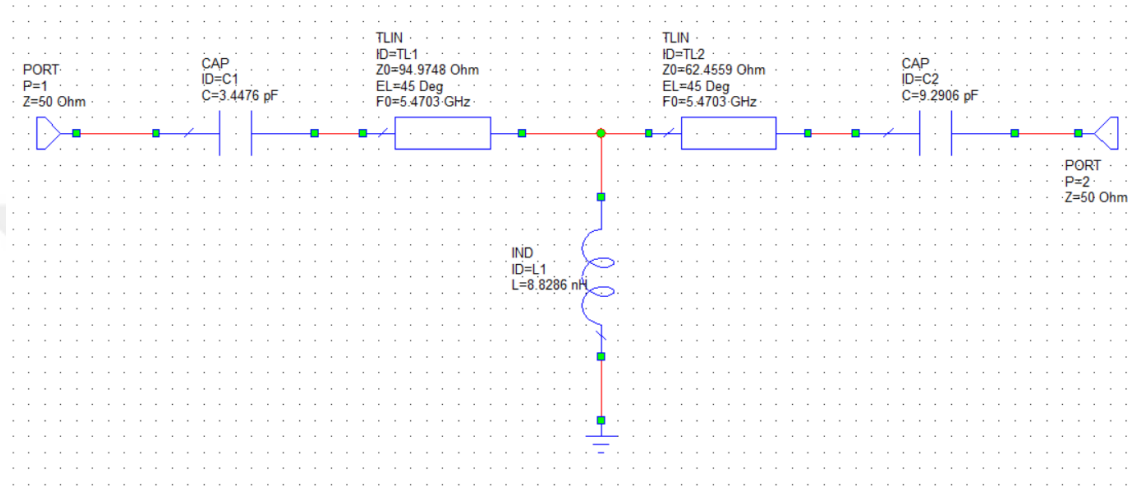


Figure 8.28 HPPSN via mixed lumped elements separated by UE at 1GHz

The scattering parameters are defined in equations (3.26-3.27). $g(p,\lambda)$, $h(p,\lambda)$, and $f(p,\lambda)$ polynomials are defined in equations (3.32-37).

Independent parameters (h_{32} , h_{10} , h_{20} , h_{30} , h_{31}) in the coefficient matrix of $h(p,\lambda)$ and the transmission delay of unit elements are assigned with random numbers. These variables are optimized in Matlab. The constant values are $h_{00}=0$ and $g_{00}=1$. The method in the optimization process is Non-Linear Least Square Method. The maximum transducer power gain is equal to 1, and the magnitude of S_{21} should also be equal to 1. Via equation (3.27), $|f(p,\lambda)| / |g(p,\lambda)|$ should be equal to 1.

The normalized angular frequency (WL) values are between 0.95 to 1.05 with 0.01 intervals and are written as

$$WL=0.95:0.01:1.05 .$$

The random variables in v matrix are written as

$$v=[0.4314 \ 0.9106 \ 0.1818 \ 0.2638 \ 0.1455 \ 0.1361] .$$

With these parameters, the independent coefficients of $g(p,\lambda)$ ($g_{32}, g_{10}, g_{20}, g_{30}, g_{31}$) are calculated via equations (3.33) for lumped elements (first column- $g_{00}, g_{10}, g_{20}, g_{30}$) and equation (3.34) for unit element (last row- g_{32}, g_{31}, g_{30}). Roots of $g(p)$ and $g(\lambda)$ polynomial are chosen in left half plane because these polynomials are strictly Hurwitz.

The optimization process is executed as described in Section 6. Boundaries of initial values in matrix v are defined as lower bound (lowb) and upper bound (upperb)

$$\text{Lowb}=[-\text{Inf} \ -\text{Inf} \ -\text{Inf} \ 0.00001 \ -\text{Inf} \ 0.01] ,$$

$$\text{upperb}=[\text{Inf} \ \text{Inf} \ \text{Inf} \ \text{Inf} \ \text{Inf} \ \text{Inf}] .$$

The total error of phase and transducer power gain is calculated via equation (6.10) to get optimized results as

$$Y=[0.4315 \ 0.9108 \ 0.1823 \ 0.2617 \ 0.1426 \ 0.1436] .$$

Y matrix contains independent coefficients of $h(p,\lambda)$ and transmission delay of the unit element, respectively. The transmission delay value of the unit element is 0.1436. The equations (3.33-3.34) are used to calculate independent variables of $g(p,\lambda)$ ($g_{32}, g_{10}, g_{20}, g_{30}, g_{31}$). g_{00} is equal to one.

After this calculation, equations (4.76-81) are used to calculate the dependent coefficients of $g(p,\lambda)$ and $h(p,\lambda)$ polynomials and scattering parameters.

The coefficient matrix of $g(p, \lambda)$ and $h(p, \lambda)$ polynomials are written as

$$M_h = \begin{bmatrix} 0.5971 & 0 & 0 \\ 0.3328 & 2.3046 & 0 \\ 0.4387 & 0.8056 & 1.9209 \\ 0 & 0.4277 & 0.4760 \end{bmatrix} ,$$

$$M_g = \begin{bmatrix} 0.5971 & 0 & 0 \\ 1.2409 & 2.3046 & 0 \\ 1.6353 & 3.2418 & 1.9209 \\ 1 & 2.0971 & 1.1075 \end{bmatrix} .$$

Normalized lumped and distributed elements values are calculated via equations in Subsection 5.3. The normalized components values are $C_1=1.0831$, $L_2=1.0194$, $C_3=2.9187$, $Z_1=1.8995$, $Z_2=1.2491$. The normalized frequency of the unit element in Microwave Office Tool is 0.8709.

Denormalized capacitor values at 1 GHz are calculated via equation (7.1). Denormalized inductor values are calculated via equation (7.2). Denormalized distributed element values are computed via equation (7.3). Denormalized lumped element values and denormalized distributed element values are $C_1=3.4476$ pF, $L_2=8.8286$ nH, $C_3=9.2906$ pF, and $Z_1=94.9748 \Omega$, $Z_2=62.4559 \Omega$., respectively. Denormalized generator impedance is $Z=50\Omega$. Denormalized load impedance is $Z=50\Omega$. The normalized frequency of the unit element in Microwave Office Tool is 5.47036 GHz.

Transducer power gain responses of high-pass and low-pass networks are given in Figure 8.29. Transducer power gain changes between 0.962 and 0.978 for the high-pass network. Transducer power gain changes between 0.949 and 0.933 for low-pass networks over 10% bandwidth at 1 GHz.

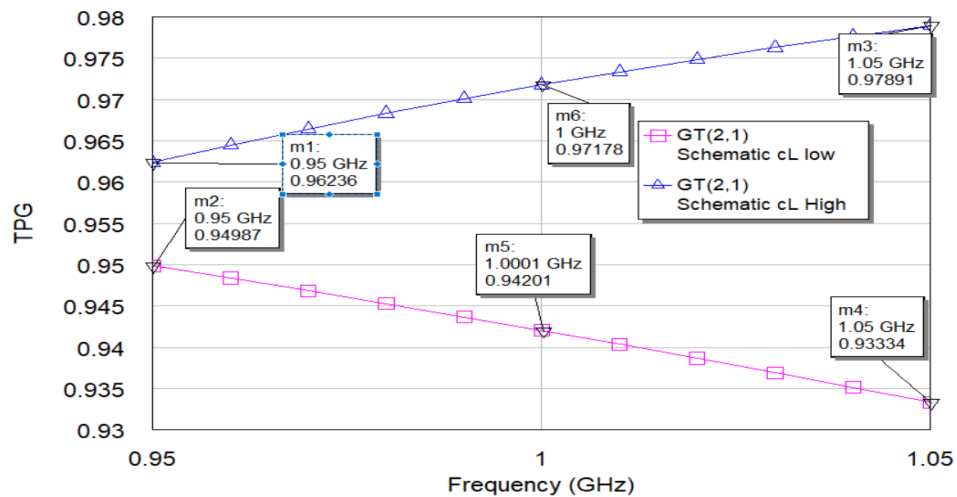


Figure 8.29 TPG of network via mixed lumped elements separated by UE at 1 GHz

The total phase response of high-pass and low-pass networks is 89.8° , as seen in Figure 8.30. The phase response of high-pass and low-pass networks is insufficient, with $+2.2^\circ$ and -1.8° phase errors around 1 GHz over 10% bandwidth (92.1° at 0.95 GHz and 88° at 1.05 GHz).

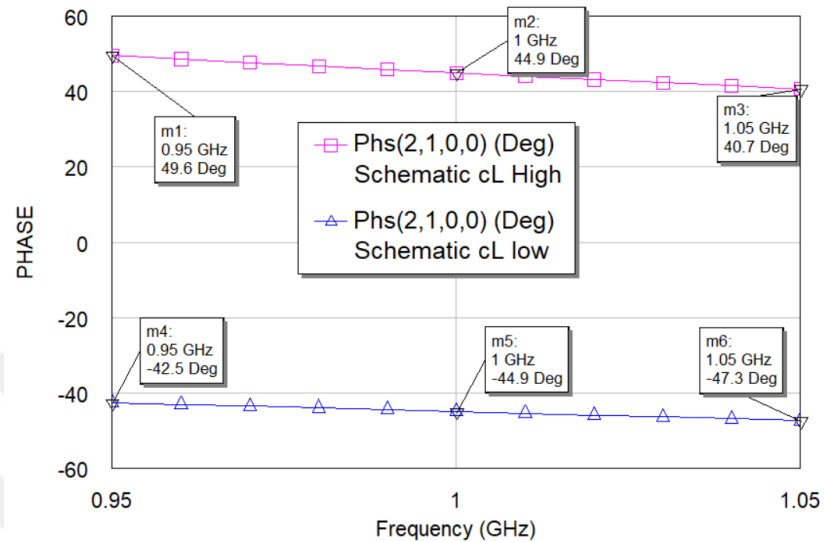


Figure 8.30 PRN via mixed lumped element separated by UE at 1 GHz

Denormalized capacitor values at 5 GHz are calculated via equation (7.1). Denormalized inductor values are calculated via equation (7.2). Denormalized distributed element values are calculated via equation (7.3). Denormalized lumped element values and denormalized distributed element values are $C_1=0.68952$ pF, $L_2=1.7657$ nH, $C_3=1.8581$ pF, and $Z_1=94.9748$ Ω , $Z_2=624559$ Ω ., respectively. Denormalized generator impedance is $Z=50\Omega$. Denormalized load impedance is $Z=50\Omega$. The normalized frequency of the unit element in Microwave Office Tool is 27.351 GHz.

Transducer power gain responses of high-pass and low-pass networks are given in Figure 8.31. Transducer power gain changes between 0.962 and 0.978 for the high-pass network. Transducer power gain changes between 0.949 and 0.933 for low-pass networks over 10% bandwidth at 5 GHz.

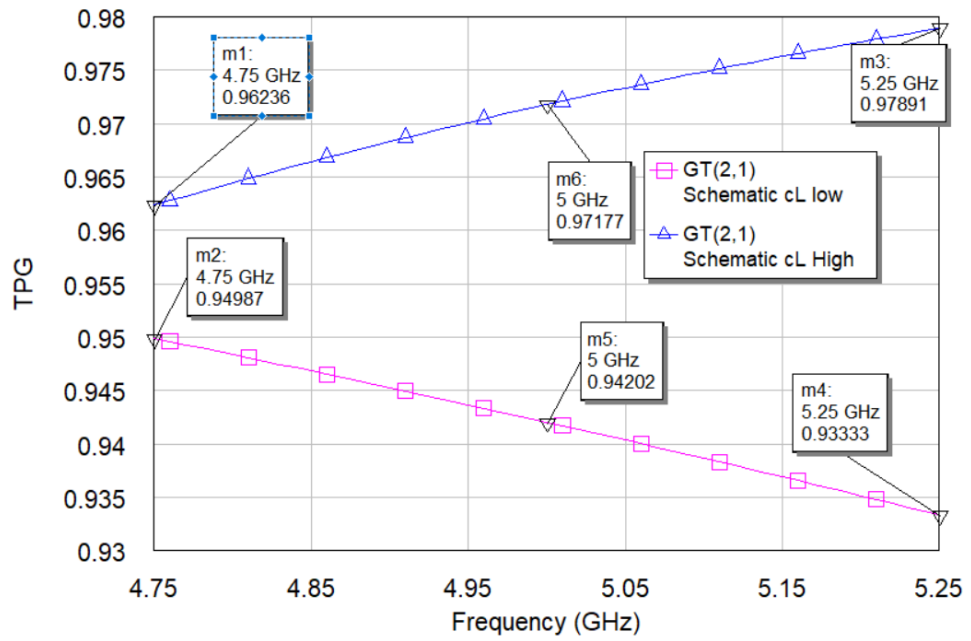


Figure 8.31 TPG of network via mixed lumped elements separated by UE at 5 GHz

The total phase response of high-pass and low-pass networks is 89.8° , as seen in Figures 8.32. The phase response of high-pass and low-pass networks is sufficient, with $+2.2^{\circ}$ and -1.8° phase errors around 5 GHz over 10% bandwidth (92.1° at 4.75 GHz and 88° at 5.25 GHz).

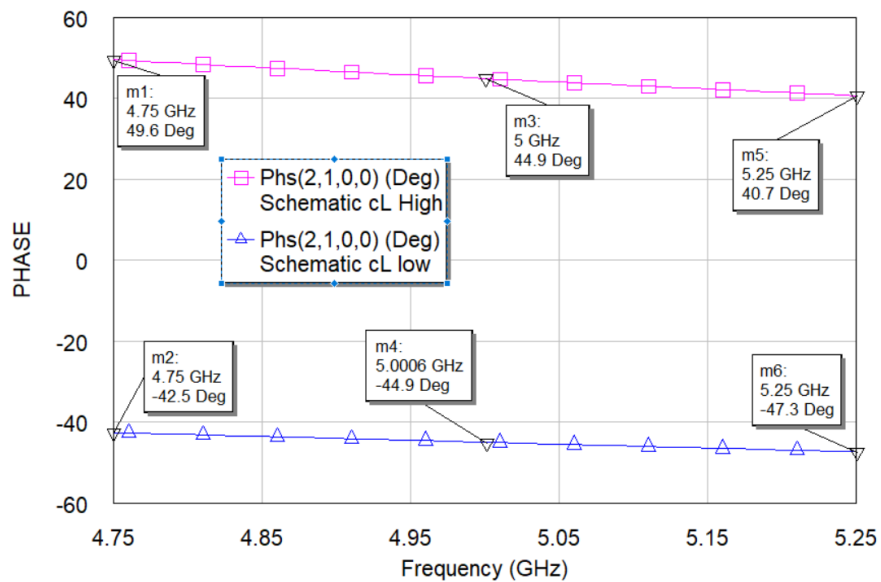


Figure 8.32 PRN via mixed lumped element separated by UE at 5 GHz

Denormalized capacitor values at 10 GHz are calculated via equation (7.1). Denormalized inductor values are calculated via equation (7.2). Denormalized distributed element values are calculated via equation (7.3). Denormalized lumped element values and denormalized distributed element values are $C_1=0.34476$ pF, $L_2=0.88286$ nH, $C_3=0.92906$ pF, and $Z_1=94.9748 \Omega$, $Z_2=62.4559 \Omega$, respectively. Denormalized generator impedance is $Z=50\Omega$. Denormalized load impedance is $Z=50\Omega$. The normalized frequency of the unit element in Microwave Office Tool is 54.703 GHz.

Transducer power gain responses of high-pass and low-pass networks are given in Figure 8.33. Transducer power gain changes between 0.962 and 0.978 for the high-pass network. Transducer power gain changes between 0.949 and 0.933 for low-pass networks over 10% bandwidth at 10 GHz.

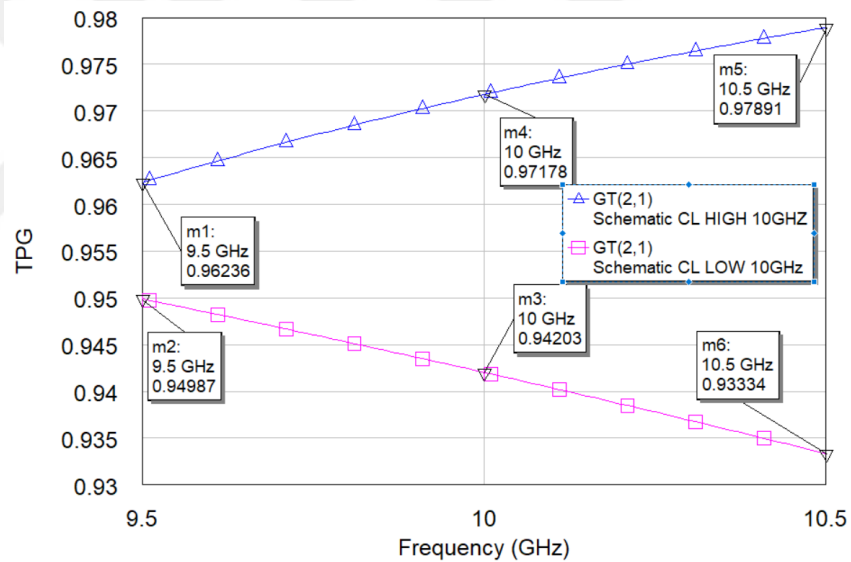


Figure 8.33 TPG of network via mixed lumped elements separated by UE at 10 GHz

The total phase response of high-pass and low-pass networks is 89.8° , as seen in Figures 8.34. The phase response of high-pass and low-pass networks is sufficient, with $+2.3^\circ$ and -1.8° phase errors around 10 GHz over 10% bandwidth (92.2° at 9.5 GHz and 88° at 10.5 GHz).

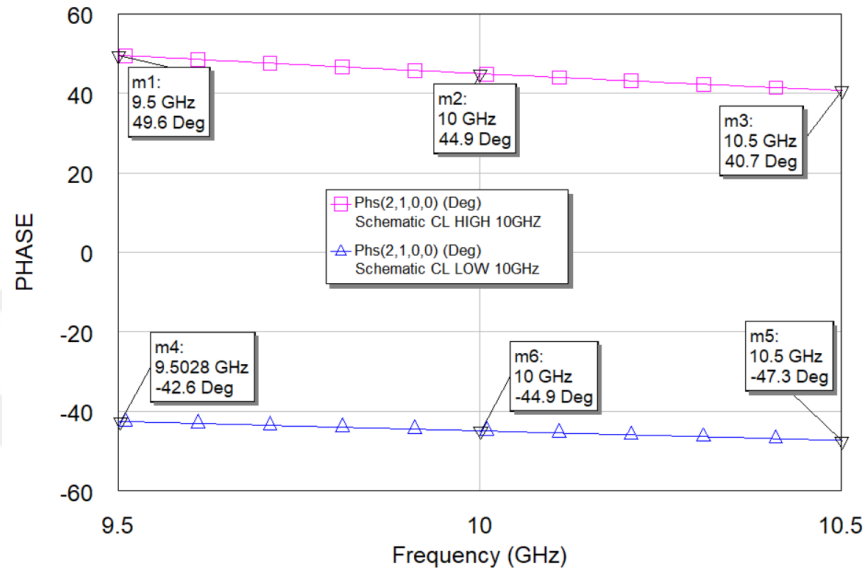


Figure 8.34 PRN via mixed lumped element separated by UE at 10 GHz

Denormalized capacitor values at 20 GHz are calculated via equation (7.1). Denormalized, inductor values are calculated via equation (7.2). Denormalized distributed element values are calculated via equation (7.3). Denormalized lumped element values and denormalized distributed element values are $C_1=0.17238$ pF, $L_2=0.44143$ nH, $C_3=0.46453$ pF, and $Z_1=94.9748 \Omega$, $Z_2=62.4559 \Omega$., respectively. Denormalized generator impedance is $Z=50\Omega$. Denormalized load impedance is $Z=50\Omega$. The normalized frequency of the unit element in Microwave Office Tool is 109.41GHz.

Transducer power gain responses of high-pass and low-pass networks are given in Figure 8.35. Transducer power gain changes between 0.962 and 0.978 for the high-pass network. Transducer power gain changes between 0.949 and 0.933 for low-pass networks over 10% bandwidth at 20 GHz.

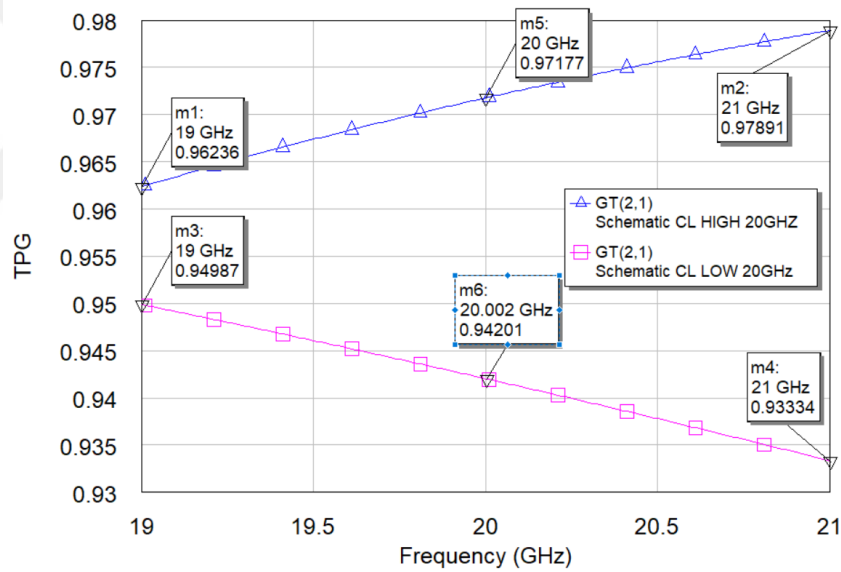


Figure 8.35 TPG of network via mixed lumped elements separated by UE at 20 GHz

The total phase response of high-pass and low-pass networks is 89.8° , as seen in Figures 8.36. The phase response of high-pass and low-pass networks is sufficient, with $+2.2^\circ$ and -1.8° phase errors around 20 GHz over 10% bandwidth (92.1° at 19 GHz and 88° at 21 GHz).

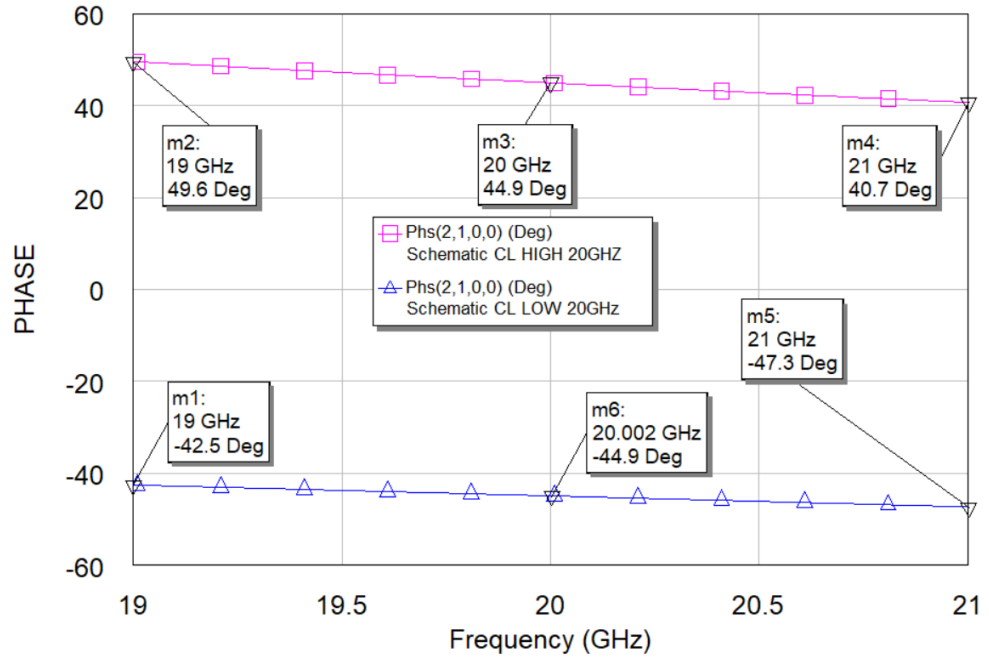


Figure 8.36 PRN via mixed lumped element separated by UE at 20 GHz

Denormalized capacitor values at 25 GHz are calculated via equation (7.1). Denormalized inductor values are calculated via equation (7.2). Denormalized distributed element values are calculated via equation (7.3). Denormalized lumped element values and denormalized distributed element values are $C_1=0.13790$ pF, $L_2=0.35314$ nH, $C_3=0.37162$ pF, and $Z_1=94.9748 \Omega$, $Z_2=62.4559 \Omega$, respectively. Denormalized generator impedance is $Z=50\Omega$. Denormalized load impedance is $Z=50\Omega$. The normalized frequency of the unit element in Microwave Office Tool is 136.76 GHz.

Transducer power gain responses of high-pass and low-pass networks are given in Figure 8.37. Transducer power gain changes between 0.962 and 0.978 for the high-pass network. Transducer power gain changes between 0.949 and 0.933 for low-pass networks over 10% bandwidth at 25 GHz.

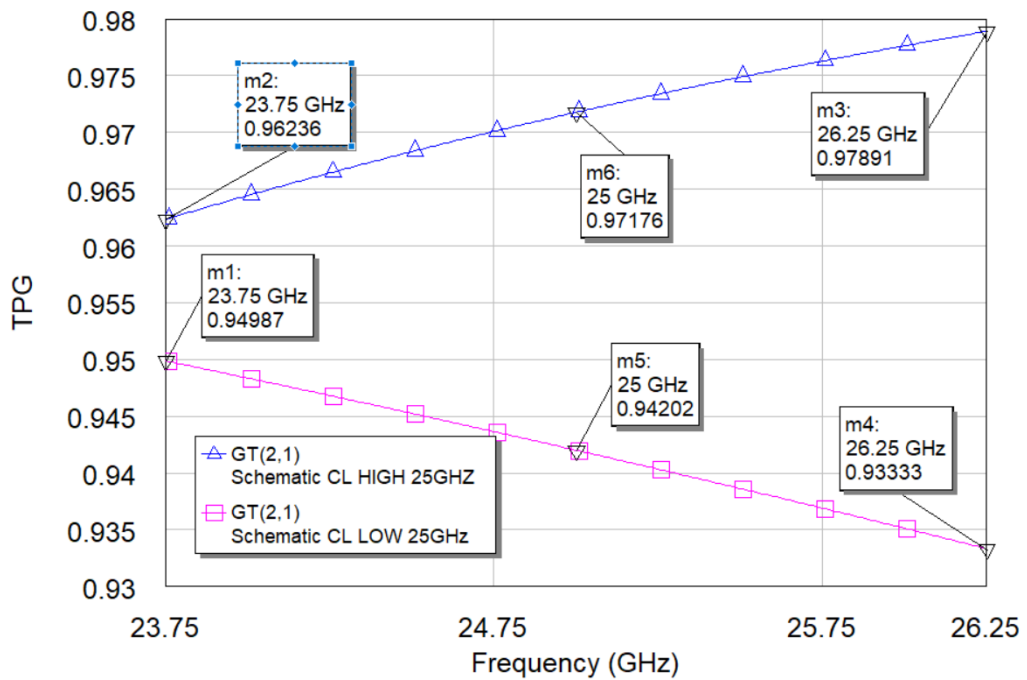


Figure 8.37 TPG of network via mixed lumped elements separated by UE at 25 GHz

The total phase response of high-pass and low-pass networks is 89.8° , as seen in Figures 8.38. The phase response of high-pass and low-pass networks is sufficient, with $+2.1^\circ$ and -1.8° phase errors around 25 GHz over 10% bandwidth (92.1° at 23.75 GHz and 88° at 26.25 GHz).

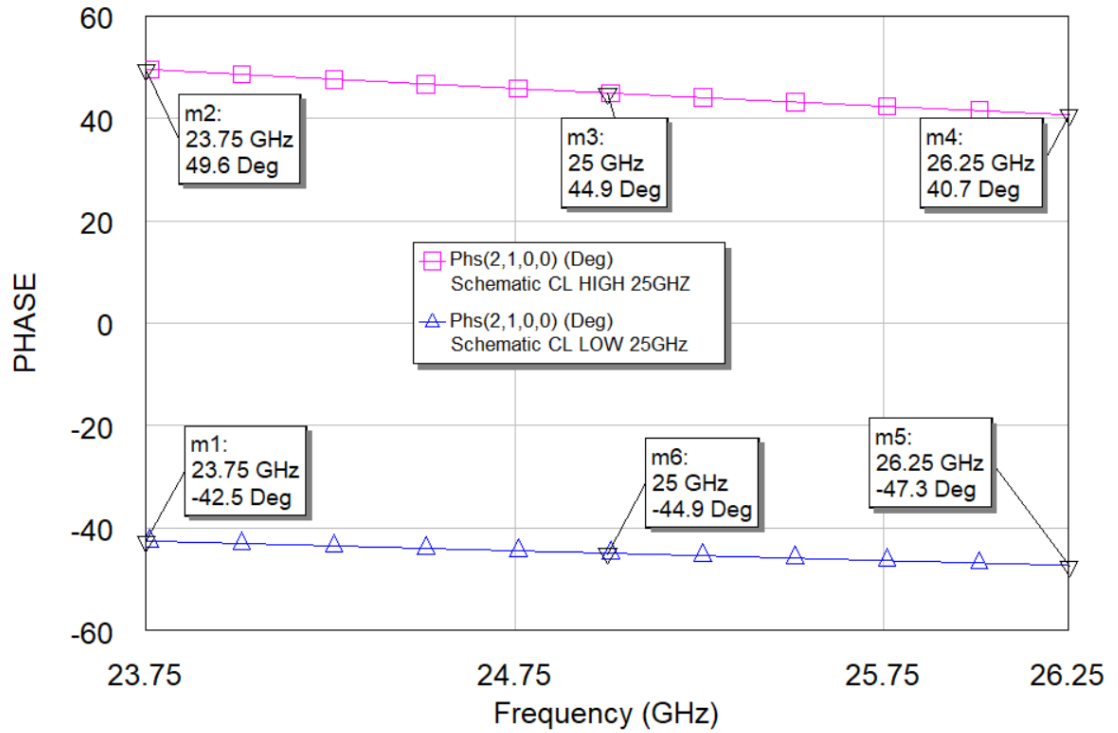


Figure 8.38 PRN via mixed lumped element separated by UE at 25 GHz

Denormalized capacitor values at 30 GHz are calculated via equation (7.1). Denormalized inductor values are calculated via equation (7.2). Denormalized distributed element values are calculated via equation (7.3). Denormalized lumped element values and denormalized distributed element values are $C_1=0.11492$ pF, $L_2=0.29429$ nH, $C_3=0.30969$ pF, and $Z_1=94.97448$ Ω , $Z_2=62.4559$ Ω ., respectively. Denormalized generator impedance is $Z=50\Omega$. Denormalized load impedance is $Z=50\Omega$. The normalized frequency of the unit element in Microwave Office Tool is 164.11 GHz.

Transducer power gain responses of high-pass and low-pass networks are given in Figure 8.39. Transducer power gain changes between 0.962 and 0.978 for the high-pass network. Transducer power gain changes between 0.949 and 0.933 for low-pass networks over 10% bandwidth at 30 GHz.

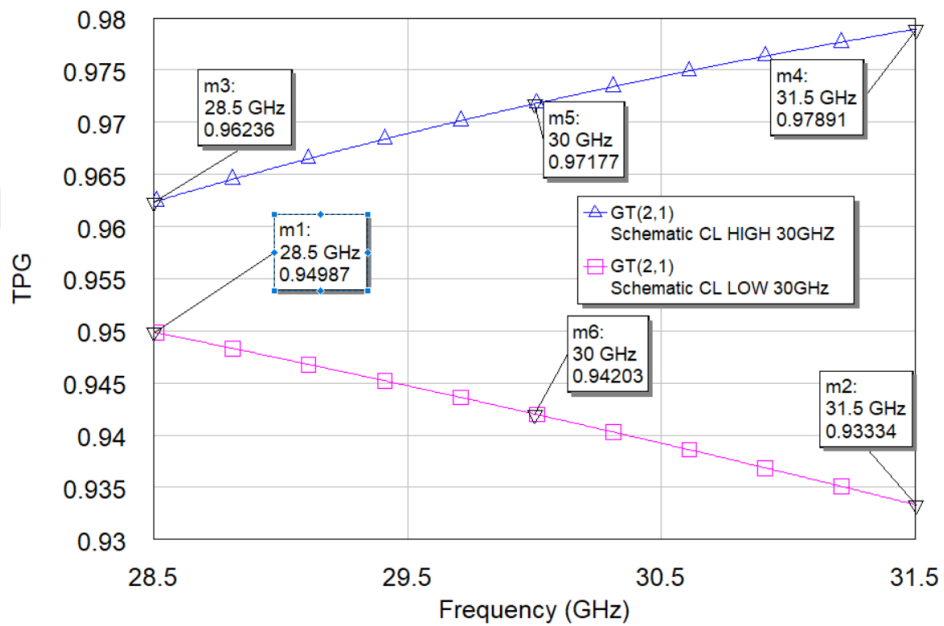


Figure 8.39 TPG of network via mixed lumped elements separated by UE at 30 GHz

The total phase response of high-pass and low-pass networks is 89.8° , as seen in Figure 8.40. The phase response of high-pass and low-pass networks is sufficient, with $+2.2^\circ$ and -1.8° phase errors around 30 GHz over 10% bandwidth (92.1° at 28.5 GHz and 88° at 31.5 GHz).

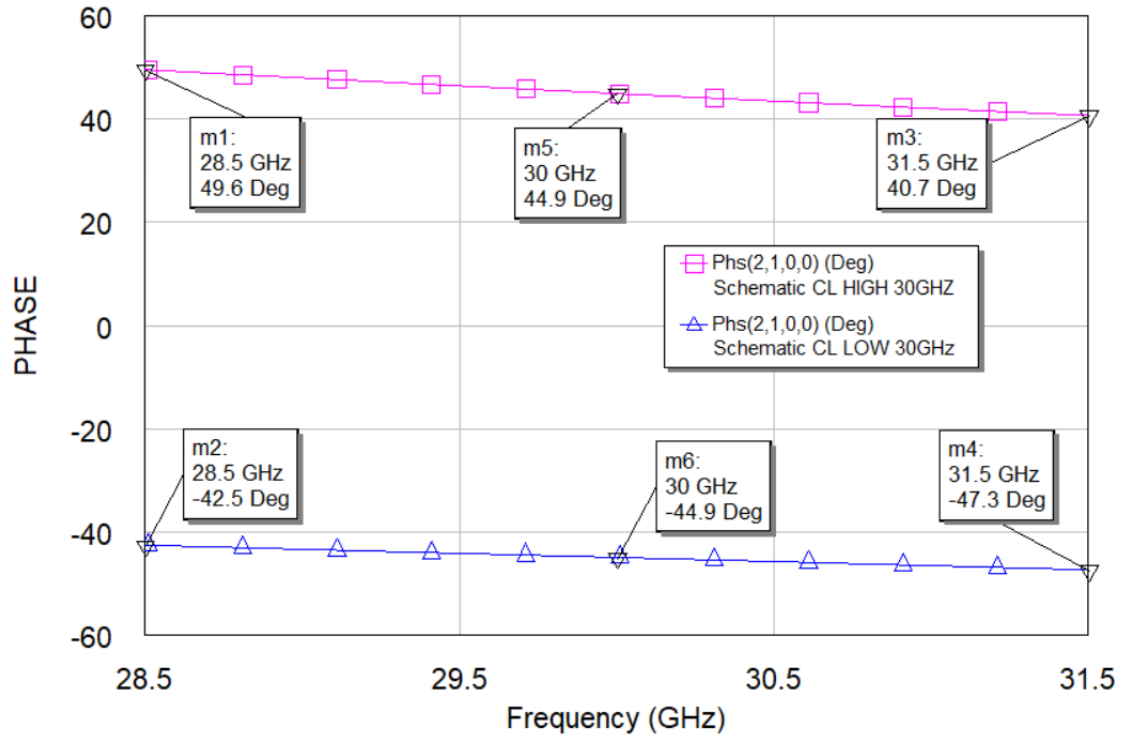


Figure 8.40 PRN via mixed lumped element separated by UE at 30 GHz

Denormalized capacitor values at 100 GHz are calculated via equation (7.1). Denormalized inductor values are calculated via equation (7.2). Denormalized distributed element values are calculated via equation (7.3). Denormalized lumped element values and denormalized distributed element values are $C_1=0.034476$ pF, $L_2=0.088286$ nH, $C_3=0.092906$ pF, and $Z_1=94.9748$ Ω , $Z_2=62.4559$ Ω ., respectively. Denormalized generator impedance is $Z=50\Omega$. Denormalized load impedance is $Z=50\Omega$. The normalized frequency of the unit element in Microwave Office Tool is 5470.3 GHz.

Transducer power gain responses of high-pass and low-pass networks are given in Figure 8.41. Transducer power gain changes between 0.962 and 0.978 for the high-pass network. Transducer power gain changes between 0.949 and 0.933 for low-pass networks over 10% bandwidth at 100 GHz.

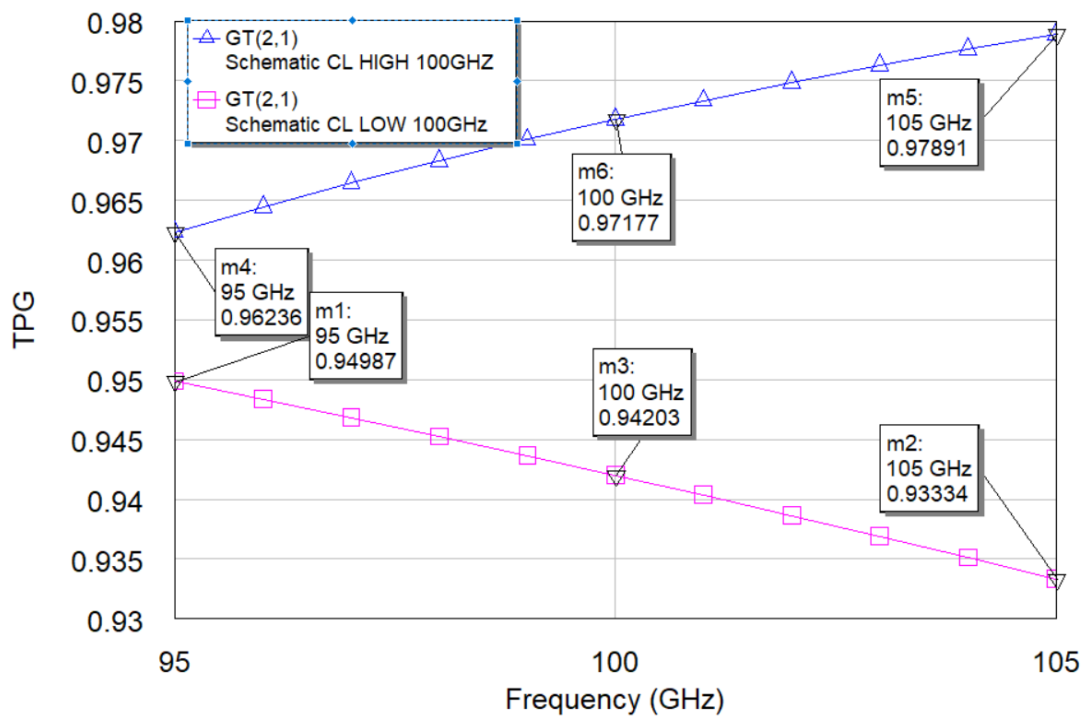


Figure 8.41 TPG via mixed lumped elements separated by UE at 100 GHz

The total phase response of high-pass and low-pass networks is 89.8° , as seen in Figure 8.42. The phase response of high-pass and low-pass networks is sufficient, with $+2.2^\circ$ and -1.8° phase errors around 100 GHz over 10% bandwidth (92.1° at 95 GHz and 88° at 105 GHz).

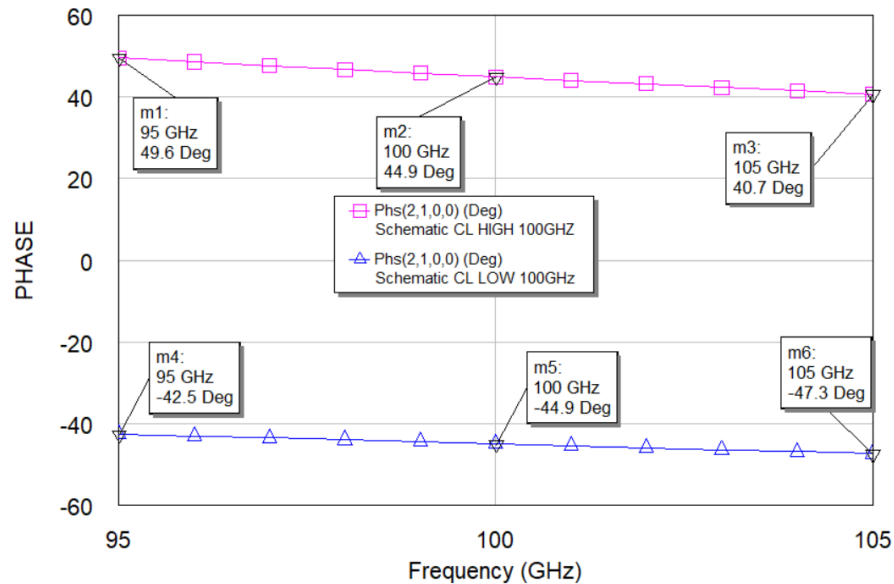


Figure 8.42 PRN via mixed lumped element separated by UE at 100 GHz

In response, networks on all central frequencies at 10% desired bandwidth have a maximum ± 2.2 phase errors, and insertion loss is lower than 11.76 dB at 1.05 GHz, as seen in Figure 8.33. In this design, increasing in bandwidth is proportional to phase error. As seen in Figure 8.34, the phase error is ± 4 around 1 GHz. Reliable communication is available at 10% narrowband at this design for long wireless communication with an acceptable phase error rate and high power handing capability. In long ranges, smart antennas direct radiation signals to desired directions electronically to provide fast tracking for radar systems and commercial communication systems, including at high central frequencies. Two types of phase shifters show an inverse relation between transducer power gain and phase responses. Network via series capacitors and shunt capacitors separated by transmission line has the advantage of low phase variations in broadband and narrowband. Still, it has higher insertion loss than described studies [19,26,44,48] and network via mixed lumped elements separated by the transmission line.

Network via mixed lumped elements separated by transmission line phase shifter has low insertion loss at 10% bandwidths and higher phase error rate than network via series capacitors and shunt capacitors separated by the transmission line. Moreover, the phase error rate is dramatically increased with bandwidth.

This design has a maximum $+0.3^{\circ}$ phase error around 90° at center 1 GHz for %10 bandwidth, and insertion loss is better than 72.78 dB. This design has $+2.87^{\circ}$ error at 0.8 GHz, and $+1.89^{\circ}$ error at 1.2 GHz around 90° at center 1 GHz for %40 bandwidth, and insertion loss is better than 27.47 dB. This design has max $+36.01^{\circ}$ at 0.6 GHz and $+1.89^{\circ}$ at 1.2 GHz around 90° at center 1 GHz for octave bandwidth, and insertion loss is better than 27.47 dB. Results are calculated due to mathematical equations in the study [26]. The phase response of this study is indicated in Figure 20, and insertion loss is shown in Figure 21 at SubSection 8.1.

Component values of lossless two-port high/low pass network via mixed lumped elements separated by unit elements are defined in Figure 27 and Figure 28. This design has $+2.27^{\circ}$ phase error at 0.95 GHz, and -1.05 at 1.05 GHz around 89.83° at center 1 GHz for %10 bandwidth, and insertion loss is better than 11.76 dB. This design has $+12.39^{\circ}$ phase error at 0.8 GHz and -5.53° error at 1.2 GHz around 89.83° at center 1 GHz for %40 bandwidth, and insertion loss is better than 10.51 dB. This design has $+39.34^{\circ}$ phase error at 0.6 GHz, and -5.53° phase error at 1.2 GHz around 89.83° at 1 GHz frequency center for octave bandwidth in Figure 43, and insertion loss is better than 5.166 dB in Figure 44.

The design of a lossless two-port high/low pass network via mixed lumped elements separated by unit elements has sufficient phase responses and insertion loss rate at only 10% bandwidth. Still, it is not as good as the study's design [26]. The design has better insertion loss rates than a two-port lossless high/low pass network via series capacitors and shunt capacitors separated by unit elements in all rate bandwidth.

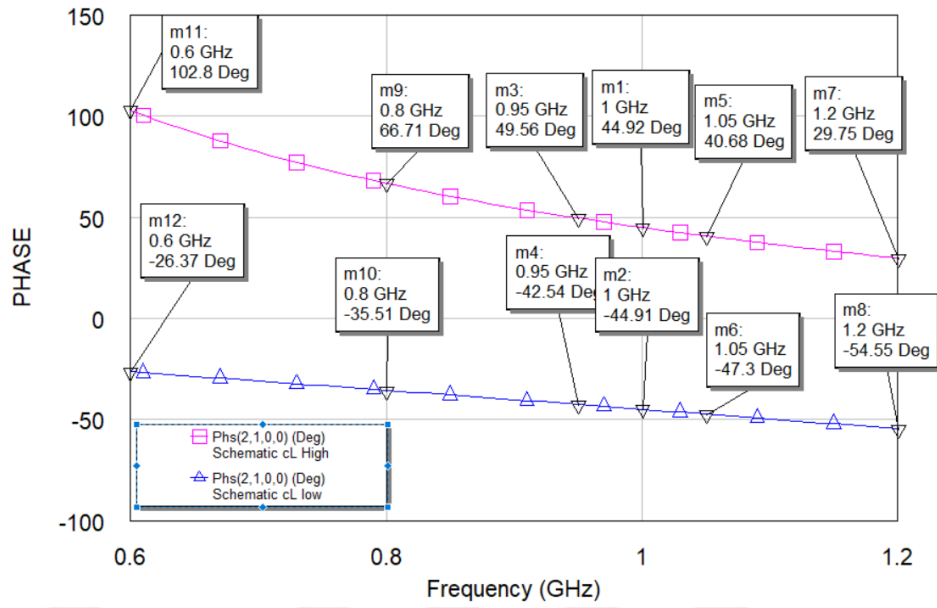


Figure 8.43 PRN via mixed lumped element separated by UE over octave bandwidth

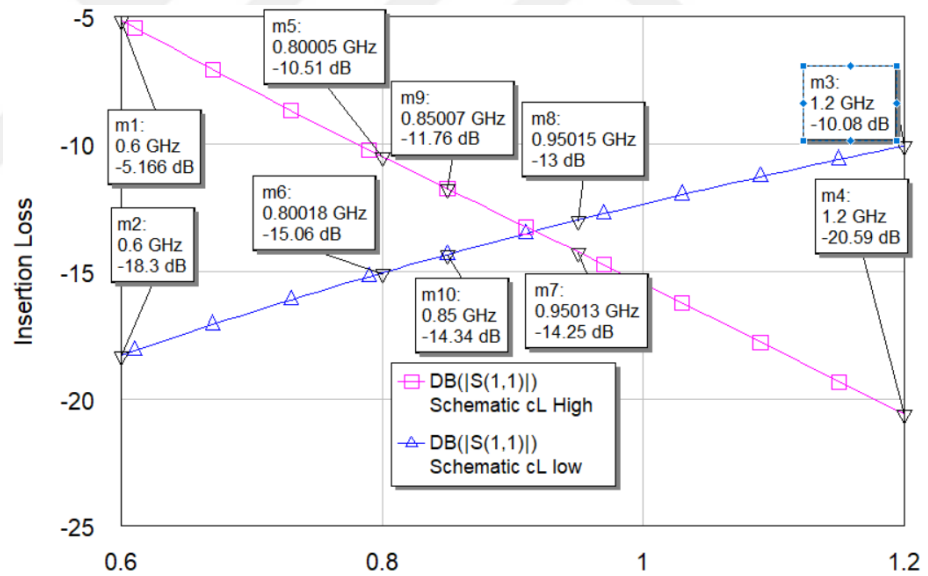


Figure 8.44 ILN via mixed lumped element separated by UE over octave bandwidth

The design consists of a resonator, two shunt transmission lines, and a reference line as seen in Figure 8.22. Phase variations are $\pm 2^\circ$ between 2.85 GHz and 7.15 GHz around 90° at center 5 GHz. The insertion loss is better than 10 dB at 129 % bandwidth with the additional effect of switch elements in the study [19].

Component values of lossless two-port high/low pass network via mixed lumped elements separated by unit elements are calculated for 5 GHz center frequency. That phase response is indicated in Figure 8.45, and insertion loss is shown in Figure 8.46. Phase responses are 135.31° at 2.85 GHz and 82.48° at 7.15 GHz at 5 GHz center frequency, but insertion loss is better than 4.357 dB. As seen, phase response and insertion loss are insufficient for 129% bandwidth. The design is appropriate for only %10 bandwidth.

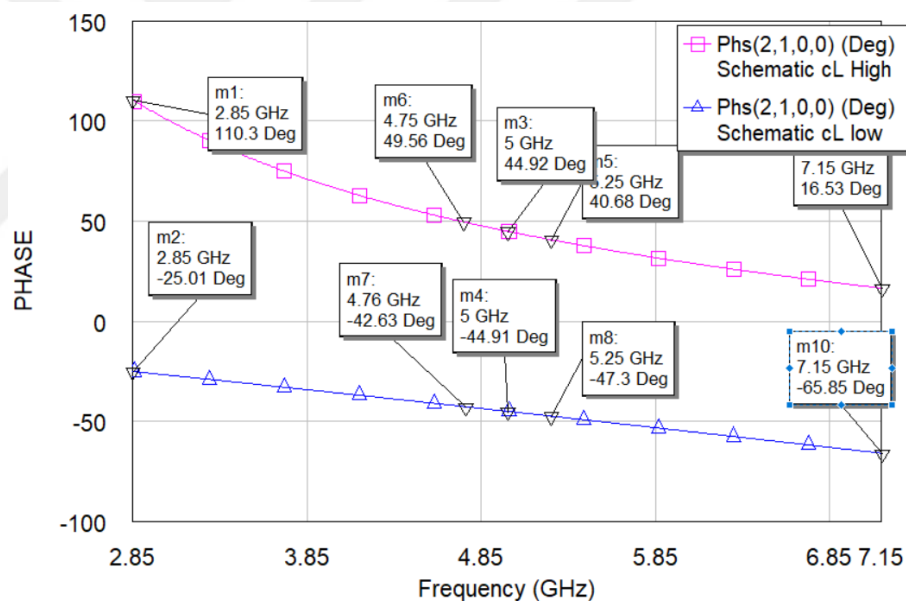


Figure 8.45 PRN via mixed lumped element separated by UE over 129% bandwidth

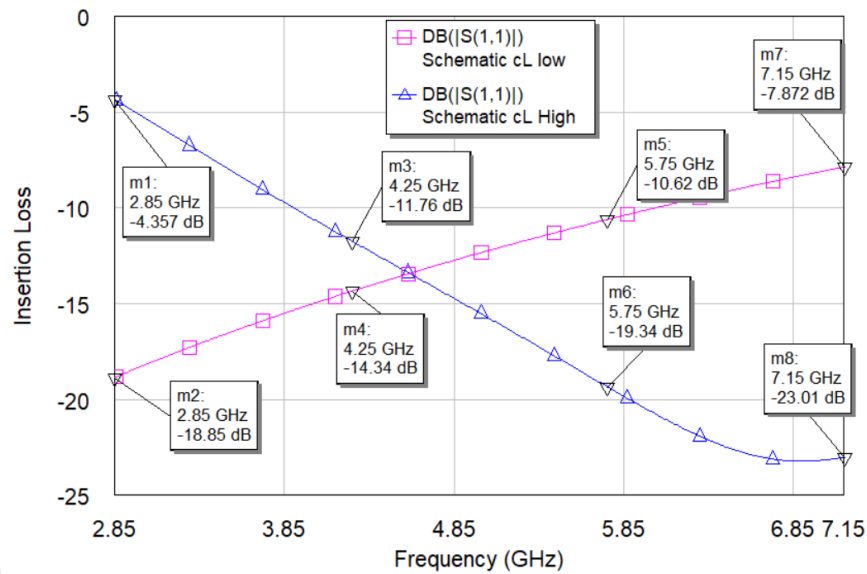


Figure 8.46 ILN via mixed lumped element separated by UE over 129% bandwidth

A Schiffman phase shifter is designed for 90° phase shifting at Ku-band (12 GHz to 18 GHz) and contains 4 port networks with a reference line and a coupled line defined time delay in the study [19]. Insertion loss is better than 10 dB, and phase variations are less than -9° at 12 GHz and $+11^\circ$ at 18 GHz.

Denormalized capacitor values at 15 GHz for the high pass network are calculated via equation (7.1). Denormalized inductor values are calculated via equation (7.2). Denormalized distributed element values are calculated via equation (7.3). Denormalized lumped element values and denormalized distributed element values are $C_1=0.22985$ pF, $L_2=0.58851$ nH, $C_3=0.61905$ pF, and $Z_1=94.9748$ Ω , $Z_2=62.4559$ Ω ., respectively. Denormalized generator impedance is $Z=50\Omega$. Denormalized load impedance is $Z=50\Omega$. The normalized frequency of the unit element in Microwave Office Tool is 82.030 GHz.

Denormalized capacitor values at 15 GHz for the low pass network are calculated via equation (7.1). Denormalized inductor values are calculated via equation (7.2). Denormalized distributed element values are calculated via equation (7.3). Denormalized lumped element values and denormalized distributed element values are $C_1=0.03336$ pF, $L_2=0.48820$ nH, $C_3=0.081642$ pF, and $Z_1=61.9653$ Ω , $Z_2=47.7354$ Ω ., respectively.

Denormalized generator impedance is $Z=50\Omega$. Denormalized load impedance is $Z=50\Omega$. The normalized frequency of unit elements in Microwave Office Tool is 827.80 GHz.

Phase response of high/low pass lossless two-port network via mixed lumped elements separated by transmission lines is 102.28° at 12 GHz, 84.25° at 18 GHz, and 89.84° at 5 GHz center frequency in Figure 8.47. Insertion loss is better than 10.17 dB in Figure 8.48 and higher than the study in [19]. This design has fewer phase variations over narrowband and tolerable insertion loss. However, this design has high rate phase variations in broadband.

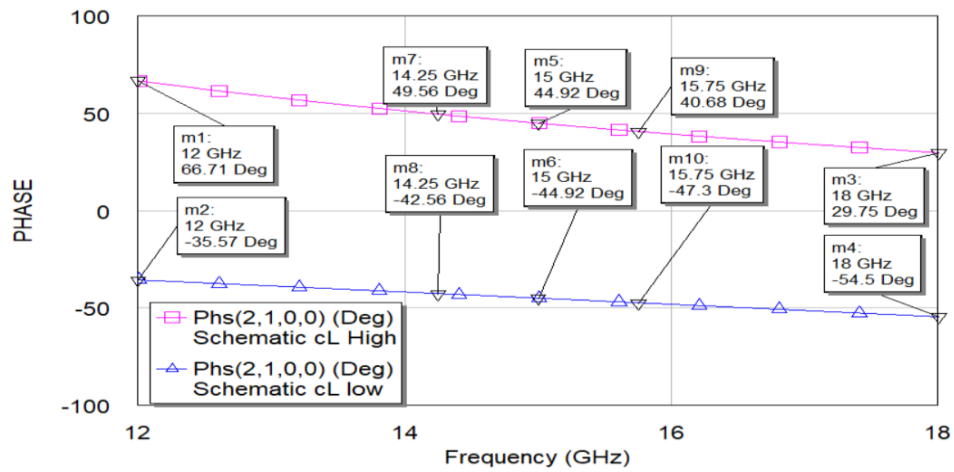


Figure 8.47 PRN via mixed lumped element separated by UE over Ku-band

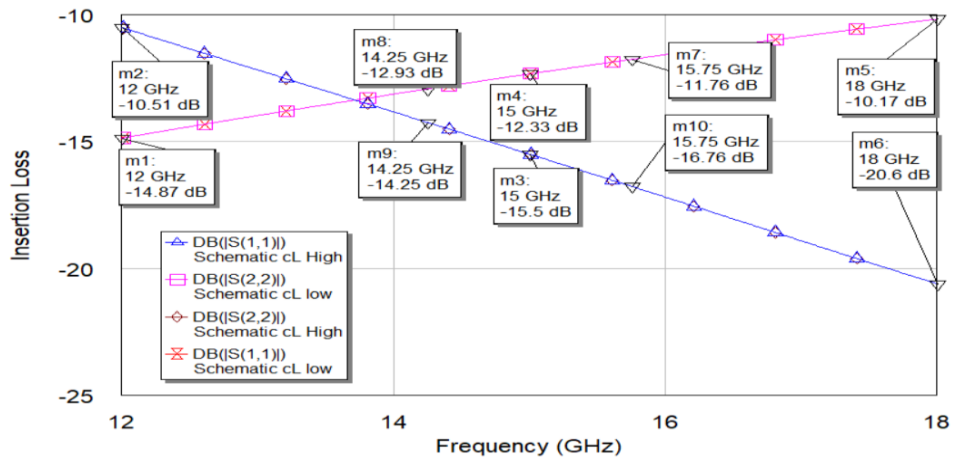


Figure 8.48 ILN via mixed lumped element separated by UE over 129% bandwidth

Phase response and insertion loss of high/low pass lossless two-port network via mixed lumped elements separated by transmission lines are good as in the study [19].



9. CONCLUSION

Phased-array antennas are used in many communication and radar systems in civilian or military applications such as global positioning, flight control, missile prevention and collision avoidance systems.

One of the elements used in a phased-array system is a switched line, reflection, loaded line or high pass / low pass phase shifter. In addition to the size advantage, high pass / low pass phase shifters are also the best choice if power consumption and phase-to-bandwidth capacities are compared to other phase shifters.

In the literature, there are many studies on high pass / low pass phase shifters. In these studies, topologies of high pass and low pass sections are determined at the beginning and element value expressions are derived. After completing the design, the results are checked if the desired phase shift is achieved, select another topology if not provided. This means to derive new element value expressions for this new topology and re-design. Furthermore, the connections between lumped elements will disrupt the performance of the phase shifter at high frequencies and result in a different phase shift than desired.

In many applications, circuits containing lumped elements are preferred because of their small sizes. But it is not possible to avoid losses caused by the connections between lumped elements at high frequencies. However, the use of these connections as circuit elements will improve the performance of the circuit. Therefore, it becomes inevitable to use circuits with mixed (lumped and distributed) elements at high frequencies.

In this thesis, high pass / low pass sections of the phase shifter consist of mixed elements. Therefore, connections between lumped elements do not cause deterioration in the performance but are used as a circuit element to achieve the desired phase shift. In the sections, four different mixed element structures are used, two of them are high pass mixed element lossless two-port and two of them are low pass mixed element lossless two-port. In one of the high pass networks, inductors and capacitors are separated by distributed elements, and in the other high pass network series capacitors are separated

by distributed elements. In one of the low pass networks, inductors and capacitors are separated by distributed elements, and in the other low pass network shunt capacitors are separated by distributed elements.

To be able to completely define a mixed element network, all the elements of coefficient matrices M_h and M_g must be calculated. In the literature, the coefficient matrices M_h and M_g of the selected three mixed element networks are obtained, and in the thesis these solutions are used. The coefficient matrices M_h and M_g defining the mixed element network with series capacitors separated by distributed elements are obtained in this thesis, and these solutions are used to form the coefficient matrices M_h and M_g .

In the thesis, the subject is to obtain phase shifting properties of mixed element high pass and low pass mixed element networks. It is necessary for a phase shifter to get the desired phase shift and maximum possible output signal level. For this purpose, firstly, phase equations of the mentioned structures are derived, and then a procedure is defined to calculate the coefficient matrices of the mixed element structure to be able to get the desired phase shift and maximum output signal level. In the defined design procedure, free parameters of the coefficient matrix M_h are initialized by the designer, and the remaining coefficients of M_h and all the coefficients of M_g are calculated.

As mentioned above, in this thesis, firstly, the necessary phase and amplitude response equations are obtained. Now it is necessary to calculate the component values of the high pass and low pass sections. Two different component value calculation process are utilized. In one of the methods, transfer scattering matrices are used. Briefly, from the calculated M_h and M_g matrices, the value of the first extracted component is calculated. Then transfer scattering matrix of the extracted component is computed. After multiplying the inverse of the transfer scattering matrix of the first component and the total transfer scattering matrix, scattering matrix of the remaining network is obtained. Then the value of the second extracted component is calculated, and the procedure is repeated until getting the termination resistance.

In the thesis, another component value calculation procedure is described. In this method, after calculating the first extracted component by using the coefficients of M_h and M_g , all the coefficients of M_h and M_g of the remaining network are separately calculated by means of the derived equations. It is seen that the precision of this method is better than the method described above.

Component values calculated via the proposed approach are normalized. So, it is necessary to calculate the real component values by means of the denormalization frequency and impedance values. In the thesis, denormalization impedance value is selected as 50 ohm, and 1 GHz, 5 GHz and 10 GHz are selected as denormalization frequency values. It is seen that the performances of the designed sections are the same at different working frequencies. So, it is enough to design high pass and low pass sections by specifying the desired phase shift, then the designed sections can be used at different real working frequencies after denormalization of all component values, it is not necessary to design all the sections for each real working frequency.

It is clear from the phase and gain graphics obtained in the design examples that the phase precision of the sections containing capacitors separated by distributed elements is better than that of the sections containing inductors, capacitors separated by distributed elements. But the gain performance of the sections containing inductors, capacitors separated by distributed elements is better than that of the sections containing capacitors separated by distributed elements.

REFERENCES

- [1] A. Aksen. "Design of lossless two-port with mixed, lumped and distributed elements for broadband matching," Ph.D. dissertation, Bochum, Ruhr University, 1994.
- [2] A. Fettweis "Some properties of scattering Hurwitz polynomials" Arch. Elektr. Übertragung.1984, vol. 38, pp. 171-176.
- [3] A. Fettweis "On the scattering matrix and the scattering transfer matrix of multidimensional lossless two-ports" Arch. Elek. Übertragung. vol. 36 no. 9 pp. 374-381 Sept. 1982.
- [4] A. Fettweis, "Cascaded synthesis of lossless two port by transfer matrix factorization," in R. Boite. Ed. Network theory, Gordon & Breach, 1972, pp: 43-103
- [5] A. Fettweis, "On the factorization of transfer matrices of lossless two-ports," in *IEEE Transactions on Circuit Theory*, vol. 17, no. 1, pp. 86-94, February 1970, doi: 10.1109/TCT.1970.1083058.
- [6] A. Kilinc and B. S. Yarman, "High Precision LC Ladder Synthesis Part I: Lowpass Ladder Synthesis via Parametric Approach," in *IEEE Transactions on Circuits and Systems I: Regular Papers*, vol. 60, no. 8, pp. 2074-2083, Aug. 2013, doi: 10.1109/TCSI.2013.2239163
- [7] A. Malczewski, S. Eshelman, B. Pillans, J. Ehmke, and C. L. Goldsmith, "X-band RF MEMS phase shifters for phased array applications," in *IEEE Microwave and Guided Wave Letters*, vol. 9, no. 12, pp. 517-519, Dec. 1999, doi: 10.1109/75.819417.
- [8] A. Sertbaş, "Two-variable scattering formulas to describe some classes of lossless two-ports with mixed lumped elements and commensurate stubs", *Turkish J. Elect. Eng. Comput. Sci.*, vol. 13, no. 2, pp. 231-239, 2005

- [9] "AWR Microwave Office," www.cadence.com, https://www.cadence.com/en_US/home/tools/system-analysis/rf-microwave-design/awr-microwave-office.html.
- [10] B. J. Edward R. S. Webb and S. Weinreb "A W-Band active phased-array antenna" *Microwave Journal*, May 1996, pp. 254-262.
- [11] B.S. Yarman, "New circuit configurations for designing 0-180 digital phase shifters," *IEE Proceedings-h Microwaves Antennas and Propagation*, vol. 134, no. 3, pp. 253-260.
- [12] B. S. Yarman, "0 degrees -360 degrees wide range digital phase shifters for large array antenna systems," *1990 IEEE International Symposium on Circuits and Systems (ISCAS)*, vol. 2, pp. 1517-1520, 1990, doi: 10.1109/ISCAS.1990.112421.
- [13] B. S. Yarman, "Novel approaches to design digital phase shifters over the complete phase plane," *Journal of Islamic Academy of Sciences*, 1990, vol. 4, pp: 14-25.
- [14] B.S. Yarman and A. Kilinc, "High Precision LC Ladder Synthesis Part II: Immittance Synthesis With Transmission Zeros at DC and Infinity," in *IEEE Transactions on Circuits and Systems I: Regular Papers*, vol. 60, no. 10, pp. 2719-2729, Oct. 2013, doi: 10.1109/TCSI.2013.2244315.
- [15] B.S. Yarman A. Kilinc and M. Un "New Digital Phase Shifter Topologies For Mobile Communication Systems" *Istanbul University Electrical and Electronics Engineering Department special report*, 2013.
- [16] Dundee, J. J. More, and N. Lab, *Levenberg--Marquardt algorithm: implementation and theory*. 1977.
- [17] D. W. Kang, H. Lee, K. H. Lee, S.-I. Jeon and S. Hong, "Design of a phase shifter with improved bandwidth using embedded series-shunt switches," *2005 European Microwave Conference*, 2005, doi: 10.1109/EUMC.2005.1610369.

- [18] D. Viveiros, D. Consonni and A. K. Jastrzebski, "A tunable all-pass MMIC active phase shifter," in *IEEE Transactions on Microwave Theory and Techniques*, vol. 50, no. 8, pp. 1885-1889, Aug. 2002, doi: 10.1109/TMTT.2002.801315.
- [19] E. Lari, G. Moradi and R. Sarrafshirazi, "Design and Fabrication of Schiffman Phase Shifter for Ku-band Applications," *2019 5th Conference on Knowledge Based Engineering and Innovation (KBEI)*, pp. 095-101, 2019, doi: 10.1109/KBEI.2019.8734962.
- [20] J. I. Alonso et al., "Low cost electronically steered antenna and receiver system for mobile satellite communications," *1996 IEEE MTT-S International Microwave Symposium Digest*, pp. 1167-1170, 1996, doi: 10.1109/MWSYM.1996.511237.
- [21] J. L. Allen, "Array antennas: New applications for an old technique," in *IEEE Spectrum*, vol. 1, no. 11, pp. 115-130, Nov. 1964, doi: 10.1109/MSPEC.1964.6500470.
- [22] J. L. Volakis, *Antenna Engineering Handbook*. USA NY New York: McGraw-Hill, 2007.
- [23] J. S. Hayden and G. M. Rebeiz, "Very low-loss distributed X-band and Ka-band MEMS phase shifters using metal-air-metal capacitors," in *IEEE Transactions on Microwave Theory and Techniques*, vol. 51, no. 1, pp. 309-314, Jan. 2003, doi: 10.1109/TMTT.2002.806520.
- [24] K. Johannsen "Mobile P-service satellite system comparison," *International Journal of Satellite Communications*, 1995, vol.13, no. 6, pp. 453-471.
- [25] K. Kurokawa, "Power Waves and the Scattering Matrix," in *IEEE Transactions on Microwave Theory and Techniques*, vol. 13, no. 2, pp. 194-202, March 1965, doi: 10.1109/TMTT.1965.1125964.

- [26] L. Chen, Y. Bai and X. Xing, "Performance of high-/low-pass phase shifter in broadband," *2010 IEEE International Conference on Ultra-Wideband*, pp. 1-4, 2010, doi: 10.1109/ICUWB.2010.5615588.
- [27] L. Stark, "Microwave theory of phased-array antennas—A review," in *Proceedings of the IEEE*, vol. 62, no. 12, pp. 1661-1701, Dec. 1974, doi: 10.1109/PROC.1974.9684.
- [28] M. A. Morton, J. P. Comeau, J. D. Cressler, M. Mitchell and J. Papapolymerou, "Sources of Phase Error and Design Considerations for Silicon-Based Monolithic High-Pass/Low-Pass Microwave Phase Shifters," in *IEEE Transactions on Microwave Theory and Techniques*, vol. 54, no. 12, pp. 4032-4040, Dec. 2006, doi: 10.1109/TMTT.2006.886162.
- [29] M. Şengül, "High-pass/low-pass section design for 0° - 360° lumped-element phase shifters via the real frequency technique," *Turkish Journal of Electrical Engineering and Computer Sciences, Turkiye Klinikleri Journal of Medical Sciences*, Vol. 25 No. 3, pp. 1922–1931.
- [30] M. Şengül, "Design of Practical Broadband Matching Networks With Mixed Lumped and Distributed Elements," in *IEEE Transactions on Circuits and Systems II: Express Briefs*, vol. 61, no. 11, pp. 875-879, Nov. 2014, doi: 10.1109/TCSII.2014.2356872.
- [31] M. Sengul, "Synthesis of Cascaded Lossless Commensurate Lines," in *IEEE Transactions on Circuits and Systems II: Express Briefs*, vol. 55, no. 1, pp. 89-91, Jan. 2008, doi: 10.1109/TCSII.2007.904171.
- [32] M. Şengül and G. Çakmak, "Analysis of Mixed-Element Structures Formed With Shunt Capacitors Separated by Transmission Lines," in *IEEE Transactions on Circuits and Systems II: Express Briefs*, vol. 66, no. 8, pp. 1331-1335, Aug. 2019, doi: 10.1109/TCSII.2018.2880262.

- [33] M. Şengül and G. Çakmak, "Component value calculations in a mixed element ladder network containing series capacitors separated by unit elements," *International Journal of Circuit Theory and Applications*, vol. 49, no. 10, pp. 3368–3377, May 2021, doi: 10.1002/cta.3076.
- [34] M. Şengül and G. Çakmak, "Mixed Element Networks with Series Capacitors Separated by Unit Elements," *Journal of Circuits, Systems and Computers*, p. 2150125, Oct. 2020, doi: 10.1142/s0218126621501255.
- [35] M. Sengül and G. Cakmak, "Synthesis of Degenerate Networks Formed with Shunt Capacitors," *7th International Conference on Advanced Technologies (ICAT'18)*, Antalya, Turkey, April 28-01 May, 2018, pp. 21-24.
- [36] M. Şengül, G. Çakmak and R. Özdemir, "Phase Shifting Properties of High-Pass and Low-Pass Mixed-Element Two-Ports," in *IEEE Transactions on Circuits and Systems II: Express Briefs*, vol. 68, no. 4, pp. 1208-1212, April 2021, doi: 10.1109/TCSII.2020.3038423.
- [37] M. Şengül and Z. Aydoğar, "Synthesis of resistively terminated high-pass LC ladder networks," *National Conference on Electrical, Electronics and Computer Engineering*, 2010, pp. 361-364.
- [38] M. Şengül and Z. Aydoğar, "Transfer matrix factorization-based synthesis of resistively terminated LC ladder networks," *2009 International Conference on Electrical and Electronics Engineering - ELECO 2009*, pp. II-74-II-77, 2009, doi: 10.1109/ELECO.2009.5355388.
- [39] N. Kingsley and J. Papapolymerou, "Organic "Wafer-Scale" packaged miniature 4-bit RF MEMS phase shifter," in *IEEE Transactions on Microwave Theory and Techniques*, vol. 54, no. 3, pp. 1229-1236, March 2006, doi: 10.1109/TMTT.2005.864099.

- [40] P. Onno and A. Plitkins, "Miniature Multi-Kilowatt PIN Diode Mic Digital Phase Shifters," *1971 IEEE GMTT International Microwave Symposium Digest*, pp. 22-23, 1971, doi: 10.1109/GMTT.1971.1122885.
- [41] R.C Johnson, H. Jasik. *Antenna Engineering Handbook*. 2nd ed. New York, NY, USA: McGraw-Hill, 1984.
- [42] R.K. Gupta, G.C. Estep, J.I. Upshur, "MMIC techniques for active phased-array antenna systems for future communications satellites," *In Asia-Pacific Microwave Conference*, Tokyo, Japan, 6–9 December 1994, pp. 897-902.
- [43] R. Tavrani *et al.*, "SiGe MMICs for phased array radar applications," *The 2005 IEEE Annual Conference Wireless and Microwave Technology*, pp. 38-38, 2005, doi: 10.1109/WAMIC.2005.1528375.
- [44] R. V. Garver, "Broad-Band Diode Phase Shifters," in *IEEE Transactions on Microwave Theory and Techniques*, vol. 20, no. 5, pp. 314-323, May 1972, doi: 10.1109/TMTT.1972.1127751.
- [45] "Solve nonlinear least-squares (nonlinear data-fitting) problems - MATLAB lsqnonlin," www.mathworks.com. <https://www.mathworks.com/help/optim/ug/lsqnonlin.html>
- [46] T. M. Hancock and G. M. Rebeiz, "A 12-GHz SiGe phase shifter with integrated LNA," in *IEEE Transactions on Microwave Theory and Techniques*, vol. 53, no. 3, pp. 977-983, March 2005, doi: 10.1109/TMTT.2004.842479.
- [47] "Tolerances and Stopping Criteria - MATLAB & Simulink," www.mathworks.com. <https://www.mathworks.com/help/optim/ug/tolerances-and-stopping-criteria.html>
- [48] X. Tang and K. Mouthaan, "A novel broadband 90° phase shifter," *2008 Asia-Pacific Microwave Conference* pp. 1-4, 2008, doi: 10.1109/APMC.2008.4958037.

[49] Z. Mao and F. Yong, "Improvement of the Design of Switched-Line Phase Shifter," *2008 China-Japan Joint Microwave Conference*, pp.78-80, 2008, doi: 10.1109/CJMW.2008.4772380



CURRICULUM VITAE

Personal Information

Name Surname : Gökhan Çakmak

Education

B. Sc. : Electronics Engineering Kadir Has University 2008

M. Sc. : Electronics Engineering Kadir Has University 2018

Languages :English

SCI Articles from M. Sc. studies

M. Şengül and G. Çakmak, "Analysis of mixed element structures formed with shunt capacitors separated by transmission line." *IEEE Transactions on Circuits and Systems II: Express Briefs*, Vol. 66 No. 6 pp. 1331-1335.

Conference Papers from M. Sc. studies

M. Sengül and G. Çakmak, "Synthesis of Degenerate Networks Formed with Shunt Capacitors," *7th International Conference on Advanced Technologies (ICAT'18)*, April 28-May 01, 2018, Antalya, Turkey.

SCI Articles from Ph. D. studies

M. Şengül, G. Çakmak and R. Özdemir, "Phase Shifting Properties of High-Pass and Low-Pass Mixed-Element Two-Ports," in *IEEE Transactions on Circuits and Systems II: Express Briefs*, vol. 68, no. 4, pp. 1208-1212, April 2021, doi: 10.1109/TCSII.2020.3038423.

M. Şengül and G. Çakmak, "Component value calculations in a mixed element ladder network containing series capacitors separated by unit elements," *International Journal of Circuit Theory and Applications*, vol. 49, no. 10, pp. 3368–3377, May 2021, doi: 10.1002/cta.3076.

M. Şengül and G. Çakmak, “Mixed Element Networks with Series Capacitors Separated by Unit Elements,” *Journal of Circuits, Systems and Computers*, p. 2150125, Oct. 2020, doi: 10.1142/s0218126621501255

